

การสร้างแบบจำลองพลวัตของการผลิตพอลิเอสเตอร์ชนิดไม่อิ่มตัวจากมาเลอิกแอนไฮไดรด์
และพรอพิลีนไกลคอล



นายสุรฉัตร ชมบ้านแพ้ว

ศูนย์วิทยทรัพยากร จุฬาลงกรณ์มหาวิทยาลัย

วิทยานิพนธ์นี้เป็นส่วนหนึ่งของการศึกษาตามหลักสูตรปริญญาวิทยาศาสตรดุษฎีบัณฑิต

สาขาวิชาเคมีเทคนิค ภาควิชาเคมีเทคนิค

คณะวิทยาศาสตร์ จุฬาลงกรณ์มหาวิทยาลัย

ปีการศึกษา 2553

ลิขสิทธิ์ของจุฬาลงกรณ์มหาวิทยาลัย

DYNAMIC MODELING OF UNSATURATED POLYESTER PRODUCTION
FROM MALEIC ANHYDRIDE AND PROPYLENE GLYCOL



Mr. Surachat Chombanphaew

ศูนย์วิทยทรัพยากร
จุฬาลงกรณ์มหาวิทยาลัย

A Dissertation Submitted in Partial Fulfillment of the Requirements
for the Degree of Doctor of Philosophy Program in Chemical Technology

Department of Chemical Technology

Faculty of Science

Chulalongkorn University

Academic Year 2010

Copyright of Chulalongkorn University

Thesis Title DYNAMIC MODELING OF UNSATURATED
POLYESTER PRODUCTION FROM MALEIC
ANHYDRIDE AND PROPYLENE GLYCOL
By Mr. Surachat Chombanphaew
Field of Study Chemical Technology
Thesis Advisor Associate Professor Lursuang Mekasut, Dr.Ing.
Thesis Co-Advisor Assistant Professor Sirilux Poompradub, D.Eng.

Accepted by the Faculty of Science, Chulalongkorn University in Partial
Fulfillment of the Requirements for the Doctoral Degree

Deputy Dean for Administrative Affairs,

Vimolvan Pimpan
..... Acting Dean, The Faculty of Science
(Associate Professor Vimolvan Pimpan, Ph.D.)

THESIS COMMITTEE

T. Vitidsant
..... Chairman
(Associate Professor Tharapong Vitidsant, Dr.de L'INPT)

L. Mekasut
..... Thesis Advisor
(Associate Professor Lursuang Mekasut, Dr.Ing.)

Sirilux P.
..... Thesis Co-Advisor
(Assistant Professor Sirilux Poompradub, D.Eng.)

Pornpote Piumsombon
..... Examiner
(Associate Professor Pornpote Piumsombon, Ph.D.)

K. Poochinda
..... Examiner
(Kunakorn Poochinda, Ph.D.)

Chesada
..... External Examiner
(Mr. Chesada Chaijareenont)

สุรจักร ชมบ้านแพ้ว: การสร้างแบบจำลองพลวัตของการผลิตพอลิเอสเตอร์ชนิดไม่อิ่มตัวจากมาเลอิกแอนไฮไดรด์และพรอพิลีนไกลคอล (DYNAMIC MODELING OF UNSATURATED POLYESTER PRODUCTION FROM MALEIC ANHYDRIDE AND PROPYLENE GLYCOL) อ. ที่ปรึกษาวิทยานิพนธ์หลัก: รศ.ดร.เลอสรวง เมฆสุต, อ. ที่ปรึกษาวิทยานิพนธ์ร่วม: ผศ.ดร.ศิริลักษณ์ พุ่มประดับ, 164 หน้า.

งานวิจัยนี้ได้พัฒนาแบบจำลองพลวัตเพื่อศึกษาผลของอุณหภูมิและอัตราการป้อนเข้าของแก๊สเฉื่อยในการสังเคราะห์พอลิเอสเตอร์ชนิดไม่อิ่มตัวจากมาเลอิกแอนไฮไดรด์และพรอพิลีนไกลคอล โดยแบบจำลองพลวัตแบ่งออกเป็น 3 ส่วนคือแบบจำลองเครื่องปฏิกรณ์แบบจำลองจลนศาสตร์ของปฏิกิริยา และแบบจำลองการถ่ายโอนมวล ผลการจำลองกระบวนการถูกตรวจสอบความถูกต้องโดยเปรียบเทียบกับข้อมูลการทดลองและยืนยันได้ว่าแบบจำลองพลวัตที่พัฒนาขึ้นมีความน่าเชื่อถือได้ ข้อมูลจากการจำลองกระบวนการพบว่าอุณหภูมิในการเกิดปฏิกิริยาและอัตราการป้อนเข้าของแก๊สเฉื่อยส่งผลกระทบต่อตัวแปรที่สำคัญในกระบวนการซึ่งเป็นผลเนื่องมาจากการเปลี่ยนแปลงลักษณะสมบัติของพอลิเมอร์อย่างต่อเนื่องระหว่างกระบวนการสังเคราะห์ โดยทั้งสองปัจจัยที่ทำการศึกษานั้นได้ส่งผลกระทบต่อโดยตรงและโดยอ้อมต่อตัวแปรที่สำคัญในกระบวนการ

การเพิ่มอุณหภูมิในการเกิดปฏิกิริยานั้นทำให้อัตราการเกิดปฏิกิริยาพอลิเมอร์ไรเซชันแบบควบแน่นสูงขึ้นเนื่องจากค่าคงที่การเกิดปฏิกิริยามีค่าสูงขึ้น ส่วนการเพิ่มอัตราการป้อนเข้าของแก๊สเฉื่อยนั้นสามารถทำให้อัตราการเกิดปฏิกิริยาพอลิเมอร์ไรเซชันแบบควบแน่นสูงขึ้นได้จากการเพิ่มพื้นที่ผิวจำเพาะของการถ่ายโอนมวล โดยที่ทั้งสองกรณีนั้นทำให้เวลาในการเกิดปฏิกิริยาลดลงได้

ศูนย์วิทยทรัพยากร
จุฬาลงกรณ์มหาวิทยาลัย

ภาควิชา.....เคมีเทคนิค.....ลายมือชื่อนิสิต.....*สุรจักร ชมบ้านแพ้ว*
สาขาวิชา.....เคมีเทคนิค.....ลายมือชื่อ อ. ที่ปรึกษาวิทยานิพนธ์หลัก.....*เลอสรวง เมฆสุต*
ปีการศึกษา.....2553.....ลายมือชื่อ อ. ที่ปรึกษาวิทยานิพนธ์ร่วม.....*ศิริลักษณ์ พุ่มประดับ*

#4873897523: MAJOR CHEMICAL TECHNOLOGY

KEYWORDS : MODELING/ SIMULATION/ UNSATURATED POLYESTER/
POLYMERIZATION/ MASS TRANSFER

SURACHAT CHOMBANPHAEW: DYNAMIC MODELING OF
UNSATURATED POLYESTER PRODUCTION FROM MALEIC
ANHYDRIDE AND PROPYLENE GLYCOL. THESIS ADVISOR:
ASSOC.PROF. LURSUANG MEKASUT, Dr.Ing., THESIS CO-
ADVISOR: ASST. PROF. SIRILUX POOMPRADUB, D.Eng., 164 pp.

This work was carried out to predict the effect of reaction temperature and the inert gas feed rate on condensation polymerization of unsaturated polyester between maleic anhydride and propylene glycol. The developed dynamic model consisted of three parts, the reactor model, the kinetic model and the mass transfer model. The simulated result was verified by comparing to the process identification from the experimental data. The comparison of the simulation and experiment gave a satisfaction and the developed model was valid. The simulation illustrated that the effect of reaction temperature and the inert gas flow were more complicate to the process parameters because of the changing in the bulk liquid properties during polymerization. Both of reaction temperature and the inert gas flow rate were influence to the process parameters via the exact and diverting paths.

Increasing of reaction temperature would increase the rate of condensation polymerization by enhancement of rate constant. Increasing of inert gas flow rate would increase the polymerization rate by increasing of specific interfacial area for mass transfer. In both two cases, the reaction time should decrease.

Department: Chemical Technology

Field of Study: Chemical Technology

Academic Year 2010

Student's Signature *Surachat Chombanphaew*

Advisor's Signature *L. S. M.*

Co-Advisor's Signature *Sirilux P.*

ACKNOWLEDGEMENTS

I would like to express my heartfelt gratitude and appreciation to my advisor Assoc.Prof.Dr. Lursuang Mekasut, and my co-advisor Asst.Prof.Dr. Sirilux Poompradub, for their kind supervision, invaluable guidance and constant encouragement.

Acknowledgements are also sincerely grateful to Assoc.Prof.Dr. Tharapong Vitidsant for serving as chairman and to Assoc.Prof.Dr. Pornpote Piumsomboon, Dr. Kunakorn Poojinda, and Mr. Chesada Chaijareenont as member of examiner of the thesis committee.

I would like to thank the Center for Petroleum, Petrochemicals and Advanced Materials (NCE-PPAM) and Graduate School Chulalongkorn University for financial support to this project, Patumwan Institute of Technology for laboratory and the Siam Chemical Industry Co., Ltd., for samples and materials. Also, I wish to express my grateful appreciation to Department of Chemical Technology, Faculty of Science, Chulalongkorn University, Bangkok, Thailand.

A very special thank you is conducted to my family and my friends for their endless encouragement, love and care.



ศูนย์วิทยทรัพยากร
จุฬาลงกรณ์มหาวิทยาลัย

CONTENTS

	Page
ABSTRACT IN THAI	iv
ABSTRACT IN ENGLISH	v
ACKNOWLEDGEMENTS	vi
CONTENTS	vii
LIST OF TABLES	xi
LIST OF FIGURES AND SCHEMES	xii
LIST OF ABBREVIATIONS	xvii
 CHAPTER	
I. INTRODUCTION	1
1.1 Motivation.....	1
1.2 Objectives of dissertation.....	2
1.3 Description of System.....	2
1.3.1 Condensation polymerization.....	2
1.3.2 System of interest.....	2
1.4 Scope of dissertation.....	3
 II. THEORY AND LITERATURE REVIEW	4
2.1 Introduction of Unsaturated polyester	4
2.2 Processing equipment and manufacturing.....	5
2.3 Unsaturated polyester resin properties	7
2.4 Application.....	9
2.5 Chemistry.....	10
2.5.1 Polyesterification	10
2.5.2 Side reaction.....	11
2.5.2.1 Isomerization.....	11
2.5.2.2 Addition of glycol to the double bond	13
2.6 Mass transfer with chemical reaction.....	13
2.6.1 Diffusion.....	13
2.6.2 Mass transfer theories at a gas-liquid interface	14

	Page
2.6.2.1 Film theory.....	15
2.6.2.2 Boundary Layer Theory	15
2.6.2.3 Penetration Theory	16
2.6.2.4 Surface renewal theory	16
2.6.3 Desorption with chemical reaction	17
2.7 Kolmogoroff's theory for turbulent flow	20
2.8 Literature reviews.....	22
III. MODEL DEVELOPMENT.....	27
3.1 Kinetic model.....	28
3.2 Resistant of water desorption in polymerization.....	32
3.3 Volumetric mass transfer coefficient.....	33
3.3.1 Mass transfer coefficient.....	33
3.3.2 Specific interfacial area.....	34
3.3.3 Power requirement.....	36
3.3.3 Physical properties estimation.....	37
3.4 Reactor model.....	38
IV. METHODOLOGY.....	41
4.1 Polymerization reactor.....	41
4.2 Temperature control system.....	41
4.3 Chemical substances.....	45
4.4 Synthesis of unsaturated polyester.....	45
4.5 Characterization.....	46
4.5.1 High performance liquid chromatography.....	46
4.5.2 Fourier transforms infrared spectroscopy.....	47
4.5.3 Gas chromatograph and mass spectrometry	47
4.6 Model flow diagram.....	47
4.6.1 Overall model flow diagram	47
4.6.2 Volumetric mass transfer model flow diagram	48

	Page
4.7 Model parameters.....	49
4.7.1 Kinetic parameters	49
4.7.2 Vapor-Liquid equilibrium estimation	50
4.8 Unsaturated polyester properties estimation.....	51
V. RESULTS AND DISCUSSION.....	53
5.1 Parameters sensitivity on energy dissipation.....	53
5.2 Parameters sensitivity on mass transfer coefficient	56
5.3 Parameters sensitivity on specific interfacial area	58
5.3.1 Gas hold-up	58
5.3.2 Bubble diameter	62
5.3.3 Specific interfacial area.....	64
5.4 Parameters sensitivity on volumetric mass transfer coefficient.....	65
5.5 Effect of synthesized condition on the rate of condensation polymerization and the reaction time	67
5.5.1 Effect of reaction temperature	67
5.5.2 Effect of inert gas flow rate	67
5.6 Characterization of Unsaturated polyester from synthesis	70
5.7 Simulation results of process parameters	71
5.7.1 Unsaturated polyester properties	72
5.7.2 Energy dissipation	72
5.7.3 Mass transfer coefficient	73
5.7.4 Gas hold-up and bubble size	74
5.7.5 Specific interfacial area	77
5.7.6 Volumetric mass transfer coefficient	78
5.8 Comparison of simulation results to experimental data	79
5.8.1 Acid number	79
5.8.2 Propylene glycol content in condensate	82
5.8.3 Accumulative condensate	82
5.8.4 Water content in unsaturated polyester	82

	Page
5.9 Concentration of each species in liquid phase	85
VI. CONCLUSIONS AND RECOMMENDATIONS.....	87
REFERENCES.....	89
APPENDICES.....	93
APPENDIX A.....	94
APPENDIX B.....	96
APPENDIX C.....	97
BIOGRAPHY.....	164



ศูนย์วิทยทรัพยากร
จุฬาลงกรณ์มหาวิทยาลัย

LIST OF TABLES

Table	Page
Table 1.1 Ingredients of unsaturated polyester in research.....	3
Table 2.1 Common Raw Materials for Polyesters.....	8
Table 2.2 General purpose unsaturated polyester properties.....	9
Table 2.3 Isomerization versus glycol type at reaction temperature 180 °C.....	12
Table 2.4 Isomerization versus reaction temperature	12
Table 3.1 Functional group in polyesterification of MA and PG	28
Table 4.1 Arrhenius parameters in polyesterification of maleic anhydride with propylene glycol.....	50
Table 4.2 Equilibrium constant in polyesterification of maleic anhydride with propylene glycol	50
Table 5.1 Synthesized conditions and molecular weight of unsaturated polyester.	70
Table 5.2 Functional group of unsaturated polyester resin and wave number.....	71
Table B.1 Unsaturated polyester synthesized conditions and initial mass of each conditions.....	96


 ศูนย์วิทยทรัพยากร
 จุฬาลงกรณ์มหาวิทยาลัย

LIST OF FIGURES AND SCHEMES

Figure and Scheme	Page
Scheme 2.1 Propylene glycol maleate structure	4
Figure 2.1 Structure of unsaturated polyester: (a) uncured resin and (b) cured resin.....	5
Scheme 2.2 General purpose unsaturated polyester	9
Scheme 2.3 Reaction of maleic acid and propylene glycol	11
Scheme 2.4 Ordelt reaction	13
Figure 2.2 Film theory conceptualization	15
Figure 2.3 Desorption conceptualization	20
Scheme 3.1 Reaction for the polyesterification of MA with PG: (E) esterification, (I) isomerization and (S) double bond saturation.	29
Figure 3.1 Model conceptualization for unsaturated polyester production.....	38
Figure 4.1 Schematic diagram of reactor setup: (1) inlet gas valve, (2) vessel cover, (3) vessel tank, (4) sampling and drain valve, (5) condenser, (6) baffles, (7) disk flat-blade turbine, (8) nozzle, (9) inert gas inlet, (10) cooling inlet, (11), cooling outlet, (12) condenser outlet, (13) and (14) flow meter.....	42
Figure 4.2 Batch polymerization reactor system which was used in this research.....	43
Figure 4.3 Schematic diagram of temperature controlling and measuring points in reactor system: (1) liquid phase, (2) gas phase, (3) cooling inlet, (4) cooling outlet, (5) outlet stream.....	43
Figure 4.4 Shinko software: (a) controlling and (b) monitoring.....	44
Figure 4.5 Reaction temperature profile	45
Figure 4.6 Overall model flow diagram	48
Figure 4.7 Volumetric mass transfer model flow diagram.....	49
Figure 4.8 MolWork software operating panel	51
Figure 5.1 Power consumption by varied inert gas flow: (a) 120 ccm, (b) 360 ccm, (c) 600 ccm and (d) 840 ccm.....	53

Figure and Scheme	Page
Figure 5.2 Effect of density and inert gas flow rate on power consumption in aerated system.....	54
Figure 5.3 Effect of density and inert gas flow rate on energy dissipation....	54
Figure 5.4 Effect of viscosity and molecular weight on diffusivity: (a) 160 °C and (b) 220 °C	55
Figure 5.5 Effect of temperature and inert gas flow rate on mass transfer coefficient, evaluate at molecular weight 500 g/mol, density 500 kg/m ³ , viscosity 0.01 Pa.s.....	56
Figure 5.6 Effect of density and viscosity on mass transfer coefficient evaluated at N ₂ flow 360 ccm: (a) 160 °C and (b) 220 °C.....	57
Figure 5.7 Effect of density and viscosity on mass transfer coefficient evaluated at 180 °C: (a) N ₂ flow 120 ccm and (b) N ₂ flow 840 ccm.....	58
Figure 5.8 Effect of parameters on gas hold-up at inert gas flow 360 ccm: (a) constant viscosity 0.01 Pa.s, (b) constant surface tension 0.5 N/m and (c) constant density 500 kg/m ³	59
Figure 5.9 Effect of viscosity and surface tension on gas hold-up, constant density 500 kg/m ³ : inert gas flow (a) 840 ccm, (b) 600 ccm, (c) 360 ccm and (d) 120 ccm.....	60
Figure 5.10 Effect of parameters on mean bubble diameter: (a) constant surface tension 0.5 N/m, (b) constant density 500 kg/m ³ and (d) constant viscosity 0.01 Pa.s	61
Figure 5.11 Bubble diameter estimated at density 500 kg/m ³ , surface tension 0.05 N/m and viscosity 0.01 Pa.s by varied inert gas flow: (a) 840 ccm, (b) 600 ccm, (c) 360 ccm and (d) 120 ccm.....	62
Figure 5.12 Effect of parameters on specific interfacial area: (a) constant surface tension 0.5 N/m, (b) constant density 500 kg/m ³ and (d) constant viscosity 0.01 Pa.s	63
Figure 5.13 Effect of viscosity and surface tension on specific interfacial area at constant density 500 kg/m ³ by varied inert gas flow rate: (a) 840 ccm, (b) 600 ccm, (c) 360 ccm and (d) 120 ccm.....	64

Figure and Scheme	Page
Figure 5.14 Effect of viscosity and density on volumetric mass transfer coefficient at surface tension 0.05 N/m and inert gas flow rate 360 ccm by varying reaction temperature: (a) 220 °C and (b) 160 °C.....	65
Figure 5.15 Effect of viscosity and density on volumetric mass transfer coefficient at surface tension 0.05 N/m and 180 °C by varied inert gas flow rate: (a) 840 ccm, (b) 600 ccm, (c), 360 ccm and (d) 120 ccm.....	66
Figure 5.16 Effect of viscosity and density on volumetric mass transfer coefficient at inert gas flow 360 ccm and 180 °C by varied surface tension: (a) 0.025 N/m, (b) 0.05 N/m, (c) 0.075 N/m and (d) 0.10 N/m.....	66
Figure 5.17 Liquid phase temperature.....	67
Figure 5.18 Effect of reaction temperature at inert gas flow 360 ccm on (a) acid number and (b) conversion: □160 °C, ○180°C, ×200 °C and Δ220 °C	68
Figure 5.19 Effect of inert gas flow rate at reaction temperature 180 °C on (a) acid number and (b) conversion: ○ 120 ccm, □ 360 ccm, × 600 ccm and Δ 840 ccm	69
Figure 5.20 Representative FTIR spectra of synthesized unsaturated polyester: (a) UP9, (b) UP8, (c) UP7, (d) UP5, (e) UP4, (f) UP2, (g) UP2 and (h) UP1.....	71
Figure 5.21 Unsaturated polyester properties from the simulation at reaction temperature 220 °C and inert gas flow 600 ccm: (a) molecular weight, (b) viscosity, (c) surface tension and (d) density.....	72
Figure 5.22 Energy dissipation at reaction temperature 180 °C: (a) 120 ccm, (b) 360 ccm, (c) 600 ccm, (d) and 840 ccm.....	73
Figure 5.23 Effect of reaction temperature on mass transfer coefficient (H ₂ O), simulated at 600 ccm: (a) 200 °C and (b) 160 °C.....	74

Figure and Scheme	Page
Figure 5.24 Effect of inert gas flow rate on mass transfer coefficient (H ₂ O), simulated at 180 °C: (a) 120 ccm, (b) 360 ccm, (c) and (d) 840 ccm.....	74
Figure 5.25 Effect of inert gas flow rate on gas hold-up, simulated at 180 °C: (a) 840 ccm, (b) 600 ccm, (c) 360 ccm and (d) 120 ccm.....	75
Figure 5.26 Effect of inert gas flow rate on gas hold-up, simulated at 180 °C: 840 ccm (a), 600 ccm (b), 360 ccm (C) and 120 ccm (d).....	75
Figure 5.27 Effect of reaction temperature on bubble size, simulated at 600 ccm: (a) 220 °C, (b) 200 °C, (c) 180 °C and (d) 160 °C.....	76
Figure 5.28 Effect of inert gas flow rate on bubble size, simulated at 180 °C: (a) 840 ccm, (b) 600 ccm, (c) 360 ccm and (d) 120 ccm.....	76
Figure 5.29 Effect of reaction temperature on specific interfacial area, simulated at 600 ccm: (a) 160 °C, (b) 180 °C and (c) 200 °C.....	77
Figure 5.30 Effect of inert gas flow rate on specific interfacial area, simulated at 180 °C: (a) 840 ccm, (b) 600 ccm, (c) 360 ccm and (d) 120 ccm.....	77
Figure 5.31 Effect of reaction temperature on volumetric mass transfer coefficient (H ₂ O), simulated at 600 ccm: (a) 160 °C, (b) 180 °C and (d) 200 °C.....	78
Figure 5.32 Effect of inert gas flow rate on volumetric mass transfer coefficient (H ₂ O), simulated at 180 °C: (a) 120 ccm, (b) 360 ccm, (c) 600 ccm and (d) 840 ccm.....	78
Figure 5.33 Acid number, simulated at inert gas flow rate 600 ccm: (a) 160 °C, (b) 180 °C, (c) 200 °C and (d) 220 °C.....	79
Figure 5.34 Acid number, simulated at 180 °C: (a) 160 ccm, (b) 360 ccm, (c) 600 ccm and (d) 840 ccm.....	80
Figure 5.35 Comparison of acid number at constant N ₂ flow 600 ccm, — simulation and • experiment: (a) 160 °C, (b) 180 °C, (c) 200 °C and (d) 240 °C	80

Figure and Scheme	Page
Figure 5.36 Comparison of acid number at reaction temperature 180 °C, ——simulation and • experiment: (a) 120 ccm, (b) 360 ccm, (c) 600 ccm and (d) 800 ccm.....	81
Figure 5.37 Propylene glycol content in condensate at N ₂ flow rate 600 ccm: simulation 160 °C, - -180 °C and —200 °C, experiment o 160 °C, □ 180 °C and Δ 200 °C.....	82
Figure 5.38 Comparison of accumulative condensate at constant N ₂ flow rate 600 ccm: simulation — 160 °C, ----- 180 °C and 200 °C, experiment Δ 160 °C, □ 180 °C and o 200 °C.....	83
Figure 5.39 Comparison of accumulative condensate at reaction temperature 180 °C, ——simulation and • experiment: (a) 120 ccm, (b) 360 ccm, (c) 600 ccm and (d) 800 ccm.....	83
Figure 5.40 Figure 5.40 Water content in unsaturated polyester (a) N ₂ flow rate 600 ccm: simulation 160 °C, - -180°C and — 200°C, experiment o160 °C, □180 °C and Δ 200 °C (b) Reaction temperature 180 °C: simulation - - 360 ccm, 360 ccm and — 360 ccm, experiment o 360 ccm, □360 ccm and Δ 360 ccm.....	84
Figure 5.41 Liquid concentration of each species, reaction temperature 160 °C and inert gas flow rate 600ccm: (a) OH, (b) COOH1D, (c) COOH2D, (d) COOR1D, (e) COOR2D, (f) COOHS, (g) COORS and (h) H ₂ O	85
Figure 5.42 Water concentration in liquid phase at reaction temperature 180 °C: (a) 120 ccm, (b) 360 ccm, (c) 600 ccm and (d) 840 ccm.....	86

LIST OF ABBREVIATIONS

Notations

a	specific interfacial area (per meter, 1/m)
c	concentration
	liquid phase (mole per kilogram, mol/kg)
	gas phase (mole per liter, mol/lit)
d_b	bubble diameter (meter, m)
D_L	diffusivity on the liquid (square meter per second, m ² /s)
E_k	turbulent kinetic energy (joule per kilogram, J/kg)
g	gravitational constant (meter per square second, m/s ²)
h	blade height of stirrer (meter, m)
H	liquid level in vessel, (meter, m)
k	rate constant (the dimension depend on the case)
k_L	mass transfer coefficient (meter per second, m/s)
K	equilibrium constant (the dimension depend on the case)
K''	gas-liquid equilibrium constant (the dimension depend on the case)
m	mass (kilogram, kg)
M_w	molecular weight (gram per mole, g/mol)
n	amount of substance (mole, mol)
\dot{n}	molar flow of substance (mole per second, mol/s)
N	stirrer speed (rounds per second, rps)
\dot{N}	molar flux of substance (mole per square meter per second, mol/m ² .s)
N_p	power number (dimensionless)
p	vapor pressure (Pascal, Pa)
p_t	total pressure (Pascal, Pa)
P	power input under gassed condition (watt, w)
P_o	power input in un-aerated system (watt, w)
Q	gas flow rate (cubic meter per second, m ³ /s and cubic centimeter per minute, ccm)
r	generation rate of functional group (mole per kilogram per second, mol/kg.s)

Re	impeller Reynolds number (dimensionless)
Sc	Schmidt number (dimensionless)
t	time (second, s)
T	stirrer diameter (meter, m)
u	velocity (meter per second, m/s)
V	volume of the liquid in the vessel (cubic meter, m ³)
V_S	superficial gas velocity (meter per second, m/s)
x	mole fraction of distillate flow (dimensionless)
y	mole fraction of outlet gas flow (dimensionless)
z	mole fraction of inlet gas flow into condenser (dimensionless)
AN	Acid number (milligram per gram, mg/g)
HN	Hydroxyl number (milligram per gram, mg/g)

Greek letters

ε	energy dissipation rate (watt per kilogram, w/kg)
ρ	density (kilogram per cubic meter, kg/m ³)
μ	viscosity (Pascal second, Pa.s)
ν	kinematic viscosity (square meter per second, m ² /s)
σ	surface tension (Newton per meter, N/m)
ϕ	gas hold-up (dimensionless)
ϕ_v	gas hold-up in viscous system (dimensionless)
τ	time scale of Kolmogoroff
η	unique length of Kolmogoroff

Subscripts and Superscript

'	outlet stream from reactor system
o	initial value
$1D$	cis-isomer
$2D$	trans-isomer
e	exposure
E	ester, esterification
G	gas phase
i	component index

- L liquid phase
 Ph interface
 S single bond, double bond saturation
 x, y, z direction
* equilibrium state



ศูนย์วิทยทรัพยากร
จุฬาลงกรณ์มหาวิทยาลัย

CHAPTER I

INTRODUCTION

1.1 Motivation

Almost of routine operation in industrial scale polymerization, operators generally run polymerization by trying to achieve a preset temperature profile that has historically proven successful. Only fine tuning some of the process conditions may bring a lot of damage and loss in the mass production if the operators do not well understand the process and effects of process condition on product qualities. Even though the process conditions are kept to operational standard, unexpected scenario may occur from uncontrolled factor and need of conditions adjustment.

A common problem in an industrial scale of polymerization processes is the lack of understanding in the process and process condition. Thus, a study of the process by using a mathematical model and its simulation result is the way to achieve the process comprehensibility and to spend not less time for perception. Furthermore, the model can predict the effect of off-bound operating conditions, unexpected scenario and estimate for the key variables needed to assess the course of the reaction. Additionally, to identify model parameters or variables, the model need to be corrected. Process models that reasonable predict the behavior of a process under changing conditions and in the presence of disturbances will be a very useful tool.

Unsaturated polyester is used in multitude of applications and high consumption. Its demand is still rather high in the global market. Unsaturated polyester can be prepared by condensation polymerization based on glycols and dibasic acids and water is generated as a byproduct. Removal of water from molten polymer during polymerization is a challenging task. Many literatures studied unsaturated polymerization by using the typical mathematical model but only a few researches directly studied and focused on this challenging task. Therefore, this polymerization system was chosen as reaction model for this research to study the effects of operating conditions on water removal and polymerization.

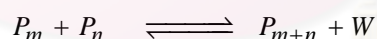
1.2 Objectives of dissertation

1. To study the effect of inert gas feed rate and temperature on the rate of condensation polymerization and the reaction time of unsaturated polyester production
2. To develop the dynamic model which is composed of the reaction and separation units of unsaturated polyester production

1.3 Description of System

1.3.1 Condensation polymerization

Polymerization processes can be divided into two main types: chain-growth (or addition) polymerization and step-growth (or polycondensation) polymerization. Polycondensation processes differ from chain growth polymerization in that the growth of the polymer molecule can occur from the reaction of any two molecules, not just by monomer addition to a growing radical chain. The step-growth process is typically much slower than the addition polymerization, resulting in a slow increase in molecular weight. The polymerization reaction frequently produces a low molecular weight by-product (usually water). Common examples of polycondensation products include nylon 6, nylon 6-6, polyethylene terephthalate and unsaturated polyester. A polycondensation reaction can be represented schematically as:



where P_i represents the growing polymer chain of length i

W represents the byproduct

Polycondensation processes are frequently equilibrium limited and thus necessitate the removal of the condensation byproduct in order to achieve desired conversions. As the reaction proceeds, the viscosity of the polymer typically increases by orders of magnitude. Then the removal of condensation byproduct becomes increasingly challenging.

1.3.2 System of interest

The unsaturated polyester studied in this project is made from maleic anhydride and propylene glycol. The chemical formulas of each compound are shown

in Table 1.1. The unsaturated polyester resin is typically produced in a batch reactor and used in applications such as coating resin and construction adhesive.

Table 1.1 Ingredients of unsaturated polyester in research

Material	Chemical formula	Molar mass (g/mol)	Boiling point (°C)
Maleic anhydride	C ₄ H ₂ O ₃	98.059	202
Propylene glycol	C ₃ H ₈ O ₂	76.096	187.35

1.4 Scope of dissertation

1. Develop the dynamic model which is composed of the reaction and separation units of unsaturated polyester production
2. Synthesize the unsaturated polyester by using maleic anhydride and propylene glycol as reactant and study the influence of operating parameters at atmospheric pressure as follows:
 - 2.1 Isothermal reaction temperature in the range of 160 - 220°C
 - 2.2 N₂ feed rate in the range of 120 - 840 ccm

ศูนย์วิทยทรัพยากร
จุฬาลงกรณ์มหาวิทยาลัย

CHAPTER II

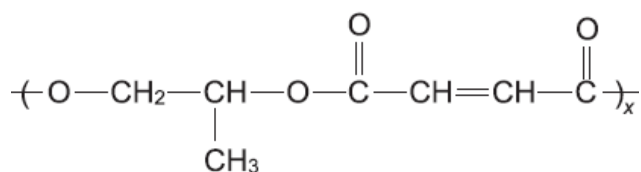
THEORY AND LITERATURE REVIEW

2.1 Introduction of unsaturated polyester

By chemical definition, polyester is a product from the reaction between polybasic acid and a polyhydric alcohol which form a series of ester linkages. The particular types of acids and alcohols which are used and other additive will determine polyester structure, properties and its application. Polyester can categorize into:

1. Alkyds: generally refer to oil-modify polyesters used for coatings, some cross linking systems are referred to as alkyd molding compound.
2. Plasticizer: certain completely saturated polyesters used to plasticize other plastic compositions are referred to as polymeric plasticizers.
3. Fiber and film: high molecular weight highly oriented polyesters based on specific acids and alcohols are used to form fibers and film.
4. Polyester foam, etc: polyester with a high concentration of hydroxyl groups which are crosslinked with isocyanates to form foams, coating, and elastomer.
5. Unsaturated polyester.

Unsaturated polyester is linear polycondensation products based on unsaturated and saturated acids/anhydrides and diols. These resins are generally pale yellow colored oligomers with low degree of polymerization. Depending on the chemical composition and molecular weight (1200-3000 g/mol), these oligomers may be viscous liquids or brittle solids. The unsaturation in the backbone provides sites for reaction with vinyl monomers using free radical initiators, thereby leading to the formation of a three dimensional network. [1]



Scheme 2.1 Propylene glycol maleate structure [2]

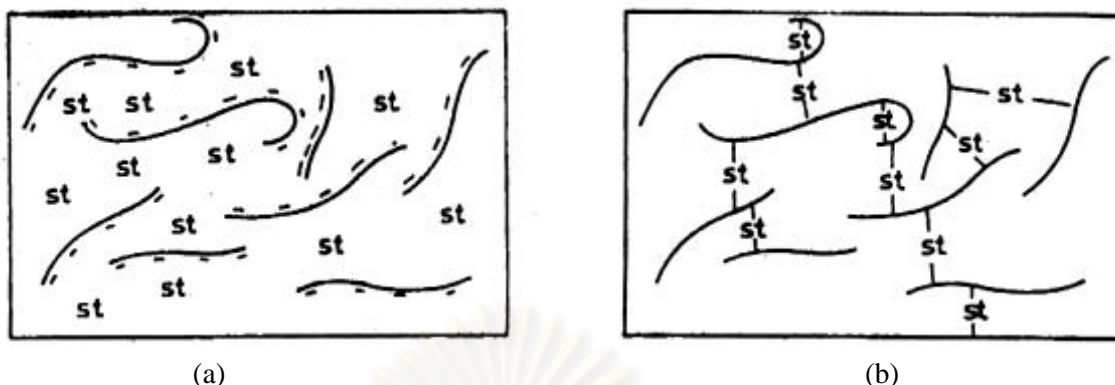


Figure 2.1 Structure of unsaturated polyester: (a) uncured resin and (b) cured resin [2]

The earliest record of chemical work with unsaturated polyesters was the study of glycol maleate in 1894. These resins were also totally unlike our present day in that they were either solid or very high viscosity, relatively immobile liquids. The key which made possible the modern unsaturated polyester resins of today is the addition of liquid unsaturated monomers such as monomeric styrene that give mixtures which would copolymerize at rates twenty to thirty times faster than the homo-polymerization rate for unsaturated polyesters by themselves. Further, the resultant mixture could be an easily handled liquid that could be readily cast or molded without the need for high molding pressures.

The modern development has propelled unsaturated polyester into the important role among modern polymer. It was found that mixing of styrene and unsaturated polyester could crosslink and yield high strength, low weight structures when reinforced with glass fibers. The fabrication of this structure could be accomplished using very low molding pressures making it possible to mold very large structures, in relatively light weight and low cost tooling. Since the end of the war, commercial development has proceeded rapidly in unsaturated polyester research and moved in all directions. Hosts of compounding materials, such as fillers, pigments, reinforcements, light stabilizers, curing catalysts, and promoters have been introduced for use with unsaturated polyesters.

2.2 Processing equipment and manufacturing

Unsaturated polyesters are synthesized in stainless steel-316 batch reactors from 3 to 15 cubic-meter capacities. The reactors have internal coil for thermal

transfer fluids and equipped with heavy duty agitators. The reactions are progressed under atmospheric pressure of inert gas to minimize oxidative degradation at reaction temperatures. It is usually necessary to use an excess of glycol in synthesis because of some glycol loss along with water from the reaction. Generally, a 5-10% excess glycol is added in the initial stages to compensate its losses during polymerization. Byproduct, water, is taken off the reactor through either packed distillation columns or partial condensers to more efficiently separate the glycol which comes off with the reaction water, so the glycol can be returned to the kettle. Xylene is added into the reactor at 3-6 wt% of the total material content to form an azeotrope with water and accelerate its removal that in turn increases the extent of reaction. The water and small non-recoverable amounts of the glycols and acids used must be dealt with in conformance with regulations that regulate the handling and disposal of industrial wastes.

The cooking operation begins with charging raw materials into the reactor. The liquid glycols are usually charged first followed by the granular and then the molten materials such as phthalic anhydride and maleic anhydride. Agitation can be started and the reactor is then slowly brought up to polymerization temperature at a programmed rate. Generally, polycondensation takes place above 160 °C and typical reaction temperatures are in the range 160° to 220 °C. The extent of reaction is controlled continuously by checking the acid number. This is done by periodically withdrawing some prepolymer samples from the reactor and titrating this with 0.1N alcoholic potassium hydroxide (KOH) solution. The reaction is carried until the desired acid number is achieved, normally less than 50. Reaction times ranging from 8 hours to 28 hours depending on the used raw materials, the degree of polymerization or molecular weight desired and the cooking temperature.

After, mixing the completed unsaturated polyester with a liquid monomer, usually styrene, is accomplished by transferring the finished molten to a thinning tank previously charged with styrene. Since the mixture of unsaturated polyester and monomer are very coreactive, polymerization inhibitors must be present in the styrene before thinning to prevent copolymerization from occurring during the thinning operation. Hydroquinone or substituted hydroquinone such as monotertiary butyl hydroquinone is commonly used. The molten is added gradually with sufficient

agitation in the thinning tank. The thinning tank, which was usually made of 316 stainless steel equip with cooling coils through which cooling water is circulated to keep the thinning tank contents below a safe temperature, usually 82° to 93°C. The molten polymer must be transferred to the thinning tank at a rate at which the heat being added to the tank by the molten polymer does not exceed the ability of the cooling system to keep the tank contents at a safe temperature level. On completion of the thinning operation, the thinned unsaturated polyester is cooled down to or near room temperature and further compounded to make the various types of unsaturated polyester resins of commerce.

The speed of the polyesterification reaction can be increased in several ways. All of which effect are more efficient to remove of the water produced as a by-product of the reaction. During reaction production, the inert gas is also introduced below the surface of the melt polymer (sparging) to minimize oxidative degradation as the main propose. At the same time, by assisting from agitation, inert gas also increases the gas-liquid interfacial area for mass transfer of water from the melt. Increasing the inert gas sparge rate or agitator speed, by increasing mass transfer area, increases the rate of water removal and hence reaction rate. The use of vacuum can also increase reaction rate by increasing the partial pressure of the by-product water, but this method may achieve undesired molecule.

The reaction can also be accelerated by the introduction of esterification catalysts. Among these are acids such as sulfuric, aryl sulfonic acids such as p-toluene sulfonic acid, tin compounds such as dibutyl tin oxide and titanates such as tetrabutyl titanate. [3]

2.3 Unsaturated polyester resin properties

Common raw materials used for preparing general propose and specialty unsaturated polyesters are shown in Table 2.1.

Unsaturated polyester resins range in viscosity from thin 0.05 Pa.s liquids to quite viscous fluids with the viscosities of 4 - 6 Pa.s and higher. Liquid resin colors can range from a very pale yellow to dark amber. These basic resin colors can further be affected by the presence of color contributing additives such as curing promoters.

The general purpose resins are synthesized using mainly propylene glycol (1,2 propanediol), maleic anhydride and phthalic anhydride. The molar ratio of phthalic anhydride to maleic anhydride is usually in the range from 1:1 to 2:1. The 100% unsaturated polyester resin from a typical general purpose resin synthesis is colorless or pale yellow solid at a room temperature having the general properties showed in Table 2.2.

Table 2.1 Common Raw Materials for Polyesters [3]

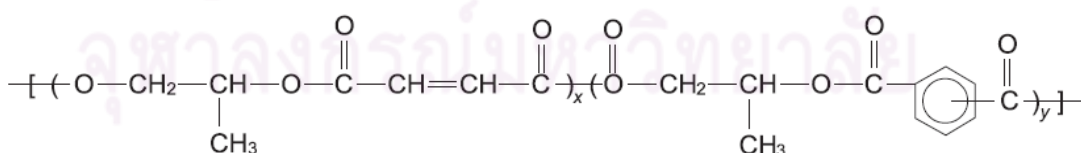
Materials	Contributes
Propylene glycol	Styrene compatibility
Ethylene glycol	Rigidity
Dipropylene glycol	Flexibility, toughness
Diethylene glycol	Flexibility, toughness
Neopentyl glycol	UV, water and chemical resistance
Trimethylpentanediol	Water and chemical resistance
Cyclohexane dimethanol	Electrical properties
Propoxylated disphenol A	Water and chemical resistance
Hydrogenated bisphenol A	Water and chemical resistance
Dibromoneopentyl glycol	Flame retardance
Phthalic anhydride	Styrene compatibility
Maleic anhydride	Provide reactive unsaturation
Adipic acid	Flexibility, toughness
Isophthalic acid	Toughness, chemical resistance
Terephthalic acid	Higher heat distortion
Fumaric acid	Provide reactive unsaturation
Glutaric acid	Flexibility, toughness
Dimer acids	Flexibility, toughness
Azelaic acid	Flexibility, toughness
Chlorendic acid	Flame retardance, chemical resistance
Tetrabromophthalic anhydride	Flame retardance, chemical resistance
Tetrachlorophthalic anhydride	Flame retardance, chemical resistance
Endomethylenetetrahydrophthalic anhydride	Air drying properties

Table 2.2 General purpose unsaturated polyester properties [3]

Properties	Characteristic/Value
Specific gravity	1.13-1.15
Solubility	Insoluble: water Soluble: ketones and aromatic solvents
Melting point	60 -77°C
Acid number	30-50

The resin properties would change as functions of the raw materials used and the molecular weight to which the resin is cooked. Although some of the unsaturated polyester resin produced is sold pure resin, most of the unsaturated polyester is sold and used as a solution in styrene monomer. The properties of unsaturated polyester resin which characterize them dominate among other thermoset plastics are: [4, 5]

1. Ease of handling in liquid form
2. Rapid cure and rapid strength gain
3. Excellent abrasion resistance
4. Excellent compressive strength and high impact strength
5. Chemical resistance, corrosion resistance
6. Heat resistance
7. Good general physical properties
8. Ease of coloring and modify for special characteristics



Scheme 2.2 General purpose unsaturated polyester [2]

2.4 Application

The unsaturated polyester resins are used in a variety of applications. They are the most widely used resin type for composites, comprising in excess of 80% of all thermoset resins (others being epoxies, phenolics, acrylics, imides, and urethanes).

They are used in the production of both fiber-reinforced plastics and non-reinforced filled products. Due to the convenience and freeness of application, they are used in various applications and end-markets, e.g. Building & Construction, Automotive and Marine. Typical application technologies and techniques for unsaturated polyester resins as reinforced application are as follows:

1. Hand lay-up and spray-up
2. Filament winding, relining and casting
3. Pultrusion resin transfer molding
4. Vacuum injection techniques
5. Closed mold technology
6. Sheet molding compound (SMC)
7. Bulk molding compound (BMC)

In field of non-reinforced application, unsaturated polyester resins are such as artificial marble or onyx, polymer concrete, and casting.

The polyester resin industry is quite mature and is predominantly characterized by well-known or established products, applications and processes. Over the next 5 years, total UPR consumption across the globe is expected to continue strong growth momentum at 9.7%. The unsaturated polyester resin market is expected to reach US \$ 7.5 billion by 2015. [6]

2.5 Chemistry

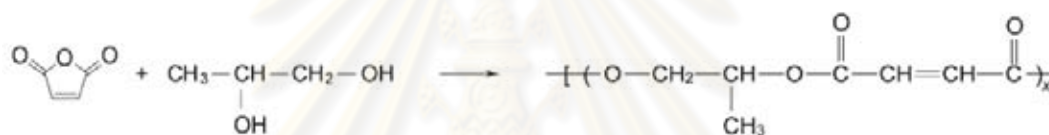
2.5.1 Polyesterification

Unsaturated polyesters are condensation polymers formed by the reaction of polyols and polycarboxylic acids with unsaturated bond contributed in one of the reactants, usually the acid. The polyols and polycarboxylic acids used are usually difunctional alcohols (glycols), and difunctional acids such as maleic. Water is produced as the byproduct of the esterification reaction and is removed from the reaction mass as soon as it is formed to drive the polyesterification reaction to completion. All of the materials used must be at least difunctional to make the polyesterification reaction possible. Monofunctional reactants such as ethyl alcohol and acetic acid can react (esterify) to form an ester but are incapable of forming a polymer (polyester). Two difunctional reactants, such as propylene glycol and maleic

acid or maleic anhydride can esterify in the esterification reaction continuing to form long chain polyester which can contain many repeating units of the basic mer, propylene glycol maleate. [2, 3]

Unsaturated polyesters are differed from saturated polyesters, such as, the polyethylene terephthalate. The acids or glycols in unsaturated polyesters having unsaturated bond included in the formula provide reactive site. This reactive unsaturate polyester can then be used to form thermoset crosslinked polymers with monomers such as styrene and methyl methacrylate which contain double bonds.

The general chemistry of unsaturated polyesters can be illustrated by the following representation of the typical UP synthesis from propylene glycol and maleic anhydride.



Scheme 2.3 Reaction of maleic acid and propylene glycol [2]

2.5.2 Side reaction

Polyesterification is the most important reaction in the preparation of unsaturated polyesters, but during the synthesis, two dominant side reactions also occur. These have been enumerated as isomerization of maleate to fumarate and addition of glycol to double bonds. [2, 3]

2.5.2.1 Isomerization

In the use of unsaturated dicarboxylic as reagents, under the conditions of polyesterification more than 90% of the maleate ester isomerizes from the cis-maleate isomer to the trans-fumarate isomer. The trans isomer has a lower energy level, less strained structure than the cis isomer configuration and the isomerization of maleate to fumarate occurs readily in the processing of most unsaturated polyesters. This is the great commercial importance because maleic anhydride is the inexpensive source for unsaturation in unsaturated polyesters. Fortunately, fumarate unsaturation is much more reactive in crosslinking reactions than maleate unsaturation and is the isomer preferred for practical reactivity levels. Use of secondary glycols such as propylene glycol in the unsaturated polyester cooked will favor a high isomerization of maleate

to fumarate. Isomerization will be less with the use of primary glycols such as ethylene glycol. [7]

V. Szmercsanyi, Marcos, and Zahran investigated the effect of different glycols on the maleate-fumarate isomerization in unsaturated polyesters. Table 2-3 shows the various isomerization incidentals to the use of different glycols they found.

Table 2.3 Isomerization versus glycol type at reaction constant temperature 180 °C [3]

Glycol	Type	Isomerization, %
1,2-Propylene	Secondary	96
Ethylene	Primary	64
Diethylene	Primary	53
1,6-Hexamethylene	Primary	36

The extent of maleate to fumarate isomerization also depends on reaction temperature and time, high temperature and longer time generally favoring greater isomerization. V. Sanercsanyi et. al, in their investigation of the kinetics of maleate% isomerization, measured the percent isomerization in the preparing of poly(propylene glycol maleate) at the temperature ranging from 105° to 180° C. These investigators found a direct dependence of isomerization on reaction temperature as shown in Table 2.4.

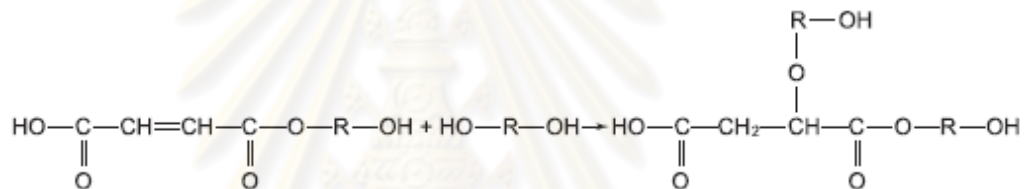
Table 2.4 Isomerization vs. reaction temperature [3]

Reaction Temperature (° C)	Isomerization to Fumarate, %
105	34
125	56
140	75
180	96

It was concluded that the rate of isomerization was mainly a function of the glycol structure and the temperature, with all glycols and temperatures, the isomerization approached a constant value.

2.5.2.2 Addition of glycol to the double bond (Ordelt saturation)

The maleate double bond in unsaturated polyester is highly electron deficient due to the presence of electron-withdrawing carbonyl groups. Addition of glycol across the double bond leads to reduction of unsaturation and branching, which affects to an uncertainty of chain end functionality. This reaction was first studied by Ordelt and co-workers. [3] The Ordelt saturation leads to the formation of branched structure and a change in the functionality of UP resins. UP formulations containing higher concentration of maleic anhydride result in the reduction of 15% unsaturation in the final product while fumaric acid retains a higher degree of unsaturation when substituted in the same formulations. This led the products to have higher reactivity and superior properties.



Scheme 2.4 Ordelt reaction [2]

2.6 Mass transfer with chemical reaction

In the following, the fundamentals of desorption with chemical reaction, which are applied to the problem of H₂O desorption in unsaturated polyester are presented.

2.6.1 Diffusion

Diffusion is mass transfer of a substance from one part of a system to another as a result of random molecular motion or a concentration gradient. Solute will flow from the region of high concentration to low concentration. The molar flux in one direction is directly proportional to the concentration gradient: [8, 9]

$$\dot{n}_A = -D_{AL} \frac{\partial C_A}{\partial x} \quad (2.1)$$

The proportionality constant is the diffusion coefficient D_{AL} , of the solute A in the liquid L. This relation is called Fick's first law. It applies to steady state diffusion only. In many cases the concentration will vary both with time t and distance x . Fick's second law of diffusion can be expressed as:

$$\frac{\partial C_A}{\partial t} = D_{AL} \frac{\partial^2 C_A}{\partial x^2} \quad (2.2)$$

The distance between the molecules in liquid is substantially smaller than in gases and the free mobility of the molecules is strongly reduced by the intermolecular forces. Thus, diffusion in liquids is very much slower than in gases. According to the Stokes-Einstein equation for large, spherical molecules diffusing into a dilute solution the diffusion coefficient D_{AL} depends on the temperature T , the viscosity μ_L of the liquid and the radius r_A of the molecule:

$$D_{AL} = \frac{k_B T}{6\pi r_A \mu_L} \quad (2.3)$$

where k_B is the Boltzmann constant.

Wilke and Chang [10] proposed a correlation for non-electrolytes in an infinitely dilute solution, in essence, it is an empirical correlation of the Stokes-Einstein equation,

$$D_{AL} = \frac{7.4 \times 10^{-8} (\Phi_L M_{wL})^{1/2} T}{\mu_L V_A^{0.6}} \quad (2.4)$$

where D_{AL} is the diffusion coefficient of A in the liquid in cm^2/s ; μ_L is the viscosity of the solution in centipoises; T is the absolute temperature in K; M_{wL} is the molecular weight of the liquid in g/mol; V_A is the molar volume of the solute at its normal boiling point in $\text{cm}^3/(\text{g-mol})$ and Φ_L is the association factor of the liquid.

2.6.2 Mass transfer theories at a gas-liquid interface

Chemical desorption is a complex process involving chemical reaction kinetics, mass transfer processes, phase equilibrium at the liquid-vapor interface as well as fluid dynamics. Several predictions have been performed to describe the behavior of complicated absorption and desorption processes with chemical reactions by using simplified models. The situations are adequate for practical purposes without introducing a large number of parameters. These are the film theory, the boundary layer theory, the penetration and the surface renewal theory.

2.6.2.1 Film Theory

The simplest and oldest model which has been proposed for the description of mass transport processes is called the film theory. [11] The film theory is based on the assumption that when two fluid phases are brought in contact with each other, a thin layer of stagnant fluid exists on each side of the phase boundary. Mass transfer by convection within this layer is assumed to be insignificant and the transport is only achieved by steady state diffusion. Beyond the thin layers the turbulence is sufficient to eliminate concentration gradients. Fig. 2.2 shows the film theory conceptualization for the case of gas absorption in liquid. The interfacial region is idealized as a hypothetical unstirred layer. The constant partial pressure, p_A , implies no resistance to mass transfer in the gas phase.

In the film theory, the mass transfer coefficient, k_L^o is directly proportional to the diffusion coefficient, D_{AL} and inversely proportional to the film thickness δ :

$$k_L^o = \frac{D_{AL}}{\delta} \quad (2.5)$$

Because the dependence of the mass transfer coefficient on the diffusion coefficient this model solution is allowed for the simple film model.

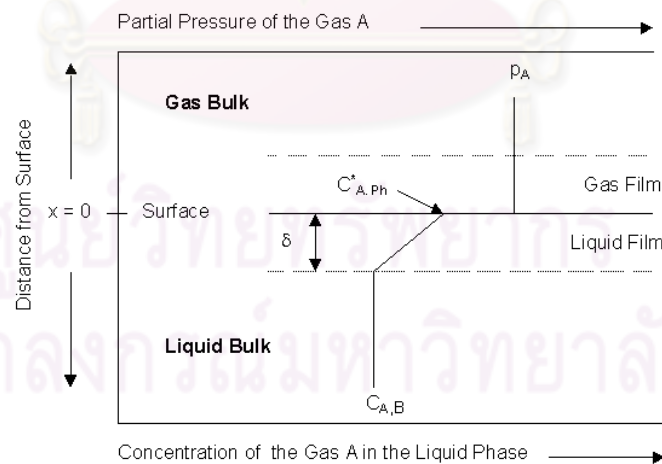


Figure 2.2 Film theory conceptualization [8, 9]

2.6.2.2 Boundary Layer Theory

Boundary layer theory differs from the film theory in that the concentration and velocity can vary in all coordinate axes. [8] However, as the change in the concentration profile is the largest in the x direction, i.e. the coordinate being

perpendicular to the phase interface which simplifies the differential equations for the concentration significantly. For diffusion through a laminar boundary layer, the average mass transfer coefficient can be found from an equation: [9]

$$k_L^o = c \frac{D_{AL}}{L} Re^n Sc^m \quad (2.6)$$

where L is the characteristic length, $Re = \frac{Lu\rho}{\mu}$ and $Sc = \frac{\nu}{D_{AL}}$ is Reynolds number and Schmidt number, respectively. The constants c , n and m depend on the type of flow and the shape of the surface which fluid flows through.

2.6.2.3 Penetration Theory

In 1935, Higbie [12] proposed a model for the gas exchange between a liquid and an adjacent gaseous phase. The gas-liquid interface is made up of a variety of small liquid elements, which are continuously brought up to the surface from the bulk of the liquid by the motion of the liquid phase itself. It means the surface is exposed by the fresh liquid elements for an exposure time. Each liquid element, as long as it stays on the surface, can be considered to be stagnant, and the concentration of the dissolved gas in the element may be considered to be everywhere equal to the bulk liquid concentration when the element reaches the surface. The residence time at the phase interface is the same for all elements. Mass transfer takes place by unsteady molecular diffusion in the various elements of the liquid surface. The mass transfer coefficient, k_L^o in the liquid phase is directly proportional to the square root of the diffusion coefficient, D_{AL} and inversely proportional to the square root of the exposure time, t_e of the element as follows:

$$k_L^o = 2 \sqrt{\frac{D_{AL}}{\pi t_e}} \quad (2.7)$$

The penetration theory represented a first step towards the development of a turbulence hypothesis which proposes that the turbulent movements reach the boundary range near the phase interface.

2.6.2.4 Surface Renewal Theory

In 1951, Danckwerts [13] proposed the surface renewal theory which is an extension of the penetration theory. It is based on the concept that the liquid elements do not stay the same time at the phase interface. He proposed the average exposure

depend on the rate of surface renewal. The mass transfer coefficient resulting from this model is proportional to the square root of D_{AL} and the rate of surface renewal, s as follows

$$k_L^o = \sqrt{D_{AL}s} \quad (2.8)$$

where s has the physical meaning of the rate of surface renewal, and $1/s$ may be regarded as the “average exposure” of surface elements.

In the penetration and surface renewal models, in which the surface film is replaced by bulk liquid after a fixed time interval, although between these periodic replacements molecular diffusion still determined the transfer between the film and the gaseous phase, the overall transfer velocity is a function of the time interval between film renewal events. Since this is shorter than the timescale of diffusion across the full width of the film, the film thickness itself is not a factor.

In many circumstances the difference between predictions made on the basis of the different models will be less than the uncertainties about the values of the physical quantities used in the calculation. The models can thus be regarded as interchangeable for many purposes, and it is then merely a question of convenience which of them is used.

2.6.3 Desorption with chemical reaction

A dissolved gas will be desorbed from a liquid into an adjacent gaseous phase, if the concentration of the gas in the bulk of the liquid is larger than that at the phase interface surface. The gas desorption can be caused by lowering the total pressure or the gas partial pressure or by increasing the temperature. The desorption of dissolved gas from a solution without reaction is called “physical desorption”. When the dissolved gas chemically reacts with other components in the solution, this desorption is called chemical desorption. [14] There are two mechanisms of gas desorption from solution. If the difference between the partial pressure of the gas in equilibrium with the bulk liquid and the partial pressure at the surface, i.e. the degree of saturation, is modest, the gas will be desorbed by diffusion from the liquid free surface in a way analogous to gas absorption. However, if the degree of saturation is large, bubbles will form in the interior of the liquid and much of the gas will be released. The growth

of gas bubbles can partially increase of turbulence and destruction of the boundary layer, in this way intensifies the mass transfer.

It can be assumed that in the reactor water is released by quiescent desorption because the partial pressure of water in equilibrium with the bulk liquid does not exceed the total pressure in the reactor.

The phenomenon of desorption with chemical reaction is made up of a number of elementary steps:

1. Chemical reaction of the dissolved gas within the liquid phase.
2. Mass transport of the dissolved gas from the bulk of the liquid to the phase interface.
3. Transport of the gas through the phase interface.
4. Mass transport of the gas from the phase interface to the bulk of the gas phase.

Steps (1) and (2) may take place simultaneously, and thus mutually interfere. The overall phenomenon resulting from steps (1) and (2) takes place in series with steps (3) and (4).

Chemical reactions affect the concentration of the dissolved gas in the bulk of the liquid. During desorption the chemical reactions continuously produce the component to be desorbed, thus providing a certain concentration of it in the bulk of the liquid, hence, a certain driving force for the mass transfer. In the absence of chemical reactions, the physical molar desorption flux of the dissolved gas species i is given by:

$$\dot{N}_{oi} = k_{Li}^o (C_{Li} - C_{Phi}) \quad (2.9)$$

where k_{Li}^o is the physical mass transfer coefficient in the liquid phase without chemical reactions, C_L is the concentration of the dissolved gas in the bulk of the liquid and C_{Ph} is the concentration at the phase interface.

The actual desorption flux in the presence of reaction should be larger than the value given by equation (2.9). The mass transfer coefficient, k_L can be defined and the chemical molar desorption flux can be written as:

$$\dot{N}_i = k_{Li} (C_{Li} - C_{Phi}) \quad (2.10)$$

The rate enhancement factor, E is defined as the ratio of the chemical desorption flux to the physical desorption flux:

$$E = \frac{\dot{N}_i}{k_{Li}^o(C_{Li} - C_{Phi})} = \frac{k_{Li}}{k_{Li}^o} \quad (2.11)$$

The resistance to desorption at the phase interface is usually negligible and physical equilibrium may be assumed to prevail. [15] The vapor liquid equilibrium ratio was applied:

$$K_{VLi} = \frac{C_{Gi}^*}{C_{Li}^*} \quad (2.12)$$

where * refer to equilibrium state. The desorption flux of interested specie i in both liquid and gas phase was given by

$$\begin{aligned} \dot{N}_i &= k_{Li}^o E (C_{Li} - C_{Phi}) \\ &= k_{Gi} (C_{Phi} K_{VLi} - C_{Gi}) \end{aligned} \quad (2.13)$$

where k_G is the mass transfer coefficient in the gas phase. The liquid phase and the gas phase mass transfer coefficients can be combined to define the overall mass transfer coefficient K_L by:

$$\dot{N}_i = K_{Li} (C_{Li} - \frac{C_{Gi}}{K_{VLi}}) \quad (2.14)$$

The total resistance to transport can be expressed as illustrated in Figure 2.3:

$$\frac{1}{K_{Li}} = \frac{1}{k_{Li}^o E} + \frac{1}{k_{Gi} K_{VLi}} \quad (2.15)$$

The liquid mass transfer coefficient k_{Li}^o is usually ranges between 10^{-5} and 10^{-3} m/s.

The gas mass transfer coefficient, k_G usually ranges from 10^{-3} to 1 m/s.

Equations (2.15), for gases that are highly soluble (low K_{VL}) or react rapidly (high E), the gas phase resistance apparently controls the transport. For gases that are less soluble (high K_{VL}) and do not react at all or only react slowly ($E \approx 1$) the liquid phase resistance predominates and controls the total resistance.

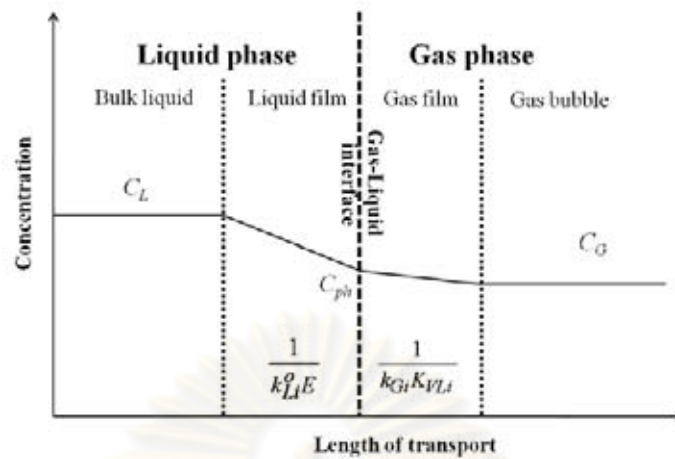


Figure 2.3 Desorption conceptualization

2.7 Kolmogoroff's theory for turbulent flow

Kolmogoroff's theory describes how energy is transferred from larger to smaller eddies, how much energy is contained by eddies of a given size, and how much energy is dissipated by eddies of each size. [16]

An eddy precludes precise definition, but it is conceived to be a turbulent motion, localized over a region of size l , which is at least moderately coherent over this region. Consider fully turbulent bulk flow at high Reynolds number.

$$Re = UL / \nu \quad (2.16)$$

Turbulence can be considered to consist of eddies of different sizes. The region occupied by a larger eddy can also contain smaller eddies. Eddies sized l have characteristics velocity $u(l)$ and timescale $t(l) = l / u(l)$.

Suppose that eddies in the large size range are characterized by the length scale, l_o which is comparable to the flow length scale, L . Their characteristic velocity $u_o \equiv u(l_o)$ which is comparable to U is on the order of the root mean square turbulence intensity:

$$u(l_o) = u' = \left(2 \frac{E_k}{3}\right)^{1/2} \quad (2.18)$$

here the turbulent kinetic energy is defined.

$$E_k = \frac{1}{2}(u'u') = \frac{1}{2}(\overline{u_x^2} + \overline{u_y^2} + \overline{u_z^2}) \quad (2.19)$$

we can now derive the following equation for this length scale:

$$l_o = \frac{E_k^{3/2}}{\varepsilon} \quad (2.20)$$

where ε is the energy dissipation rate (m^2/s^3).

This length scale is usually referred to as the integral scale of turbulence. The Reynolds number associated with these large eddies is referred to as the turbulence Reynolds number Re_L , which is defined as:

$$Re_L = \frac{E_k^{1/2} l_o}{\nu} = \frac{E_k^2}{\varepsilon \nu} \quad (2.21)$$

The large eddies are unstable and can be broken up, transferring their energy to somewhat smaller eddies. These smaller eddies undergo a similar break-up process and transfer their energy to smaller eddies. This energy cascade continues transferring successively to smaller and smaller eddies until the Reynolds number is sufficiently small that the eddy motion is stable and molecular viscosity is effective in dissipating the kinetic energy. At these small scales, the kinetic energy of turbulence is converted into heat. [16]

The large eddies have order of energy u_o^2 and timescale $\tau_o = l_o / u_o$ so the transfer of energy can be expressed as:

$$\varepsilon = u_o^2 / \tau_o = u_o^3 / l_o \quad (2.22)$$

Consequently, at high Reynolds numbers the energy cascade indicates that ε is proportional to u_o^3 / l_o and independent of ν .

Kolmogoroff's theory has hypothesis for homogenous turbulence, the turbulent kinetic energy, E_k is the same everywhere. For isotropic turbulence, the eddies behave the same kinetic energy in all directions:

$$\overline{u_x^2} = \overline{u_y^2} = \overline{u_z^2} \quad (2.23)$$

Kolmogoroff argued that the directional biases of the large scales are lost in the chaotic scale-reduction process as energy is transferred to successively smaller eddies. Hence Kolmogoroff's hypothesis of local isotropy states that at sufficiently high Reynolds numbers, the small-scale turbulent motions are statistically isotropic. The term local isotropy means isotropy at small scales. Large scale turbulence may still be anisotropic.

Kolmogoroff also argued that not only the directional information get lost as the energy passes down the cascade, but also all information about the geometry of the eddies gets lost. As a result, the statistics of the small-scale motions are universal. They are similar in every high Reynolds number turbulent flow, independent of the mean flow field and the boundary conditions. These small scale eddies depend on the rate of received energy from the larger scales which is approximately equal to the dissipation rate, ε and the viscous dissipation, which is related to the kinematic viscosity.

Given the two parameters ε and ν we can form the following unique length, velocity, and time scales.

$$\text{length scale: } \eta = (\nu^3 / \varepsilon)^{1/4} \quad (2.24)$$

$$\text{velocity scale: } u_\eta = (\varepsilon \nu)^{1/4} \quad (2.25)$$

$$\text{time scale: } \tau_\eta = (\nu / \varepsilon)^{1/2} \quad (2.26)$$

$$Re_\eta = \frac{\eta u_\eta}{\nu} \quad (2.27)$$

The cascade proceeds to smaller and smaller scales until the Reynolds number is small enough for energy dissipation to be effective. These scales are indicative of the smallest eddies present in the flow.

2.8 Literature Review

Paatero et al. [17] proposed a rate model base on a reaction mechanism for the melt polyesterification of dicarboxylic acids with diols for the case that no catalyst was used. The model included the esterification, the cis-trans isomerization and the double saturation reaction. All three reactions were the acid catalyzed. The overall reaction order of the main reaction increased with conversion progress due to a shift of the ionic equilibria in the liquid phase. This increase of the reaction order was described by a semi-empirical function. The experiments were carried out by the esterification of maleic acid with propylene glycol in the range of 160° to 220 °C in a laboratory scale reactor. The derived rate model successfully described the isomerization of maleic acid to fumaric acid, the saturation of the double bonds and the polyesterification of maleic and fumaric acids.

Salmi et al. [18] studied the kinetic of melt polymerization of maleic anhydride and phthalic anhydride with propylene glycol in a laboratory scale batch reactor operating at 160-220 °C and at atmospheric pressure. Maleic anhydride and phthalic anhydride were suitable model molecules for the polyesterification study, since in the polymerization of phthalic anhydride only the esterification reaction took place. However, in the polymerization of maleic anhydride the double bond isomerized and became partially saturated by the alcohol. A kinetic model was developed including the polyesterification, isomerization and double saturation during the polymerization. The kinetic model was based on the principle of equal reactivity of the functional groups. The rate equations were coupled to the reactor mass balances, in which the change of the reaction mass due to water evaporation was included. The rate parameters for esterification, isomerization and double saturation were estimated from the experimental data by using non-linear regression analysis.

Lehtonen et al. [19] developed a generally applicable model for the kinetic analysis of the reaction network in the polyesterification of unsaturated dicarboxylic acids with diols in the presence of homogeneous acid catalyst. The network consisted of the esterification reaction as well as the side reactions, i.e. the cis-trans isomerization and double bond saturation reactions. Rate equations based on plausible reaction mechanisms were derived and the parameters of the rate equations were determined by non-linear regression analysis using the polyesterification of maleic acid with propylene glycol at 140-190 °C as a demonstration system. Comparisons of the model predictions with the experimental data showed the approach provides a reasonable description of the polyesterification network.

Salmi et al. [20] developed a systematic stoichiometry and kinetic model for the acid-catalyzed polyesterification of unsaturated dicarboxylic acids and mixtures of dicarboxylic acids. The model was based on a rigorous treatment of the functional groups and their reactions: esterification, cis-trans isomerization and double-bond saturation through Ordel reaction. The model was applied on the polyesterification of maleic and phthalic acids with ethylene glycol, propylene glycol, diethylene glycol and dipropylene glycol in a semi-batch reactor at 160-195 °C. Kinetic and thermodynamic parameters included in the model were estimated with non-linear regression. It was found that the important simplifications can be introduced. The rate

constants of the different esterification and isomerization reactions can be set equal, whereas the rate constants of the different double-bond saturation reactions were treated by individual rate constants. A comparison of model predictions with experimental data revealed that the proposed kinetic treatment was relevant for polyesterification of complex mixture.

Nalampang et al. [21] studied the kinetics of the individual key reactions by involving in the formation of unsaturated polyester resins using the reactive glycol, 2-methyl-1,3-propanediol (MPD). This diol reacted in turn with maleic anhydride (MA), phthalic anhydride (PA) and isophthalic acid (IA) under the isothermal condition in the temperature range of 180–210 °C and the kinetic constants of the following reactions were obtained: MA+MPD, PA+MPD, IA+MPD, MA+PA+MPD and MA+IA+MPD. The relative reactivity of MPD with MA and PA measured by monitoring the loss of carboxyl groups at 180 and 200 °C were found to be 2.26 and 1.70, respectively. At 200 °C, PA was more reactive than IA in homopolyesterification. The differences in reactivity might be expected to have a significant effect on the coreactant sequence lengths in polymers formed by PA, IA and MPD. Thus the final properties of the cured resins were different.

Zetterlund et al. [22] modified the kinetic model for the formation of unsaturated polyester resins by reaction between diols and anhydrides to take into account the difference in reactivity between the two hydroxyl groups of 1,2-propylene glycol in polyesterification and the changes in the concentrations caused by glycol and water removal through distillation during batch polymerization at elevated temperature. The aim was to estimate the relative difference in reactivity between maleic and phthalic anhydride and to obtain the necessary data for use in computer modeling and simulation. It has been found that the relative reactivity of maleic and phthalic anhydride toward 1,2-propylene glycol after completing the ring opening step of both anhydrides were increased from approximately 1.7 to 2.3 as the temperature was increased from 160 to 220°C. The polymerization rate appeared to be an anti-synergistic effect in this copolyesterification, i.e., the total rate of reaction of carboxyl groups was lower than the summation of the rates of reaction of the individual acids with the same concentration and at the same temperature. Simulated results were in good agreement with experimental finding.

Korbar et al. [23] studied the progress of the synthesis of unsaturated polyester based on anhydrides of phthalic and maleic acid and propylene glycol without catalysts. The reaction was carried out both at the laboratory and industrial scales. The acid number and molecular weight distribution were also determined. In the laboratory synthesis, the amount of water produced during the reaction was measured. Two steps in the reaction were observed. The first reaction was the reaction of anhydrides with glycol producing monoester and then the second step was the step-growth polymerization reaction producing polymer. The kinetic of step-growth polymerization reaction was found to be third order with an activation energy $E_a = 54.3 \text{ kJ mol}^{-1}$ and $k_o = 15.2 \text{ kg}^2\text{mol}^{-2}\text{s}^{-1}$. The kinetic model was prepared and compared with the results obtained from reaction carried out on an industrial scale. A method was presented for determining a heating program based on a limited reaction rate and a maximal reaction temperature for a particular system. The molecular weight distribution of polyester resin was determined and the disagreement was found compared to the most probable molecular weight distribution.

Salmi et al. [24] continuously developed the kinetic model. A simple two parameters model was proposed for the kinetic of polyesterification reaction. The kinetic model was based on the true reaction mechanism, i.e., the shift of the ionic equilibria in the carboxylic acid protolysis during the reaction and the bimolecular nucleophilic substitution of the protolysed acid with the alcohol. The model described the increase of the reaction order with respect to the carboxylic acid from 1 to 2 as the esterification proceeds. The rate equation $r = kC_{COOH}^n C_{OH}$ was used, where n is a function of the carboxylic acid concentration. The kinetic model was tested with the classical data of Flory obtained for diethylene glycol–adipic acid and the lauryl alcohol–adipic acid reactions. The model provided an excellent description data over the entire range of conversions of the carboxylic acids and it can be extended to new polyesterification systems.

Dairanieh et al. [25] prepared the laboratory procedure of a recently developed unsaturated polyester resin and followed by the preparation of the resin on a large scale (10-200 liters pilot plant reactors). The process heating rate, reaction temperature, and agitator tip speed were kept constant on scale-up. The resin was successfully reproduced and its properties were unchanged upon scale-up. The effects

of reaction temperature and inert gas flow rate on the polyesterification reaction rate were investigated. It was found that a 10°C increase in temperature or a 50% increase in the gas flow rate results in a 50% increase in the reaction rate.

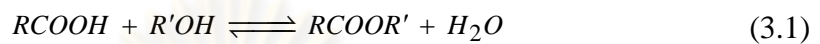
Boodhoo et al. [26] described the performance of a thin film reactor in the form of a spinning disc reactor which may be used for continuous condensable polymerization of esters. Test results suggested that it might be possible to significantly enhance the rate of polymerization by addressing the mass transfer and mixing limitations thereby performing the reaction at its inherently faster kinetic speed. This technology may provide an opportunity for the intensification of condensation polymerization processes.

Lehtonen et al. [27] proposed a dynamic model for a system containing a semi-batch wise operating reaction vessel connected to a distillation unit. The approach consisted of kinetic equations for the reactions as well as a dynamic model for the distillation unit. As an example reaction, the catalyzed polyesterification of maleic acid with propylene glycol was used. The kinetic and the mass transfer parameters at 170°C were estimated from experimental data. The fit of the model to the data indicated that the approach was suitable for the description of semibatch liquid phase reaction-separation systems.

CHAPTER III

MODEL DEVELOPMENT

The esterification between diacids and diols is a reversible reaction as presented in equation (3.1). The equilibrium constant (K) is shown in equation (3.2).



$$K = \frac{[RCOOR'][H_2O]}{[RCOOH][R'OH]} \quad (3.2)$$

According to equation (3.1), it is found that water is obtained as a byproduct. Therefore, the removal of water from the reaction system can drive towards more completion of polyester. However, the high viscosity resulting from the melt polymer during the esterification makes the removal more difficult. [28] Thus, the rate of esterification is limited by the mass transfer process. Technological advance in the production has mainly concentrated on removing water from the melt polymer to increase polymerization rate and reduce reaction time. In industrial, the production usually takes place in a batch reactor. During the entire batch, the inert gas, such as, nitrogen is fed into the reactor to minimize oxidative degradation and act as a carrier gas to bring the water out of the reactor.

The higher gas-liquid mass transfer area will increase amount of water transfer out. Enhancement of mass transfer area in the reaction can be done by bubbling the inert gas pass through the sparger below the surface of the melt polymer. [3] As much as mass transfer increase, a volumetric mass transfer coefficient should be increased too. Thus, the water removal rate will be increased and the reaction time should be decreased.

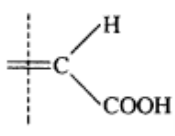
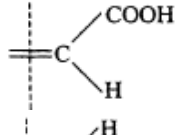
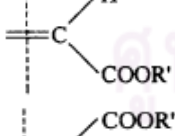
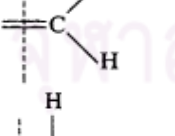
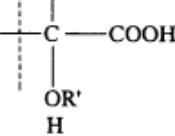
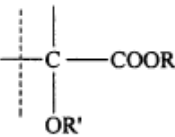
In the previous work, the model which simulated this reaction system used constant value of volumetric mass transfer coefficient. In fact, this value should be varied with time as the reaction proceeds because of higher viscosity from longer chain of polymer. In this research, the polymerization between MA and PG is prepared as a model reaction. The volumetric mass transfer coefficient was calculated as a function of polymer properties which changed with time. Then, inserted this

estimated value in the developed dynamic model to investigate the effect of inert gas feed rate and temperature on polyesterification.

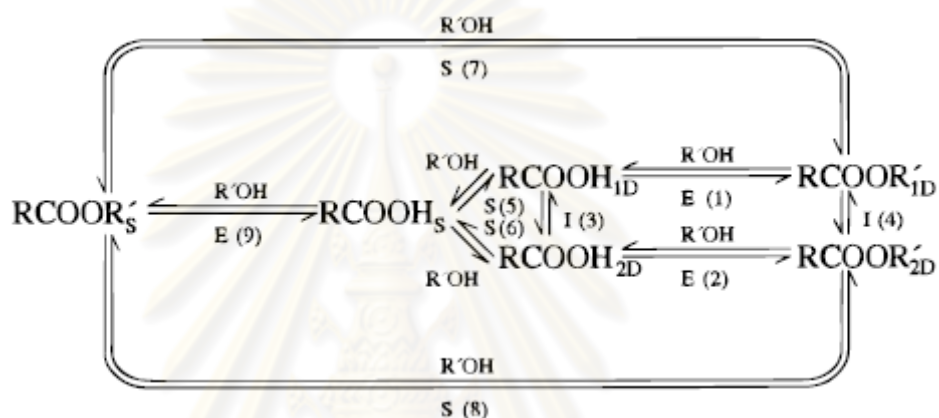
3.1 Kinetic model

Both MA and PG have two reactive groups in molecules. To obtain the correct stoichiometry we must define new functional groups. For example, the functional group of a dicarboxylic group was defined to have only one carbonyl group and a half of the double bond. [23] Other function groups and its abbreviation are listed in Table 3.1.

Table 3.1 Functional group in polyesterification of MA and PG

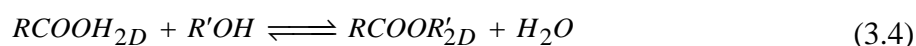
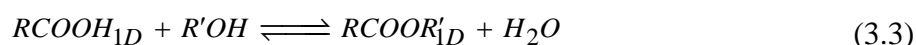
Functional groups		Abbreviations	
Formula	Name	Reaction scheme	Model
---OH	hydroxyl group	$R'OH$	OH
	cis-acid	$RCOOH_{1D}$	$COOH_{1D}$
	trans-acid	$RCOOH_{2D}$	$COOH_{2D}$
	cis-ester	$RCOOR_{1D}$	$COOR_{1D}$
	trans-ester	$RCOOR_{2D}$	$COOR_{2D}$
	saturated acid	$RCOOH_S$	$COOH_S$
	saturated ester	$RCOOR_S$	$COOR_S$

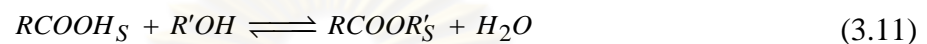
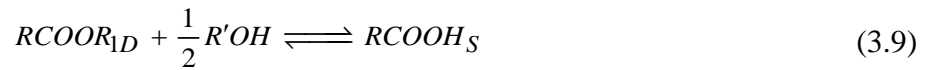
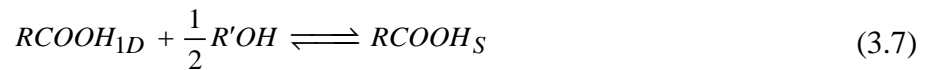
The presence of unsaturated carboxylic acids in polymerization reaction makes the whole systems essentially complicate as presented by Flory [27]. The double bonds can be saturated by reacting with the hydroxyl group from diols also known as the Ordelt reaction. This reaction has an important impact on polyesterification process, excess of diols need to be used because of diols consumption in this side reaction. Furthermore, the double bond of the acid undergoes the cis-trans isomerization. [18]



Scheme 3.1 Reaction for the polyesterification of MA with PG: (E) esterification, (I) isomerization and (S) double bond saturation [29]

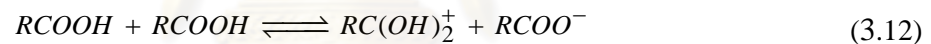
During esterification, three types of carboxylic groups are participated, i.e. the carboxylic group of maleic, fumaric and substituted butanedioic acid. [29] The fumaric acid group is found via the isomerization of maleic acid group, and the saturated butanedioic acid group is generated through the double bond saturation reaction. These reactions are illustrated in Scheme 3.1. Reactions path 1, 2 and 9 are esterification reactions, 3 and 4 represent cis-trans isomerizations, and 5-8 are double bond saturation reactions. These reactions could be summarized as follow:



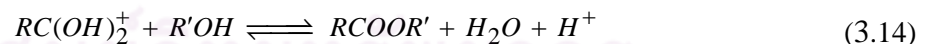


It should be noticed that the stoichiometric coefficient $\frac{1}{2}$ was included in equation (3.7) - (3.10) because the double bonds in Table 3.1 were defined as only a half of the actual double bond.

All three reaction types are acid catalyzed. When acid catalyst is absent, the carboxylic itself acts as catalyst agent via autoprotolysis. The following protolysis equilibria were considered:



The separated ions dominated at the beginning and the ion pair dominated at the end of reaction. Both types of ion reacted with $R'OH$ via esterification as follow: [27]



Steps (3.12) and (3.13) were assumed to be rapidly occur while step (3.14) and (3.15) were rate determining. The concentrations of cation and anion formed in equation (3.12) were assumed to be equal. Applied quasi-equilibrium to the rapid step:

$$C_{RC(OH)_2^+} = K_{12}^{1/2} C_{RCOOH} \quad (3.16)$$

$$C_{RC(OH)_2^+ RCOO^-} = K_{13} C_{RCOOH}^2 \quad (3.17)$$

Thus the rate equations for reaction (3.14) and (3.15) can be obtained:

$$r_{14} = k_{14}K_{12}^{1/2}C_{RCOOH}C_{R'OH} - k_{-14}C_{RCOOR'}C_{H_2O}C_{H^+} \quad (3.18)$$

$$r_{15} = k_{15}K_{13}C_{RCOOH}^2C_{R'OH} - k_{-15}C_{RCOOR'}C_{RCOOH}C_{H_2O} \quad (3.19)$$

Combined equation (3.18) and (3.19) together, we have:

$$r_{14} + r_{15} = (k_{14}K_{12}^{1/2} + k_{15}K_{13}C_{RCOOH})C_{RCOOH}C_{R'OH} - (k_{-14}C_{H^+} + k_{-15}C_{RCOOH})C_{RCOOR'}C_{H_2O} \quad (3.20)$$

Combination of $r_{14} + r_{15}$ was esterification rate and can be written down as follow:

$$r_E = (k_{14}K_{12}^{1/2} + k_{15}K_{13}C_{RCOOH})(C_{RCOOH_{1D}}C_{R'OH} - \frac{C_{RCOOR'_{1D}}C_{H_2O}}{K_E}) \quad (3.21)$$

where

$$K_E = \frac{(k_{14}K_{12}^{1/2} + k_{15}K_{13}C_{RCOOH})}{(k_{-14}C_{H^+} + k_{-15}C_{RCOOH})} = \frac{k_E}{k_{-E}} \quad (3.22)$$

From equation (3.21), at the beginning the term $k_{14}K_{12}^{1/2}$ dominates, and at higher conversion the carboxylic acid term $k_{15}K_{13}C_{RCOOH}$ dominates. This can explain the shift of reaction order as the reaction proceeds. [29] By applying above analogy to the nine reversible reactions, the rate equations of each reaction paths 1-9 could be generated as follows:

$$r_1 = k_1(C_{RCOOH_{1D}}C_{R'OH} - \frac{C_{RCOOR'_{1D}}C_{H_2O}}{K_1}) \quad (3.23)$$

$$r_2 = k_2(C_{RCOOH_{2D}}C_{R'OH} - \frac{C_{RCOOR'_{2D}}C_{H_2O}}{K_2}) \quad (3.24)$$

$$r_3 = k_3(C_{RCOOH_{1D}} - \frac{C_{RCOOH_{2D}}}{K_3}) \quad (3.25)$$

$$r_4 = k_4(C_{RCOOR'_{1D}} - \frac{C_{RCOOR'_{2D}}}{K_4}) \quad (3.26)$$

$$r_5 = k_5(C_{RCOOH_{1D}}C_{R'OH} - \frac{C_{RCOOH_s}}{K_5}) \quad (3.27)$$

$$r_6 = k_6(C_{RCOOH_{2D}}C_{R'OH} - \frac{C_{RCOOH_s}}{K_6}) \quad (3.28)$$

$$r_7 = k_7(C_{RCOOR'_{1D}}C_{R'OH} - \frac{C_{RCOOR'_s}}{K_7}) \quad (3.29)$$

$$r_8 = k_8 \left(C_{RCOOR'_{2D}} C_{R'OH} - \frac{C_{RCOOR'_S}}{K_8} \right) \quad (3.30)$$

$$r_9 = k_9 \left(C_{RCOOH_S} C_{R'OH} - \frac{C_{RCOOR'_S} C_{H_2O}}{K_9} \right) \quad (3.31)$$

Symbols in equations are explained in Notation. From the reaction stoichiometry and the rate equations (3.32)-(3.31) the generation rates of each species are obtained as follows:

$$r_{COOH_{1D}} = -r_1 - r_3 - r_5 \quad (3.32)$$

$$r_{COOH_{2D}} = -r_2 + r_3 - r_6 \quad (3.33)$$

$$r_{COOH_S} = -r_9 - r_5 - r_6 \quad (3.34)$$

$$r_{COOR'_{1D}} = r_1 - r_4 - r_7 \quad (3.35)$$

$$r_{COOR'_{2D}} = r_2 + r_4 - r_8 \quad (3.36)$$

$$r_{COOR'_S} = r_7 + r_8 + r_9 \quad (3.37)$$

$$r_{R'OH} = -(r_1 + r_2 + r_9) - \frac{1}{2}(r_5 + r_6 + r_7 + r_8) \quad (3.38)$$

$$r_{H_2O} = \frac{1}{2}(r_1 + r_2 + r_9) \quad (3.39)$$

We presumed that all esterification constants were equal, all isomerization constants were equal and all double bond saturation constants were equal, too. [18, 24] Hence we have:

$$k_E = k_1 = k_2 = k_9$$

$$K_E = K_1 = K_2 = K_9$$

$$k_I = k_3 = k_4$$

$$K_I = K_3 = K_4$$

$$k_D = k_5 = k_6 = k_7 = k_8$$

$$K_D = K_5 = K_6 = K_7 = K_8$$

3.2 Resistance of water desorption in polymerization

Water removal from bulk polyester is a desorption process. Generally, polyesterification affects the concentration of the dissolved gas in the bulk of the liquid. During desorption process the polyesterification continuously produces the

water, desorbed species. According to equation (2.15), assumption for water that it was less soluble in polyester (high K_{VL}), low resistant of mass transfer in the gas phase (high k_G) and the rate of polymerization was slow ($E \approx 1$), thus, the liquid-phase resistance should predominate and control the total resistance. Equation (2.15) can be transform in the form of molar flow:

$$\dot{N}_i = k_{Li} \left(C_{Li} - \frac{C_{Gi}}{K_{VLi}} \right) \quad (2.15)$$

$$\dot{n}_i = k_{Li} A \left(C_{Li} - \frac{C_{Gi}}{K_{VLi}} \right) \quad (3.40)$$

where A is total mass transfer area which could be replaced by the term specific interfacial area (a), mass transfer area per unit volume of liquid phase.

$$\dot{n}_i = k_{Li} a V_{total,L} \left(C_{Li} - \frac{C_{Gi}}{K_{VLi}} \right) \quad (3.41)$$

The term $k_{Li}a$ in equation (3.41) is known as the volumetric mass transfer coefficient.

3.3 Volumetric mass transfer coefficient

A fundamental approach was applied to estimate volumetric mass transfer coefficient, $k_{Li}a$ in stirred tank reactors. In a first step, it was necessary to separate $k_{Li}a$ into two parameters, k_{Li} and a . The mass transfer coefficient, k_{Li} was estimated by the Higbie's penetration theory, the description of the rate of mass transfer process in the continuous phase around the bubbles. The specific interfacial area, a was estimated from gas hold-up and mean bubble size. [30]

3.3.1 Mass transfer coefficient, k_L

The model was developed based on high turbulent regime then the penetration theory was adapted. This theory is widely accepted for gas-liquid transfer description. By following this theory, when a gas bubble moves through a liquid, it continually creates new interfacial area. Each liquid element, as long as it stays on the surface, may be considered to be stagnant and mass transfer takes place by unsteady molecular diffusion in the various elements of the liquid surface. During a contact or exposure time, the mass transfer coefficient can be calculated from equation (2.7)

$$k_L = \frac{2}{\sqrt{\pi t_e}} \sqrt{D_L} \quad (2.7)$$

Consequently, the experimental results showed that the exposure time is necessarily affected by eddies or turbulence at a microscopic scale. [31, 32] Therefore, the rate of energy dissipation in the liquid per unit mass, ε , is the most adequate magnitude to characterize this time scale. The exposure time that characterizes the residence time of micro-eddies at the interface is generally unknown, but it can be estimated by Kolmogoroff's theory of isotropic turbulence. At high turbulent regime, we can presume here that a small liquid element in penetration theory is approach to the Kolmogoroff length scale. Thus, the exposure time in penetration theory can replace by the Kolmogoroff time scale. Considered the eddy of length scale, η that had velocity scale, u_η both parameters depended on the rate of energy dissipation per liquid unit mass and the kinematic viscosity as written down in equations (2.24) – (2.26):

$$\eta = (\nu^3 / \varepsilon)^{1/4} \quad (2.24)$$

$$u_\eta = (\varepsilon \nu)^{1/4} = (\varepsilon \eta)^{1/3} \quad (2.25)$$

$$t_e = \tau_\eta = (\nu / \varepsilon)^{1/2} = (\mu / \rho \varepsilon)^{1/2} \quad (2.26)$$

This exposure time value has been previously used in some works for the prediction of volumetric mass transfer coefficient.

Unsaturated polyester resins are normally Newtonian fluid. [33] By assuming Newtonian media, k_L could be estimated from equations (2.7) and (2.26):

$$k_L = \frac{2}{\sqrt{\pi}} \sqrt{D_L} \left(\frac{\varepsilon \rho}{\mu} \right)^{1/4} \quad (3.42)$$

A correlation of D_L for non-electrolytes in an infinitely dilute solution can be estimated by equation (2.4).

3.3.2 Specific interfacial area, a

Assuming spherical bubbles, the specific interfacial area can be calculated from the values of the gas hold-up and average bubble size by the following equation: [30]

$$a = \frac{6 \times (\text{gas hold-up})}{\text{bubble diameter}} = \frac{6\phi}{d_b} \quad (3.43)$$

The specific interfacial area is a strong function of the geometrical design and the hydrodynamics into the reactor. This area can be increased by creating smaller bubbles or increasing the number of bubbles. For a given volume of gas, a greater interfacial area is provided if the gas is dispersed into many small bubbles rather than a few large ones.

Gas hold-up, ϕ , is one of the most important parameters defining the hydrodynamics of bubble columns. It can be defined as the percentage by volume of the gas in the two or three phase mixture in the reactor, on one hand it defines the gas-phase residence time. Gas hold-up can be estimated by the equation derived by using the isotropic turbulence theory as follows:

$$\frac{\phi}{1-\phi} = 0.5 \frac{V_s^{2/3}}{(gl)^{1/3}} \left(\frac{\rho_L}{\rho_L - \rho_G} \right) \quad (3.44)$$

In this equation, l is the Kolmogoroff length scale and assuming that the size of the bubbles formed in the turbulent regime is affected by the stirrer speed. For a range of Reynolds number $10^3 \leq Re \leq 2 \times 10^5$ the following equation for l has been proposed: [34]

$$l = 2 \left(\frac{\sigma}{0.4\rho_L} \right)^{3/5} \left(\frac{(h/6)^{2/5}}{(\pi TN)^{6/5}} \right) \left(\frac{\rho_L}{\rho_G} \right)^{0.1} \quad (3.45)$$

Combining equation (3.45) and (3.46) together, the following equation can be derived:

$$\frac{\phi}{1-\phi} = 0.819 \frac{V_s^{2/3} N^{2/5} T^{4/15}}{g^{1/3}} \left(\frac{\rho_L}{\sigma} \right)^{1/5} \left(\frac{\rho_L}{\rho_L - \rho_G} \right) \left(\frac{\rho_L}{\rho_G} \right)^{-1/15} \quad (3.46)$$

When the liquid phase is viscous, the above equation needs to be modified to take the viscous forces which neglected in the previous analysis into account. The following equation can then be used: [35]

$$\left(\frac{\phi_v}{1-\phi_v} \right) = \frac{\phi}{1-\phi} \left(\frac{\mu_L}{\mu_G} \right)^{-1/4} \quad (3.47)$$

From Kolmogoroff's theory, the velocity scale can write down in term of the length scale and the energy dissipation, equation (2.25). For microscopic scale, we could assume the length scale had the same order of magnitude as the bubble

diameter. The dynamic pressure force can be expressed in terms of the velocity and bubble diameter.

$$u = (\varepsilon d_b)^{1/3} \quad (3.48)$$

$$\tau \cong \rho_L u^2 \cong \rho_L \left[\left(\frac{P}{V} \right) \frac{d_b}{\rho_L} \right]^{2/3} \quad (3.49)$$

Equilibrium bubble diameter can be obtained by a balance between the dynamic pressure force exerted on the bubble by the turbulent liquid flow and the surface tension.

The ratio between these two forces is the Weber dimensionless number which could be assumed to have a constant value, according to:

$$W_e = \frac{\tau \cdot d_b}{\sigma} = \text{constant} \quad (3.50)$$

From equations (3.49) and (3.50) the following correlation was derived.

$$d_b \propto \frac{\sigma^{3/5}}{(P/V) \rho_L^{1/5}} \quad (3.51)$$

Many equations have been proposed from this assumption. In this work, we used the following equation for an average bubble size which was proposed by Bhavaraju et al: [36]

$$d_b = 0.7 \frac{\sigma^{0.6}}{(P/V)^{0.4} \rho_L^{0.2}} \left(\frac{\mu_L}{\mu_G} \right)^{0.1} \quad (3.52)$$

3.3.3 Power requirement

The stirrer speed and the mixing intensity play a major role in breaking up of bubbles. The impeller Reynolds number was estimated by the following equation:

$$Re_i = \frac{T^2 N \rho_L}{\mu_L} \quad (3.53)$$

In stirred reactor, the power number could be considered constant in the turbulent regime. This value depended on the impeller type and geometry. For disk flat-blade turbines at a value of impeller Reynolds number higher than 10^4 , power number is constant at 5. [37]

$$N_p = 5 \quad (\text{at } Re \geq 10^4) \quad (3.54)$$

The power consumption in un-aerated system calculated by:

$$P_o = N_p \rho_L N^3 T \quad (3.55)$$

In aerated systems, the presence of gas has an effect on power consumption. The sparged gas bubbles reduce density and decrease power consumption. Thus, the power consumption in the aerated systems, P , is always lower than in the un-aerated system. The dimensional analysis shows that the power deliver to an incompressible fluid by a rotating impeller in stirred tanks is proportional to the agitation rate raise to the third power and the impeller diameter raise to the fifth power. For Newtonian fluids, a good estimated of P could obtain using the following relationship: [38]

$$P = \alpha \left(\frac{P_o^2 N T^3}{Q^{0.56}} \right)^\beta \quad (3.56)$$

where the constants α and β depend on the stirrer type and the configuration of the system agitation. From the experimental data in a wide range of operational conditions for a simple impeller disk flat-blade turbines, α and β were 0.783 and 0.459, respectively. While for dual impeller system the values were 1.224 and 0.432, respectively. [39]

In order to determine k_L , the local energy dissipation rate near the interface needed to be estimated. Assuming that energy at the gas-liquid interface was consumed in the contact between liquid elements and gas bubbles. The average energy dissipation rate per mass unit in stirred tanks is approximately:

$$\mathcal{E} \approx \mathcal{E}_{avg} = \frac{P}{\left(\frac{\pi T^2}{4} \right) H \rho} \quad (3.57)$$

Combining equations (3.42), (3.43), (3.47), (3.52), and (3.57) together could obtain $k_L a$.

3.3.4 Physical properties estimation

During polyesterification process the carboxyl and hydroxyl group were reduced. The acid number (AN) and hydroxyl number (HN) were estimated from the remaining of both groups per gram of bulk polymer. [40] The molecular weight of bulk polymer determined from AN and HN using the following equation: [41]

$$M_w = \frac{2 \times 56100}{(AN + HN)} \quad (3.58)$$

The physical properties which used for estimating $k_L a$ such as density, viscosity, and surface tension of UP were estimated from the Modify Joback's method by using the MOLWORK software. All of the physical properties were written down in form of correlated equation which relate to M_w that could use in the simulation.

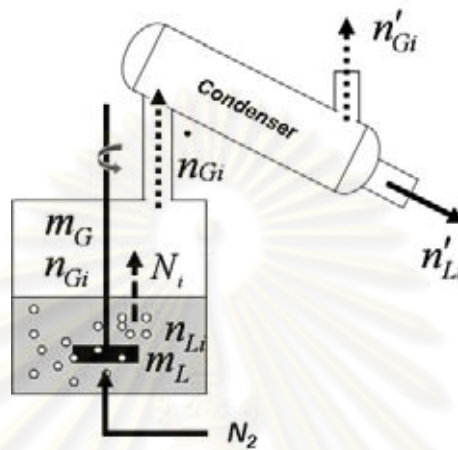


Figure 3.1 Model conceptualization for unsaturated polyester production

3.4 Reactor model

To simplify the reactor system, condenser was considered as a flash condenser connected to the reactor as show in Figure 3.1. Distillate flowed out from the condenser and did not return to the reactor. The water was removed continuously from the reactor and equilibrium of the reaction was shifted to the product side. The balance at liquid and gas phase were written in equations (3.59), and (3.60), respectively:

$$\frac{dn_{L_i}}{dt} = r_i m_L - n_{L_i} \quad (3.59)$$

$$\frac{dn_{G_i}}{dt} = n_{L_i} - n_{G_i} \quad (3.60)$$

From equations (2.15) and (3.41) at gas-liquid interface, desorption of each species from bulk polymer was limited by viscous liquid phase.

$$\frac{1}{K_{Li}} = \frac{1}{k_{Li}^o E} + \frac{1}{k_{Gi} K_{VLi}} \quad (2.15)$$

$$n_i = k_{Li} a V_{total,L} \left(C_{Li} - \frac{C_{Gi}}{K_{VLi}} \right) \quad (3.41)$$

In this model it was more convenient to use the concentration in liquid phase, C_{Li} , in unit term of mole per unit mass, thus, equation (3.41) needed to be modified:

$$\dot{n}_i = k_{Li} a \times m_L \times (c_{Li} - \frac{C_{Gi}}{K'_{VLi}}) \quad (3.61)$$

$$c_{Li} = \frac{n_{Li}}{m_L} \quad (3.62)$$

$$C_{Gi} = \frac{n_{Gi} C_G}{\sum n_{Gi} + n_{N_2}} \quad (3.63)$$

where c_{Li} and C_{Gi} denoted concentration of each species in liquid and gas phase respectively. Total concentration in gas phase, C_G , could be calculated from the ideal gas law. [27] K'_{VL} was defined vapor-liquid equilibrium ratio which relate to liquid concentration mol/kg.

The following expression was used for the flow out from the gas phase.

$$\dot{n}_{G_i} = \frac{n_{G_i}}{\sum n_{G_i} + n_{N_2}} (\sum \dot{n}_{Li} + \dot{n}_{N_2}) \quad (3.64)$$

where \dot{n}_{N_2} was the molar flow rate of the inert gas, nitrogen. The balance at flash condenser was obtained:

$$z_i \dot{n}_G = y_i \dot{n}'_G + x_i \dot{n}'_L \quad (3.65)$$

where z_i was the mole fraction in the feed to condenser. The mole fraction x_i and y_i in liquid and gas outlet streams from flash condenser were calculated from the Rachford-Rice equation: [42]

$$x_i = \frac{z_i}{1 + \left(\frac{\dot{n}'_{Gi}}{\dot{n}_G} \right) (K_i - 1)} \quad (3.66)$$

The gas-liquid equilibrium ratio calculated from Raoult's law:

$$K_i = \frac{p_i}{p_t} \quad (3.67)$$

The final equation was written down for the overall mass balance:

$$m_L = m_{oL} - m'_L + m'_G \quad (3.68)$$

The generate equations of each species and k_{La} were inserted in the reactor model. By assuming only PG and water were volatile species, the dynamic model had eight differential equations for liquid phase and two differential equations for the gas phase. The real liquid-gas phase and condenser temperature were used as input data in the dynamic model. In this simulation, the rate expression and other constants were adopted from literature. [17, 18, 19, 22, 27 and 29] The ten ordinary differential equations can be solved by using MATLAB program.



ศูนย์วิทยทรัพยากร
จุฬาลงกรณ์มหาวิทยาลัย

CHAPTER IV

METHODOLOGY

This chapter showed the details about the experimental set up for studying the effect of processing conditions on unsaturated polyester production. Descriptions of polymerization reactor and experimental set up, utilized chemical substances and experimental procedure were described. The model flow diagrams including loop control were also summarized here.

4.1 Polymerization reactor

A 2.65 liter stainless steel reactor at 130 mm diameter was set up by following typical arrangement mechanical agitation reactor as shown in Figure 4.1. The baffled vessel with liquid depth approximating the tank diameter provided adequately free space to allow for the gas hold up during gas flow. Gas was introduced below the impeller through a single nozzle sparger. The nozzle diameter was 1.5 mm. Standard baffling consisted of four flats, vertical strips arranged radially at 90 ° interval around the tank wall, extending for the full liquid depth. The standard baffle width was 10% of tank diameter and set at a clearance from the vessel wall of about one-six the baffle width to eliminate liquid stagnant. The presence of baffles reduced swirl and increased the vertical liquid current in the vessel. The impeller was disk flat-blade turbine which was used for mass transfer operation. Impeller diameter was 1/3 of tank diameter, width at 1/5 of diameter and placed at depth 2/3 of liquid level. [35] The condenser was connected to the reactor. Cooling inlet water was controlled at 15 ° C by automatic chiller and took into the condenser at flow rate 10 cm³ /minute. The condensate was collected and weighed as the polymerization progressed.

4.2 Temperature control system

The reaction temperature was controlled by 2 outputs controller. The first output was proportional current for electrically heater and the other was on/off output for turn on/off solenoid valve. This valve was used to let coolant media into the

cooling coil for cool down the molten polymer in the case of overshoot temperature or over control limit. Cool compressor air at 15 °C and 6 kg/cm³ was use as coolant.

There were 5 positions in the reactor system which were measured and recorded temperature as shown in Figure 4.3. The temperature was controlled at liquid phase. The cooling inlet temperature was measured to guarantee that chill water was in acceptable limit 5° C. Figure 4.4 shows the temperature controlling and monitoring panel of a commercial software name “SHINKO” which used in the reactor system. This software was linked the temperature controller to personal computer. The temperature data could monitor and record as a spread sheet file at the minimum interval 1 second over the entire reaction time.

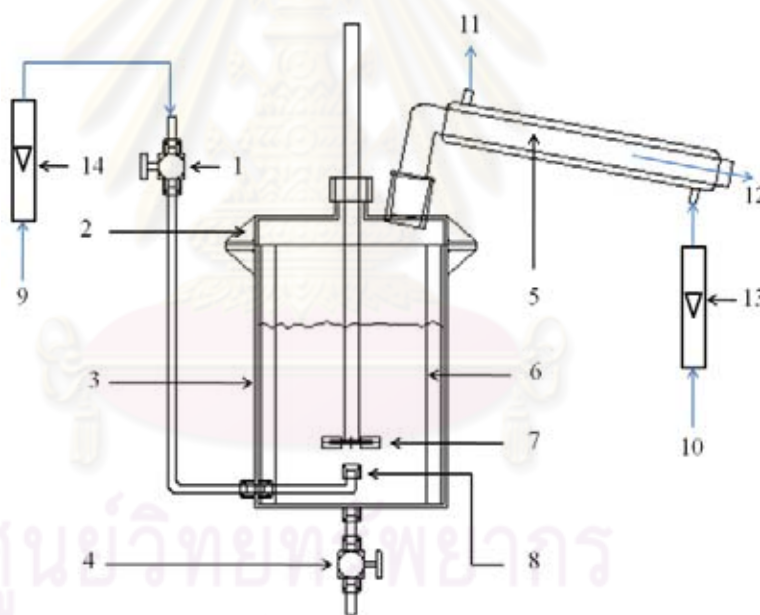


Figure 4.1 Schematic diagram of reactor setup: (1) inlet gas valve, (2) vessel cover, (3) vessel tank, (4) sampling and drain valve, (5) condenser, (6) baffles, (7) disk flat-blade turbine, (8) nozzle, (9) inert gas inlet, (10) cooling inlet, (11), cooling outlet, (12) condenser outlet, (13) and (14) flow meters



Figure 4.2 Batch polymerization reactor system which was used in this research

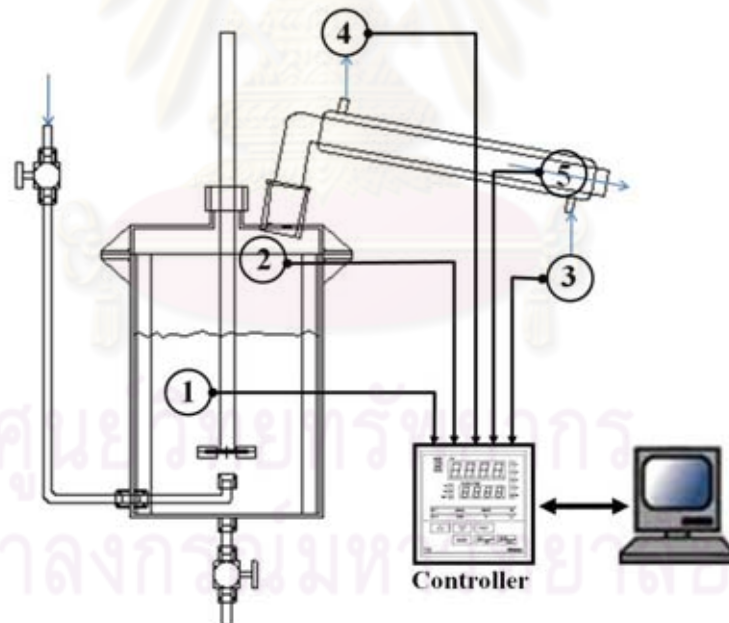
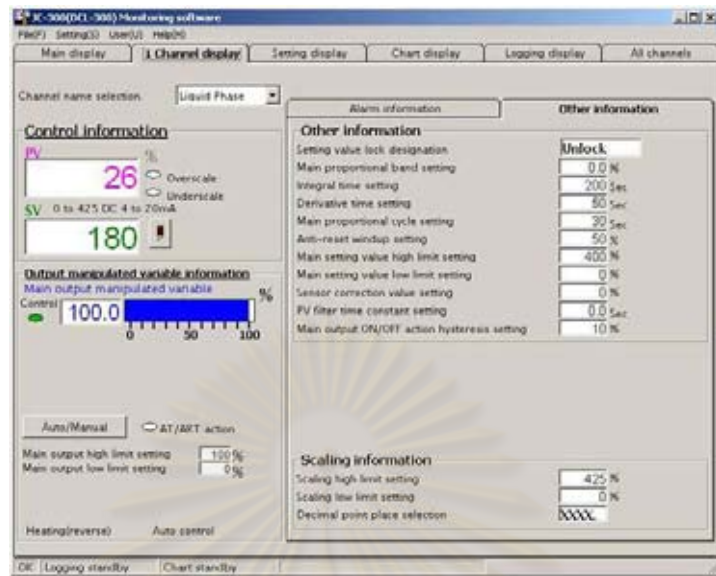
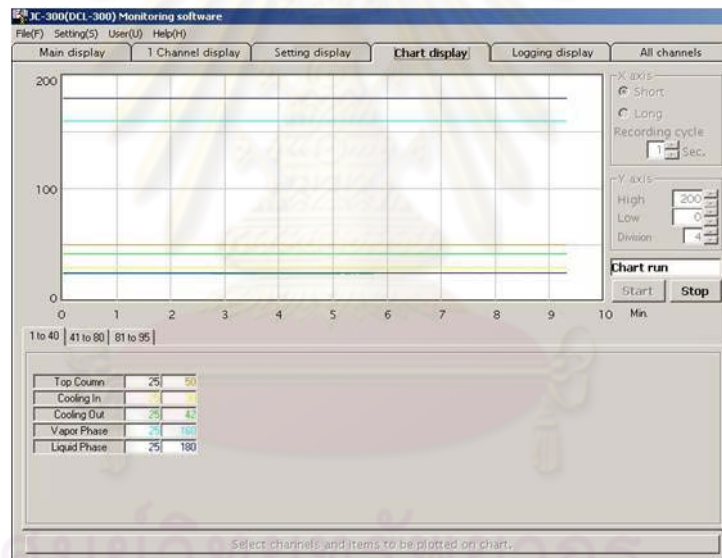


Figure 4.3 Schematic diagram of temperature controlling and measuring points in reactor system: (1) liquid phase, (2) gas phase, (3) cooling inlet, (4) cooling outlet, (5) outlet stream



(a)



(b)

Figure 4.4 Shinko software: (a) controlling and (b) monitoring

The temperature control profile was separated in four steps as shown in Figure 4.5. Step 1 and 3 were heat up, while step 2 and 4 were controlled. The 1st controlling point (step 2) was the melting of maleic anhydride and the 2nd controlling point (step 4) was polymerization temperature.

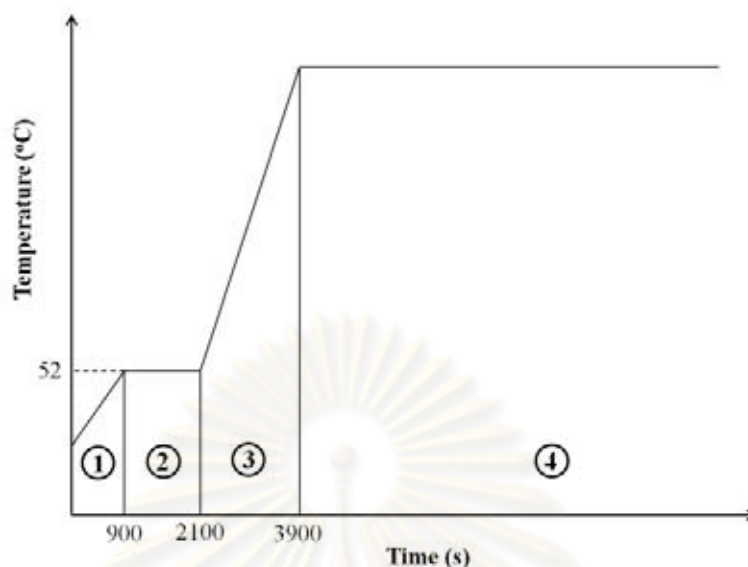


Figure 4.5 Reaction temperature profile

4.3 Chemical substances

The desired synthetic unsaturated polyester, propylene glycol maleate resin, and other chemical substances were prepared from the following reagents:

- 1,2-propanediol ($C_3H_8O_2$) (Siam Chemical Industry co., ltd.)
- Maleic anhydride ($C_4H_2O_3$) (Siam Chemical Industry co., ltd.)
- Xylene (C_8H_{10}) (Siam Chemecal Industry co., ltd.)
- Sodium hydroxide (NaOH) (97% purity, Carlo Erba)
- Hydranal composite5 (Fluka)
- Hydranal solvent (Fluka)
- Acetone (97% purity, Fluka)
- Nitrogen gas (99.99% purity)

4.4 Synthesis of unsaturated polyester

The constant process temperature varied in the range of 160-220 °C. The entire reaction was carried out in an inert atmosphere, nitrogen. The constant nitrogen flow rate was varied from 120-840 cm^3/min .

1. The correct amount of propylene glycol and maleic anhydride were charged into the vessel at 10% excess of glycol and 2% weight of xylene

was added. Then, oxygen was excluded by flushing out the vessel with sluggish N_2 for 10 minute.

2. N_2 was fed and heater was started and heated up to design temperature. This should be recorded to zero time. The stirrer should also be started and continue throughout the process. The speed of stirrer was constant at 15 rps for ensuring high turbulent zone.
3. The reaction temperatures, 5 measuring points were recorded every 1 second through the reaction. When the batch temperature was about $100\text{ }^\circ\text{C}$, condensing was started at constant coolant flow rate $10\text{ cm}^3/\text{min}$.
4. 15 minutes after starting condenser, a few gram of resin was sampling from the batch during $\frac{1}{2}$ - 1 hour and determined:
 - a. The acid number by titration with 0.1 N NaOH, used 20 ml of acetone to dissolve the resin, record the acid number as milligram of KOH per gram of resin. This titration was analyzed by auto titration. (Mettler Toledo DL5X)
 - b. Water content in polymer by titration with Hydranal composite 5, used 20 ml of Hydranal solvent to dissolve the resin. Record the water content as % water in polymer. This titration was analyzed by auto titration. (Mettler Toledo V30)
5. The accumulated of condensate was weighed and sampling a few gram of condensate during $\frac{1}{2}$ - 1 hour to analyze propylene glycol content.
6. The reaction was continuously progressed until the acid number fallen to 50 then stopped the reaction.

4.5 Characterization

4.5.1 High performance liquid chromatography

The molecular weight of unsaturated polyester from each condition was analyzed by high performance liquid chromatography (Shimadzu LC-10ADvp) equipped with a RID-10A refractive index detector. The stationary phase was a GPC AT- 805S column (8.0 x 250 mm) and the mobile phase was toluene at flow rate of 1.0 ml/min. The column temperature was controlled at $40\text{ }^\circ\text{C}$.

4.5.2 Fourier transform infrared spectroscopy

For the FTIR analysis, the functional groups of unsaturated polyester from each condition was monitored between $650 - 4000 \text{ cm}^{-1}$ with the resolution of 4 cm^{-1} and 64 number of scan at room temperature by a Nicolet, model NEXUS 670, FTIR spectrometer equipped with a ZnSe Disc ($32 \times 2 \text{ mm}$) detector at transmission mode. All the recorded spectra were implemented in the OMNIC[®] (Thermo Nicolet Corp.) software.

4.5.3 Gas chromatograph

The condensate which sampling from polymerization during an appropriate interval time was characterized by a gas chromatography (Shimadzu GC-10ADvp) equipped with a flame ionization detector. GCsolution software was used to collect and analyze the data. A Restek Crop (Bellefonte, PA) DB-WAX GC-column ($30\text{m} \times 250\text{mm} \times 0.25\mu\text{m}$) was used in analysis.

4.6 Model flow diagram

4.6.1 Overall model flow diagram

The overall model flow diagram was carried out by following a procedure shown in Figure 4.6. Assume here that only propylene glycol and water was volatile species in the system. From this scheme, the set of mole balances in both liquid and vapor phases were generated in the form of equation (3.59) - (3.60). The mole balance equations were obtained, 8 equations for liquid and 2 equations for vapor. The generation rate of each species, r_i , was calculated from equation (3.32) - (3.39). The initial mole and process condition such as temperature, inert gas flow rate and stirrer speed were input to the model. These ten ordinary differential equations were integrated by MATLAB and obtained a column vector with ten members as the answer. Each member in the vector was mole of each species in liquid and vapor phase respectively. Follow a dash line in the lower loop, the gas molar flow of each volatile species was calculated by used equation (3.64). The flow was passed through the condenser. The Rachford-Rice equation (3.66) was applied, the mole fraction in the outlet gas and condensate were solved by trial and error. Total mole and mass outlet were subtracted from the initial value, equation (3.68), the remaining were used as initial mole for the next loop of calculation. For a continuous line in the upper loop,

this path was used to estimate the volumetric mass transfer coefficient. The amount of carboxylic and hydroxyl group in the liquid phase were calculated from the liquid mole of each species in the column vector. The acid and hydroxyl number were used for predicting the molecular weight of the resin, equation (3.58). Then unsaturated polyester properties such as density and surface tension were estimated by group contribution method from “Mol Work” software. The next procedure, the volumetric mass transfer coefficient was estimated and used in the next loop of calculation. One cycle of both two loops was meant for 1 second time scale.

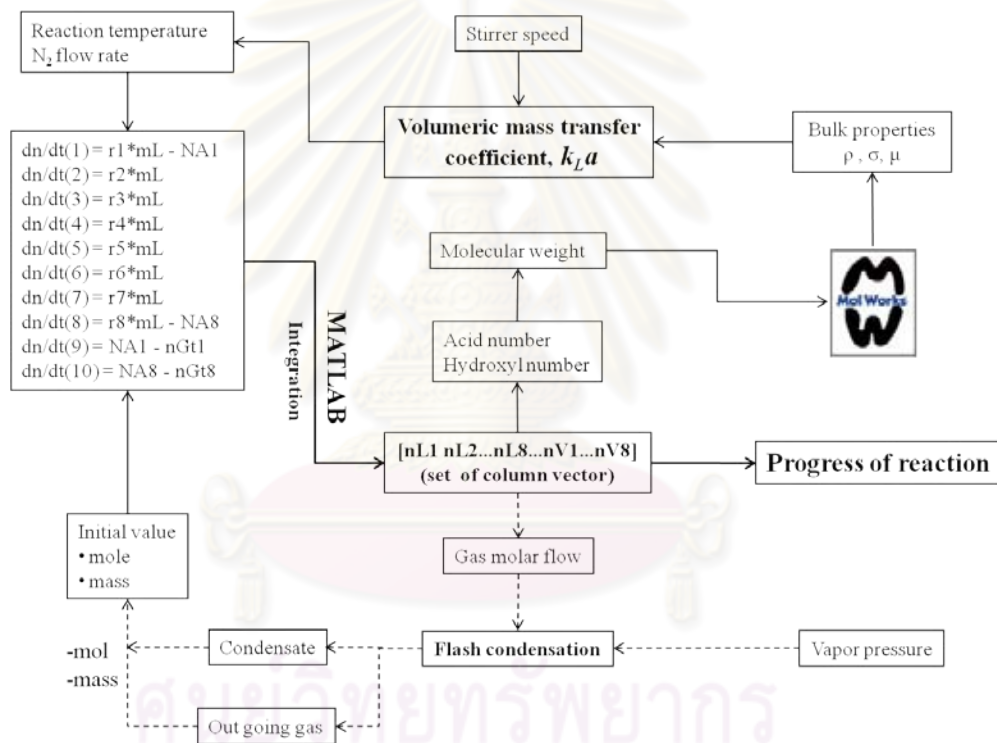


Figure 4.6 Overall model flow diagram

4.6.2 Volumetric mass transfer model flow diagram

The same method as the upper loop of Figure 4.6, the acid and hydroxyl number could obtain from the column vector. The unsaturated polyester properties were predicted. The gas hold-up and bubble diameter was estimated from equation (3.46), (3.47) and (3.52), respectively, followed by equation (3.43) for specific

interfacial area. The mass transfer coefficient was started with equations (3.56) and (3.57) for estimating the power consumption and energy dissipation, respectively. By applying both penetration and Kolmogoroff's theories the mass transfer coefficient could be estimated from equation (3.42). Finally, the volumetric mass transfer coefficient was obtained.

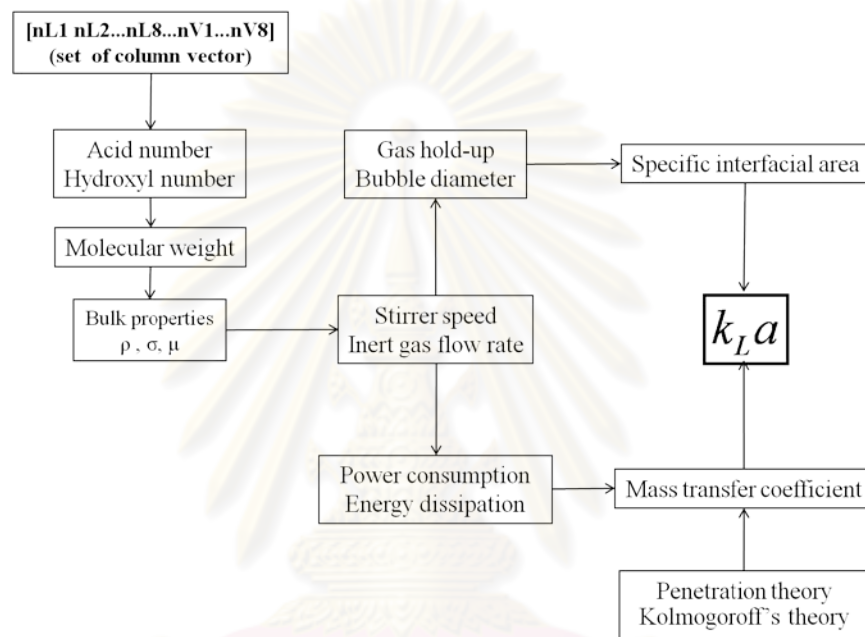


Figure 4.7 Volumetric mass transfer model flow diagram

4.7 Model parameters

4.7.1 Kinetic parameters

In this modeling and simulation study, the rate expressions and rate constants have been adopted from the literature. E. Paatero and coworker [16] studied the kinetic and rate expression for main and side reaction of the melt polyesterification of maleic anhydride and propylene glycol. The Arrhenius parameters and the equilibrium constants from this research were summarized in Table 4.1 and 4.2, respectively.

J. Lethonen and coworkers [29] developed the kinetic model and determined the rate parameter for polyesterification of unsaturated polyester. They proposed that

the reaction path 6 in scheme 2.1 was considered as an irreversible reaction and reaction path 8 in the same scheme was discarded.

Table 4.1 Arrhenius parameters in polyesterification of maleic anhydride with propylene glycol

Reaction	Frequency factor, A	Activation energy, E_a (kJ/mol)
Esterification	1,200,000 kg mol ⁻¹ min ⁻¹	75
Isomerization	127,000 min ⁻¹	56
Double bond saturation	476,000 kg mol ⁻¹ min ⁻¹	48

Table 4.2 Equilibrium constant in polyesterification of maleic anhydride with propylene glycol

Temperature (°C)	K_E	K_I	K_S
160	25	12.5	0.87
180	19	9.1	2.30
200	14	45	2.60
220	36	12.4	-

4.7.2 Vapor-Liquid equilibrium estimation.

The last parameter, which used to estimate the molar flow out from the liquid phase in the model, was vapor-liquid equilibrium ratio in equation (3.61).

$$\dot{n}_i = k_{Li} a \times m_L \times (c_{Li} - \frac{C_{Gi}}{K_{VLi}''}) \quad (3.61)$$

The term K_{VLi}'' was related to liquid concentration mol/kg of resin. As the presumption in the model that only propylene glycol and water were volatile species then the estimation of these parameters were needed. The estimation used the method of

minimization the sum of residual squares. Each temperature condition was estimated separately. $K''_{VL_{PG}}$ was verified with percent of propylene glycol content in the condensate while $K''_{VL_{H_2O}}$ was verified with the accumulation of the condensate.

The initial estimation of $K''_{VL_{PG}}$ was obtained by neglecting the effect of $K''_{VL_{H_2O}}$ and set as constant. For the first estimation cycle, each loops of calculation for $K''_{VL_{PG}}$ was trial until it got the minimum of the sum residual square. The obtained $K''_{VL_{PG}}$ was used to estimate $K''_{VL_{H_2O}}$ in the same way. After received both the $K''_{VL_{PG}}$ and $K''_{VL_{H_2O}}$ from the first cycle, the estimation cycle was repeated until both parameters were convergent.

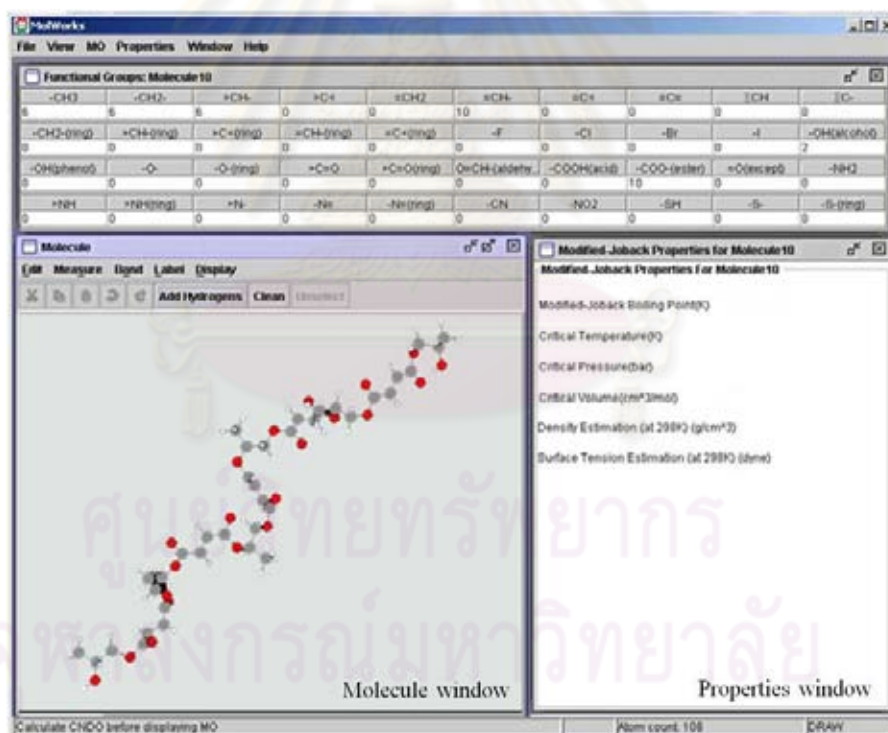


Figure 4.8 MolWork software operating panel

4.8 Unsaturated polyester properties estimation

The unsaturated polyester properties were estimated by group contribution method from the freeware name “MolWorks” version 2.0 as shown in Figure 4.8. MolWorks is an integrated software tool for molecular design. The designed

molecule was built up reasonable in molecule window then the software automatically arranged each atom in three dimensions to optimize internal energy. Each functional group was counted and used to estimate the properties of the molecules based on group contribution method.



ศูนย์วิทยทรัพยากร
จุฬาลงกรณ์มหาวิทยาลัย

CHAPTER V

RESULTS AND DISCUSSION

This chapter presented the results and discussion of the simulation from the developed dynamic model. The comparison between the simulation and experimental results were discussed.

Base on the Newtonian liquid, several simulations of process parameters were performed to predict their sensitivities. By using the equations proposed in chapters 2 and 3, the model was able to predict the influence of operating conditions on gas hold-up, specific interfacial area and finally on the volumetric mass transfer coefficient. Remind that all of the simulation results were simulated at constant stirrer speed 15 rounds per second.

5.1 Parameters sensitivity on energy dissipation

The presence of gas in the vessel contents resulted in lowering the power required to turn an impeller at a given speed, as showed in Figure 5.1, probably because of the lowered mean density of the mixer. At high turbulent regime, the power consumption was proportional to liquid density.

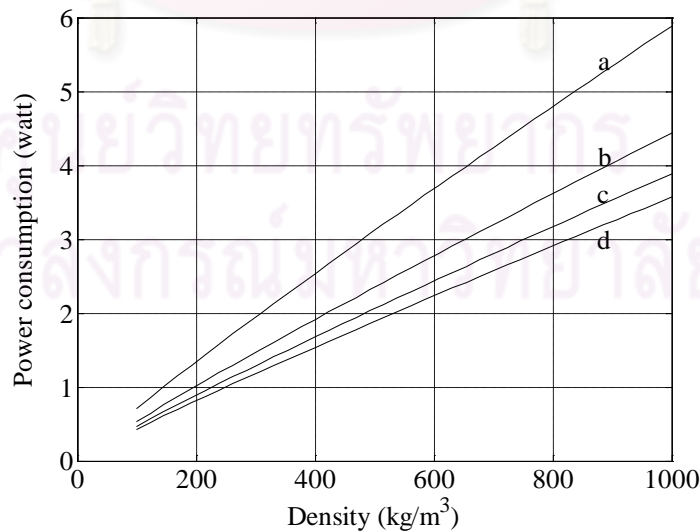


Figure 5.1 Power consumption by varied inert gas flow: (a) 120 ccm, (b) 360 ccm, (c) 600 ccm and (d) 840 ccm

Meanwhile, the reaction time progress, the density of polymer was increased from longer polymer chain then the impeller needed more power as shown in Figure 5.2. This figure presented the plot from equation 3.56 and illustrated that too high gas flow rate did not achieve the lowest power.

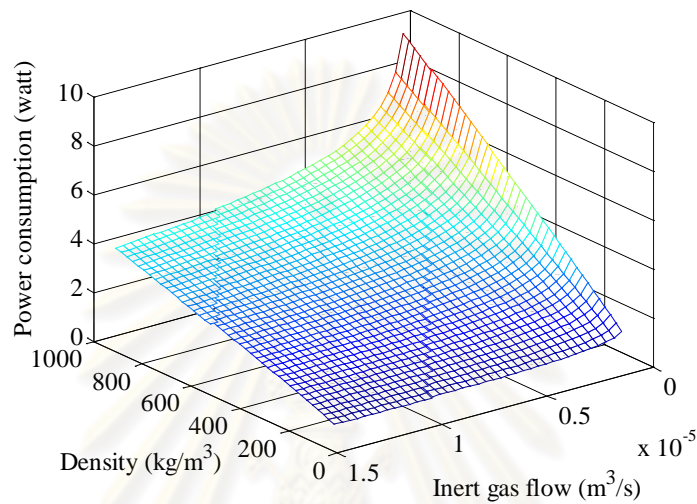


Figure 5.2 Effect of density and inert gas flow rate on power consumption in aerated system

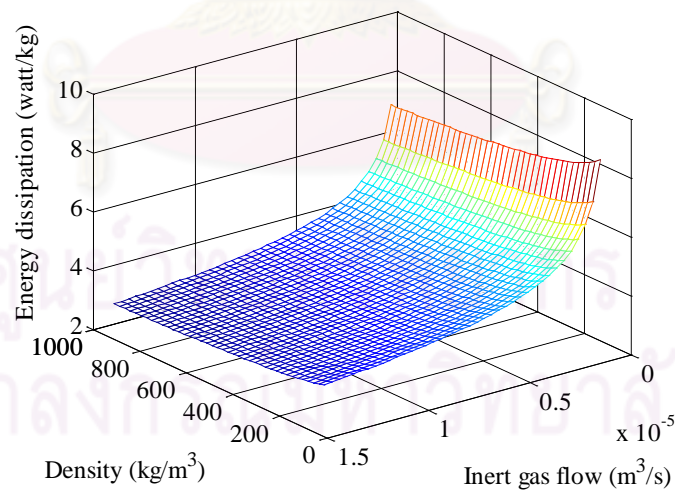
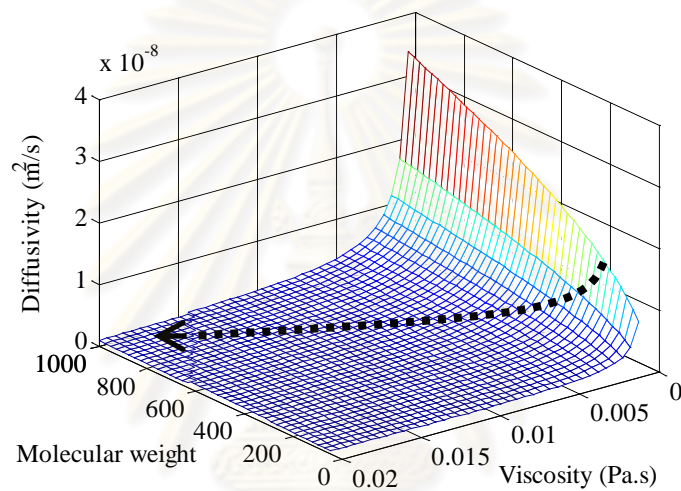


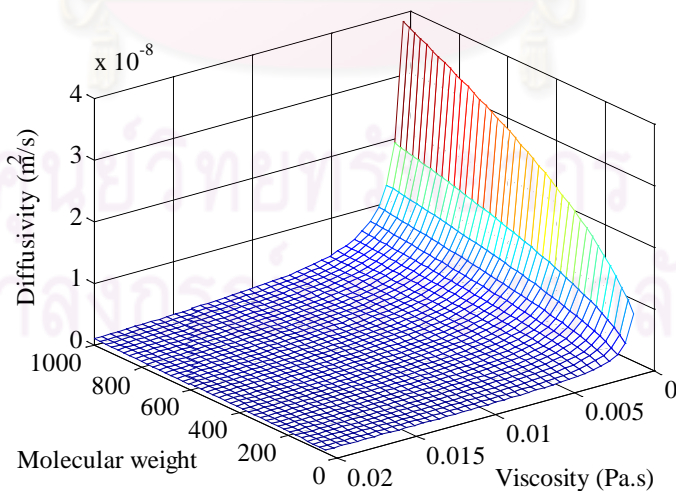
Figure 5.3 Effect of density and inert gas flow rate on energy dissipation

The plot of energy dissipation from equation (3.57) was presented in Figure 5.3. This term was inverse proportion to both density and inert gas flow. Normally gas is easy to disperse in a thin liquid medium, but in a thick or dense liquid medium the dispersion is rather difficult. At high reaction time of polymerization, the density of

polymer increased then the gas dispersion was not good, thus bubble diameter became large. For increasing of inert gas flow at constant stirrer speed, the bubble gas was trapped and became coalescence then obtaining a large bubble, too. As mentioned in section 3.3.3, the energy was consumed in the contact between liquid elements and gas bubbles, in case of a very small bubble. It meant that the energy dissipated throughout the liquid and the rate of dissipation was high. As gas bubble became bigger, both of energy dissipation and dissipation rate would be decreased.



(a)



(b)

Figure 5.4 Effect of viscosity and molecular weight on diffusivity: (a) 160 °C and (b) 220 °C

5.2 Parameters sensitivity on mass transfer coefficient

The predictions of mass transfer coefficient started with the diffusivity which was the function of molecular weight, viscosity and temperature, equation 2.3). The effect of these three parameters were showed in Figure 5.4. If the size of molecule was growth up, the space between the molecules increased causing conveniently diffusion and diffusivity was high. At very low viscosity the diffusivity was high and rapidly decreased at higher viscosity. During polymerization, both of molecular weight and viscosity gradually increased. Thus, the estimated diffusivity should follow the black dash arrow as showed in Figure 5.4(a). The temperature influence was represented by Figure 5.4(a) and (b) at 160 °C and 220 °C, respectively. Increasing of temperature obtained the higher diffusivity. We can presume here that nearly completed polymerization, every reaction temperature, the diffusivity was convergence to a very low value.

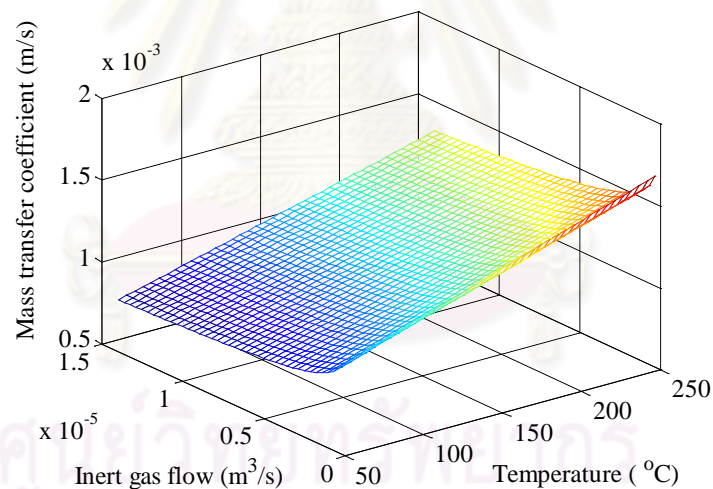
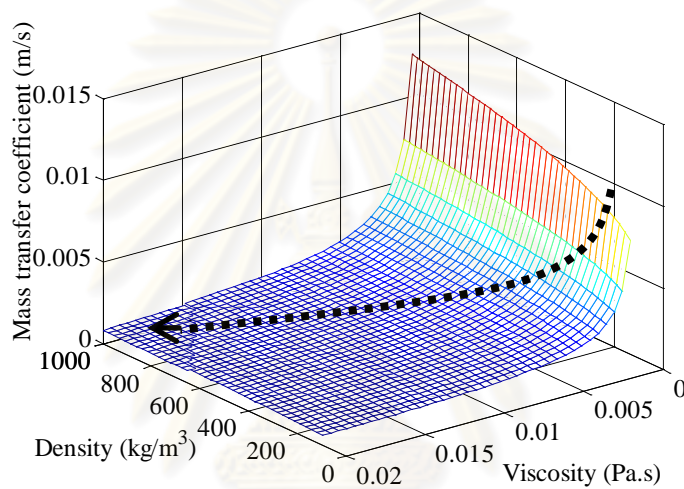


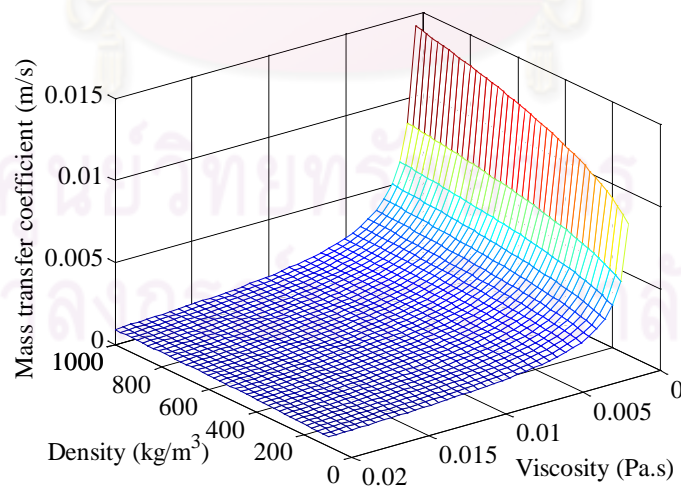
Figure 5.5 Effect of temperature and inert gas flow rate on mass transfer coefficient, evaluated at molecular weight 500 g/mol, density 500 kg/m³, viscosity 0.01 Pa.s

The mass transfer coefficient was proportional to reaction temperature and inversely proportional to the inert gas flow rate as shown in Figure 5.5. The proceeding of mass transfer coefficient during entire reaction was simulated and exemplified. In Figure 5.6, the inert gas flow was fixed and varied reaction temperature, meanwhile Figure 5.7, temperature was fixed and varied inert gas flow. Surface plot gave the higher mass transfer coefficient at high reaction temperature,

comparing Figures 5.6 (a) and (b). The surface plot gave the inverse proportional when increase inert gas flow, comparing Figure 5.6 (a) and (b). At very high viscosity, these four surface plots showed the same results that the value of mass transfer coefficient slightly changed. This phenomenon illustrated the same characterization as the diffusivity. When density and viscosity increased as reaction progress, the mass transfer coefficient value should be proceeded by following the dash arrow in these figures.

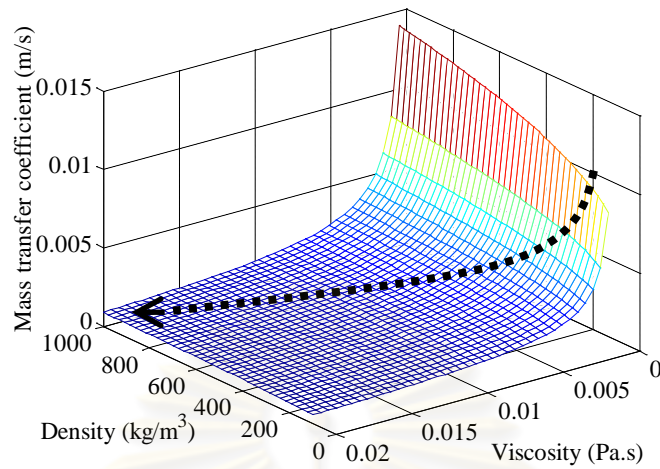


(a)

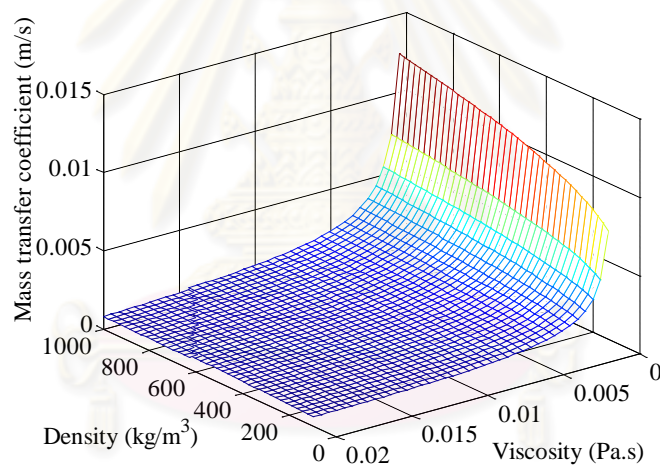


(b)

Figure 5.6 Effect of density and viscosity on mass transfer coefficient evaluated at N₂ flow 360 ccm: (a) 160 °C and (b) 220 °C



(a)



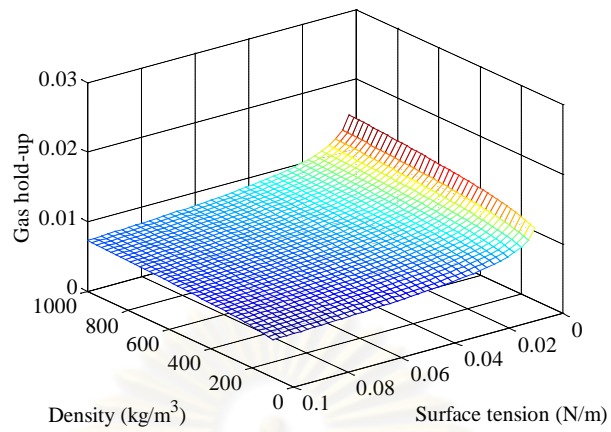
(b)

Figure 5.7 Effect of density and viscosity on mass transfer coefficient evaluated at 180 °C: (a) N₂ flow 120 ccm and (b) N₂ flow 840 ccm

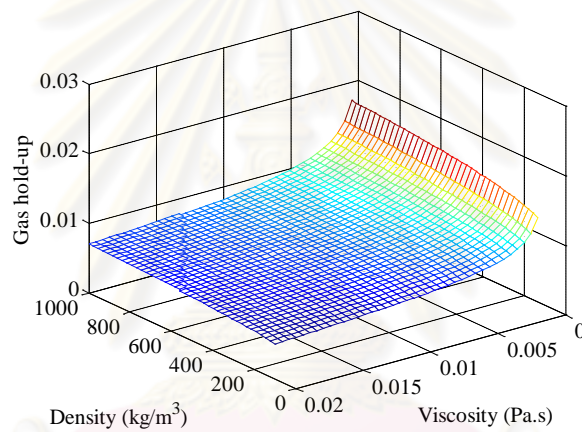
5.3 Parameters sensitivity on specific interfacial area

5.3.1 Gas hold-up

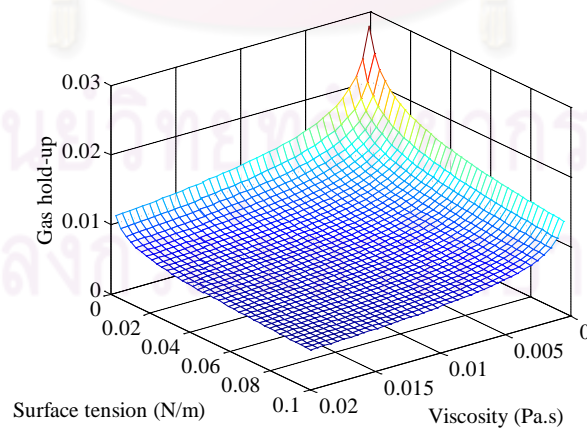
Gas hold-up was one of the most important parameters characterizing the hydrodynamics of bubble. From equations 3.44) and 3.46), the gas hold up depended on many parameters. Figures 5.8(a), (b) and (c) illustrated the three dimensional plots which simulated from each pair of parameters by fixing other parameters as constant. From these three surface plots, the density of polymer was a little bit influence on the



(a)



(b)



(c)

Figure 5.8 Effect of parameters on gas hold-up at inert gas flow 360 ccm: (a) constant viscosity 0.01 Pa.s, (b) constant surface tension 0.5 N/m and (c) constant density 500 kg/m^3

gas hold-up as shown in Figure 5.8(a) and (b), but gas hold-up was sensitive on surface tension and viscosity as shown in Figure 5.8(c).

By varying the inert gas flow rate, the surface plots of equation 3.46) at constant density were shown in Figure 5.9. They indicated that the total gas hold up was increased with increasing of inert gas flow, linearly related to superficial gas velocity. At constant stirred and low inert gas flow rate, the bubble size was small and uniform. These bubbles traveled upwards without any major collision or coalescence, thus the liquid and gas phase seemed to be a homogeneous mixture. When the inert gas flow rate was too high, the bubbles were coalescence, therefore at high inert gas flow rate all the bubbles should be large. The large bubbles had higher rising velocity than small bubbles then the residence time of large bubbles decreased and caused to reduce the gas hold up. These phenomena were illustrated by Figure 5.9 at surface plot layers (a), (b), (c) and (d) respectively.

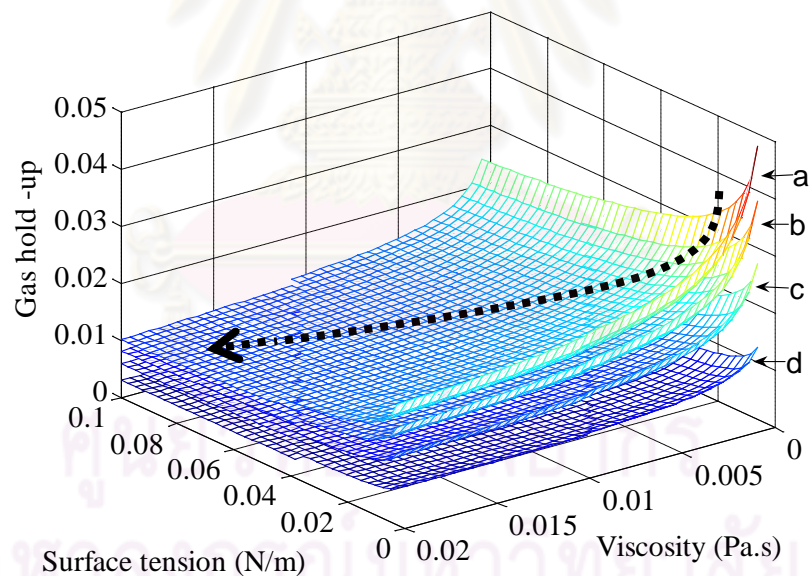
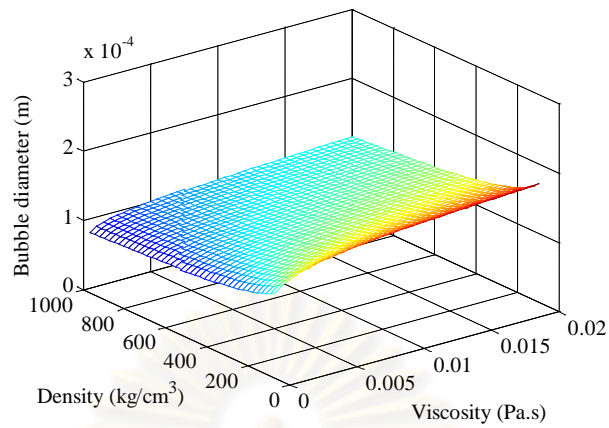
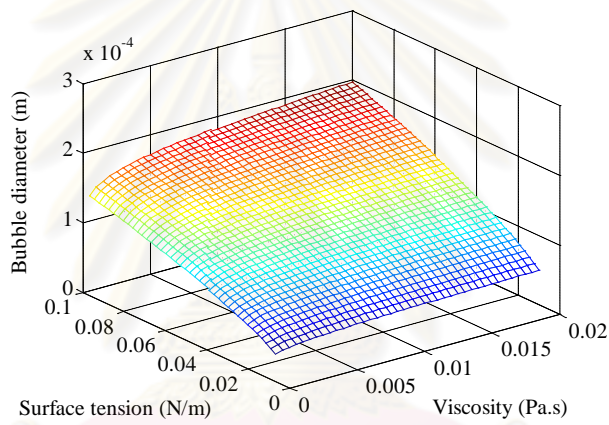


Figure 5.9 Effect of viscosity and surface tension on gas hold-up, constant density 500 kg/m^3 : inert gas flow (a) 840 ccm, (b) 600 ccm, (c) 360 ccm and (d) 120 ccm

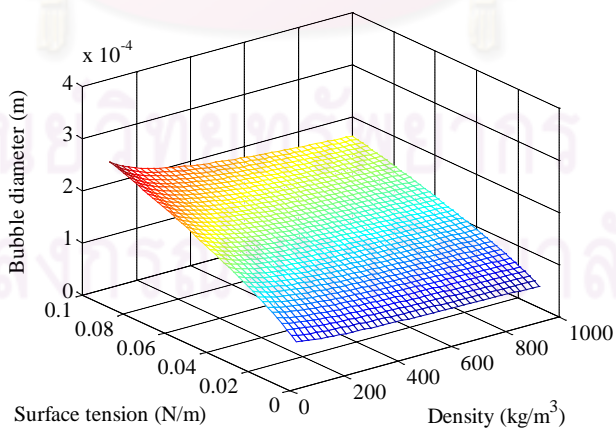
Furthermore, Figure 5.9 indicated that at the low surface tension and viscosity, their effects were dominated and obtained the higher gas hold-up because the liquid surface was easy to break down for the gas dispersion.



(a)



(b)



(c)

Figure 5.10 Effect of parameters on mean bubble diameter: (a) constant surface tension 0.5 N/m, (b) constant density 500 kg/m^3 and (d) constant viscosity 0.01 Pa.s

When the viscosity and surface tension increased as reaction progress, the gas hold-up should be proceeded by following the dash arrow in this figure. Too high of inert gas flow rate might change the system from homogeneous to heterogeneous regime and dropped in gas hold-up. The heterogeneous regime was out off scope of this research.

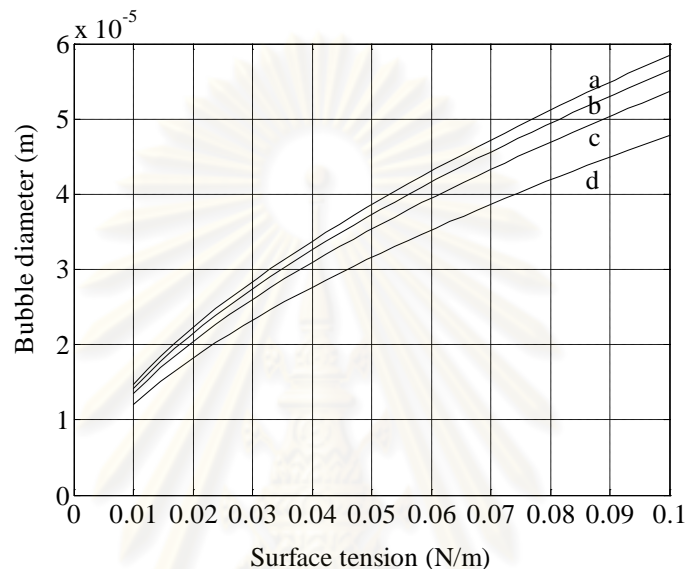


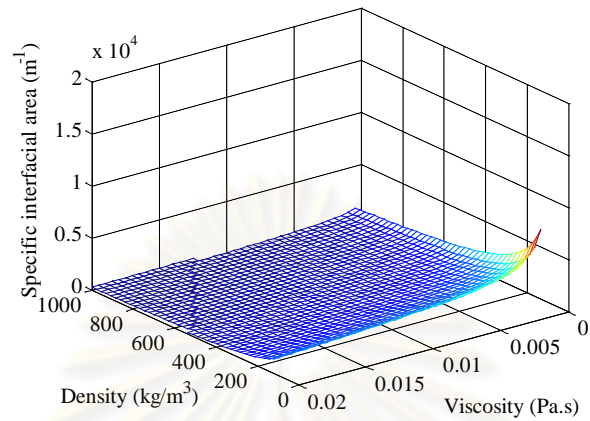
Figure 5.11 Bubble diameters estimated at density 500 kg/m^3 , surface tension 0.05 N/m and viscosity 0.01 Pa.s by varying inert gas flow: (a) 840 ccm , (b) 600 ccm , (c) 360 ccm and (d) 120 ccm

5.3.2 Bubble diameter

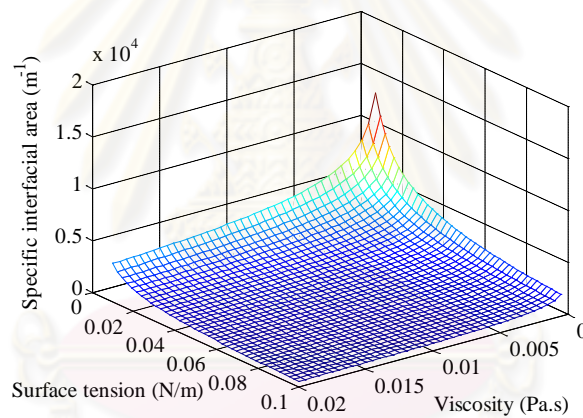
The bubble diameter of inert gas in liquid phase was obtained from equation (3.52) which related to many parameters. Figures 5.10(a), (b) and (c) illustrated the three dimension plots simulated from each pair of parameters by fixing other parameter as constant. From this three dimensional plots, the density and viscosity of polymer were a little bit influence on the bubble size as shown in Figure 5.10(a). On the other hand, surface tension was the most sensitive on the bubble size as shown in Figure 5.10(a) and (b). If the surface tension was higher, the bubble diameter was bigger because we need more power to break down the liquid surface at high tension then the dispersion of inert gas in liquid phase was difficult.

To understand the effect of inert gas flow rate on bubble size, the simulation graphs in Figure 5.11 was calculated by fixing all parameters constant except surface

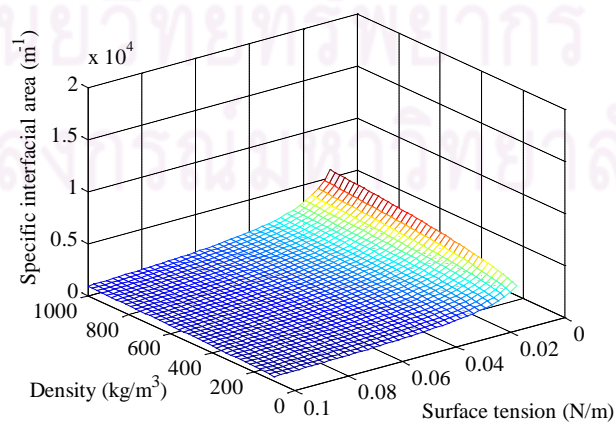
tension. Increasing the inert gas flow rate at constant stirrer speed brought up the coalescence of bubbles therefore the bubbles will be larger.



(a)



(b)



(c)

Figure 5.12 Effect of parameters on specific interfacial area: (a) constant surface tension 0.5 N/m, (b) constant density 500 kg/m^3 and (d) constant viscosity 0.01 Pa.s

5.3.3 Specific interfacial area

Specific interfacial area was six times of ratio between the gas hold-up and the bubble diameter, and then the characteristic of the interfacial area was depending on these two terms. Figures 5.12(a), (b) and (c) presented the simulation results from equation 3.43), each pair of parameters were simulated their affectation by fixing other parameter as constant. Figure 5.12(a) and (c) showed that density was slightly influence on specific interfacial area meanwhile Figure 5.12(b) indicated that surface tension and viscosity were potently influence. Especially at low surface tension and viscosity, the effects from both parameters were obvious and obtained high interfacial area.

The effect of the inert gas flow rate on specific interfacial area was studied. The simulated results were plotted in Figure 5.13 by fixed all parameters constant except surface tension and viscosity. Increasing inert gas flow rate induced higher specific interfacial area. The proceeding of interfacial area should follow the dash arrow in this figure as the polymerization progress.

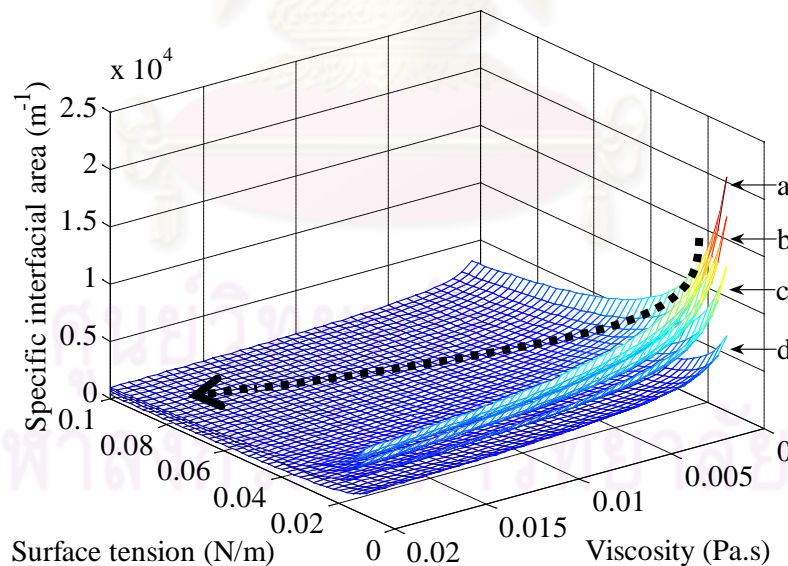


Figure 5.13 Effect of viscosity and surface tension on specific interfacial area at constant density 500 kg/m^3 by varying inert gas flow rate: (a) 840 ccm, (b) 600 ccm, (c) 360 ccm and (d) 120 ccm

5.4 Parameters sensitivity on volumetric mass transfer coefficient

Volumetric mass transfer coefficient was obtained from the multiple between the mass transfer coefficient and specific interfacial area, equations 3.42) and 3.43). The first term was depending on the density and viscosity, while the second term was depending on the density, viscosity and surface tension. Because the viscosity and density were coordinate parameters. Then they were used as the basement axis of three dimension plot in this section. The parameter which wanted to study its effect was varied and the others were fixed as shown in Figures 5.14, 5.15 and 5.16.

The results in section 5.2 and 5.3.3 indicated that density was a little effect on mass transfer coefficient and specific interfacial area, thus it still had the small effect on volumetric mass transfer coefficient too. Viscosity and surface tension still had the same influence as discussion in section 5.3.3, the volumetric mass transfer coefficient got high at the zone which low viscosity and surface tension as showed in Figure 5.16. Figure 5.14 illustrated the effect of reaction temperature, the volumetric mass transfer was higher when increased temperature but in this research the temperature range was narrow then its effect did not dominate here.

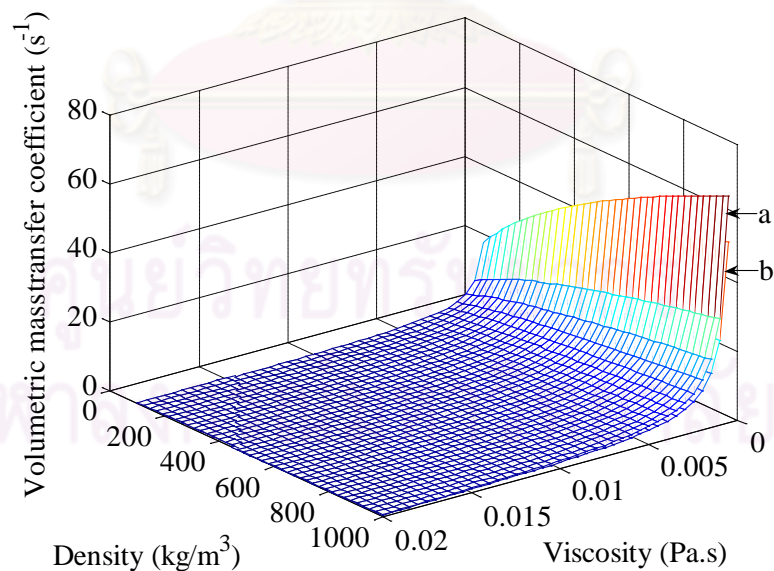


Figure 5.14 Effect of viscosity and density on volumetric mass transfer coefficient at surface tension 0.05 N/m and inert gas flow rate 360 ccm by varying reaction temperature: (a) 220 °C and (b) 160 °C

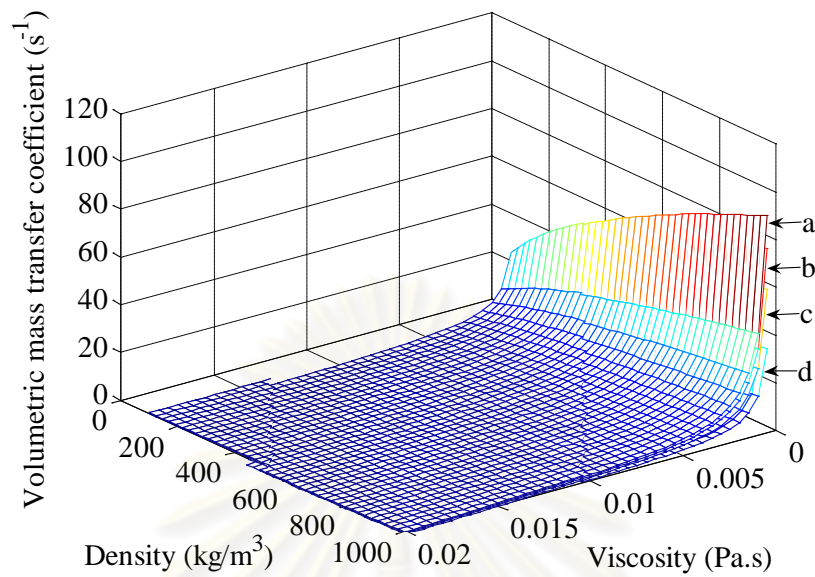


Figure 5.15 Effect of viscosity and density on volumetric mass transfer coefficient at surface tension 0.05 N/m and 180 °C by varied inert gas flow rate: (a) 840 ccm, (b) 600 ccm, (c), 360 ccm and (d) 120 ccm

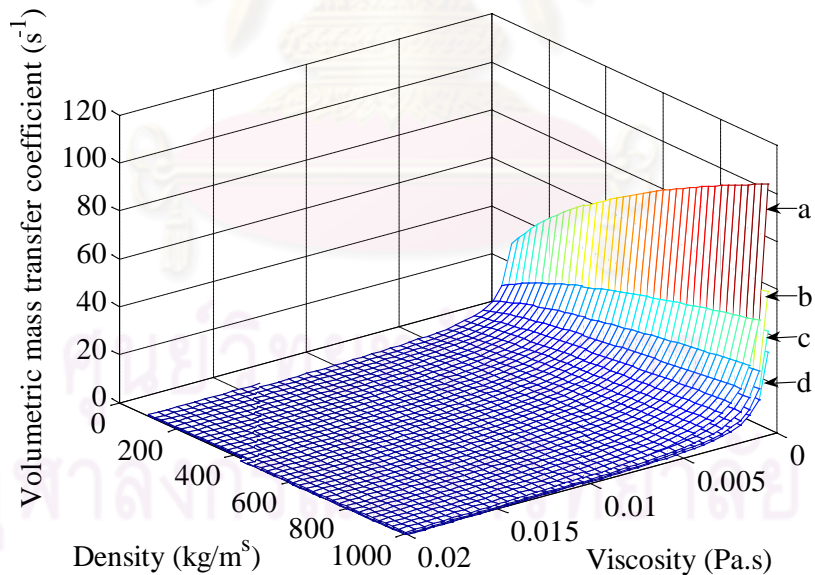


Figure 5.16 Effect of viscosity and density on volumetric mass transfer coefficient at inert gas flow 360 ccm and 180 °C by varied surface tension: (a) 0.025 N/m, (b) 0.05 N/m, (c) 0.075 N/m and (d) 0.10 N/m

For the inert gas flow rate, its effect was presented in Figure 5.15. Although Figure 5.5 in section 5.2 indicated that the mass transfer coefficient was reduced when

increased the inert gas flow rate, but the higher inert gas flow induced very high specific interfacial area as presented in Figure 5.13. Thus the volumetric mass transfer coefficient was increased finally.

5.5 Effect of synthesized condition on the rate of condensation polymerization and the reaction time

5.5.1 Effect of reaction temperature

Polyesterification is exothermic reaction and reacts at high temperature. When the liquid phase reached the reaction temperature, polyesterification progresses and the system release high thermal energy. Figure 5.17 showed the overshoot temperature cause of high exothermic reaction. The release energy brought up the reaction temperature and accelerated the reaction rate at the beginning as illustrated in Figure 5.18. The acid number (Figure 5.18a) and reaction conversion (Figure 5.18b) were rapidly changed at beginning and obtained the high polymerization rate. Both of acid number and conversion graphs indicated that increasing of reaction temperature would obtain high polymerization rate.

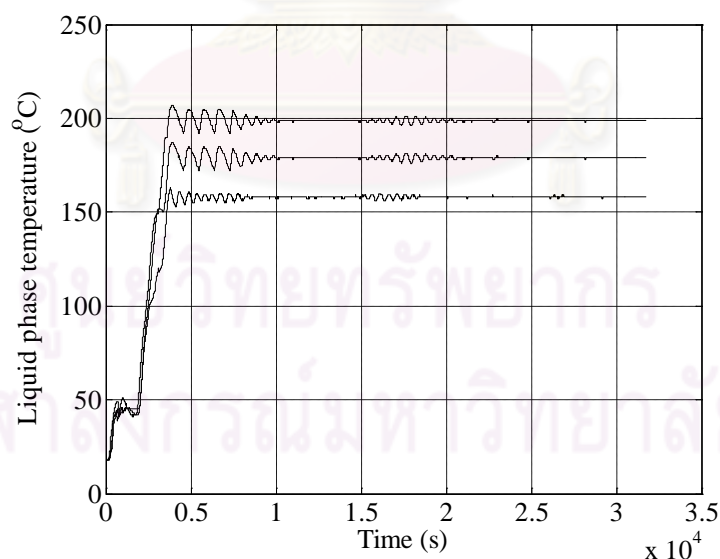
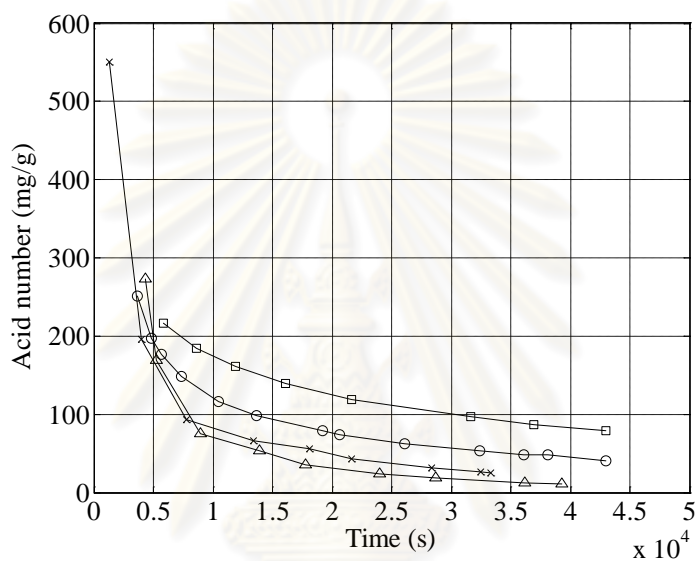


Figure 5.17 Liquid phase temperature

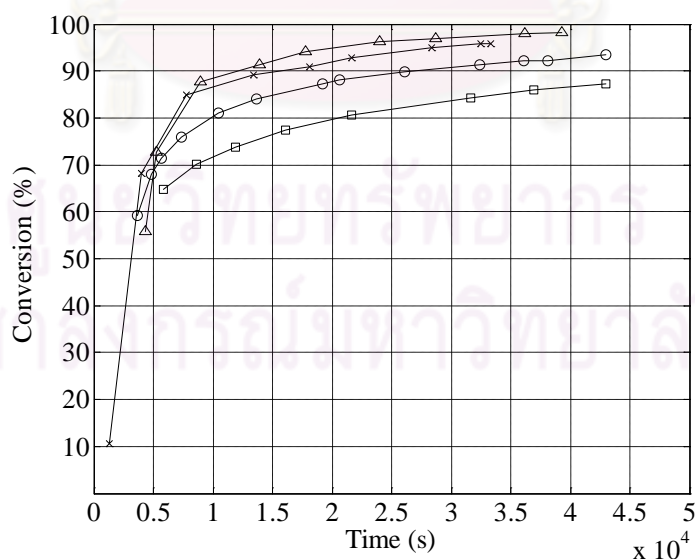
5.5.2 Effect of inert gas flow rate

The main objective of inert gas flow is to prevent oxidizing but at the same time it acts as carrier gas to bring out condense byproduct, water, from the system.

Although inert gas flow rate is not directly accelerate the polymerization but it can increase specific interfacial area for mass transfer as discussion in section 5.3.3. The higher amount of interfacial area should gain the water transfer out and drive the equilibrium toward product side. The results in Figure 5.19 confirmed and proved effect of inert gas flow rate, the acid number was more reduced (Figure 5.19a) or the conversion was higher (Figure 5.19b) as increasing of the inert gas flow rate.



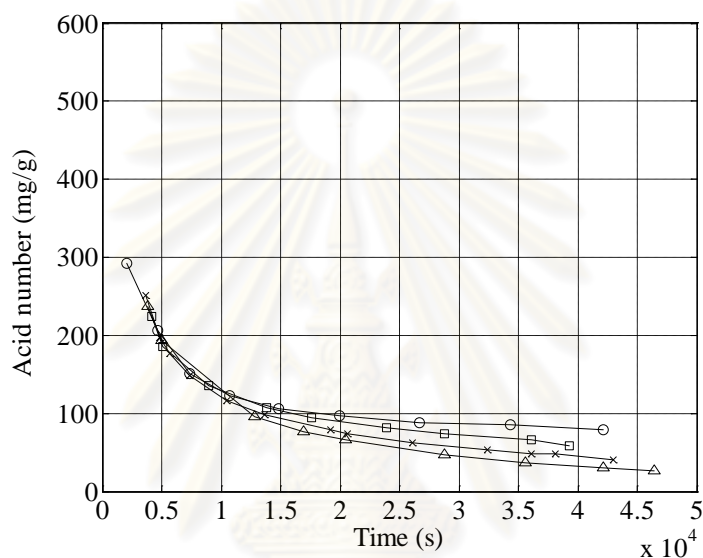
(a)



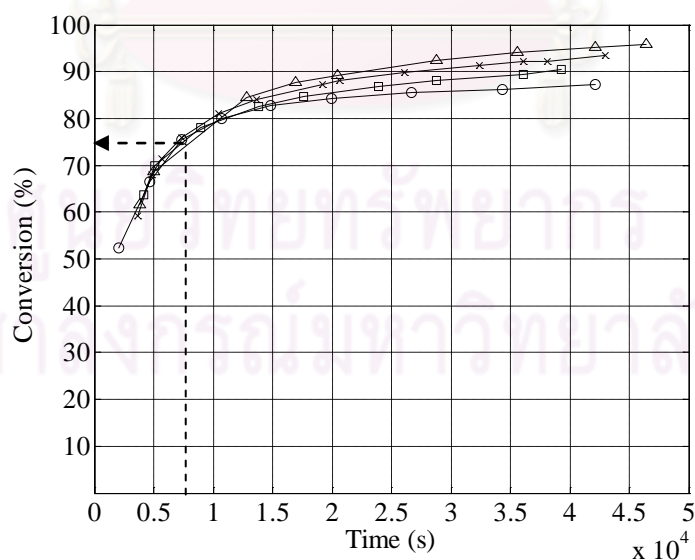
(b)

Figure 5.18 Effect of reaction temperature at inert gas flow 360 ccm on (a) acid number and (b) conversion (b): □160 °C, ○180°C, ×200 °C and Δ220 °C

Both of acid number and conversion graphs (Figure 5.18 and 5.19) illustrated that increasing of reaction temperature and the inert gas flow rate could obtain the higher polymerization rate and reduce the reaction time. For general proposed unsaturated polyester with the acid number 50 mg/g or more than 90 % conversion, the result from Figure 5.19 indicated that the reaction time will decrease around 160 minute if the inert gas flow increased from 360 to 600 ccm.



(a)



(b)

Figure 5.19 Effect of inert gas flow rate at reaction temperature 180 °C on (a) acid number and (b) conversion: O 120 ccm, □ 360 ccm, × 600 ccm and Δ 840 ccm

5.6 Characterization of Unsaturated polyester from synthesis

Table 5.1 was listed the synthesized conditions, reaction time and their molecular weight. Temperature was varied in range 160-220 °C and inert gas flow was varied in the range 120-840 ccm. Both the number average molecular weight (M_n) and weight average molecular weight (M_w) were analyzed from GPC. The quantity M_w/M_n of the synthesized polyester were quite small if compare to typical condensation polymer which has the M_w/M_n around 2.0. [43] This feature indicated that the breadth of molecular weight distribution of synthesized polyesters were rather narrow, especially at low molecular weight. Thus, in the model and simulation that used M_n represented for the molecular weight of the liquid phase was reasonable.

Table 5.1 Synthesized conditions and molecular weight of unsaturated polyester

Sample	Reaction condition		Reaction time (s (HR))	Conversion (%)	M_n	M_w	M_w/M_n
	Temp. (°C)	N ₂ Flow (ccm)					
UP5	160	600	43523 (12:06)	87.26	596	726	1.21763
UP1	180	120	42912 (11:55)	87.24	489	539	1.10354
UP2	180	360	43553 (12:05)	90.54	591	704	1.19081
UP3	180	600	44680 (12:24)	93.50	649	830	1.27995
UP4	180	840	47374 (13:09)	95.74	750	1018	1.35685
UP8	200	360	34122 (09:29)	94.32	788	1081	1.34831
UP6	200	600	44993 (12:30)	95.89	-	-	-
UP7	200	840	31753 (10:49)	96.13	823	1001	1.21570
UP9	220	600	39250 (10:54)	98.25	856	1251	1.46281

Figure 5.20 showed the analyzed results of synthesized polyesters from FTIR. The characteristic bands of unsaturated polyester show their resemblance to standard unsaturated polyester, as listed in Table 5.1. The FTIR results illustrated that the inert gas flow rate had not effect to the molecular structure of unsaturated polyester product although the increasing flow accelerated the polyesterification.

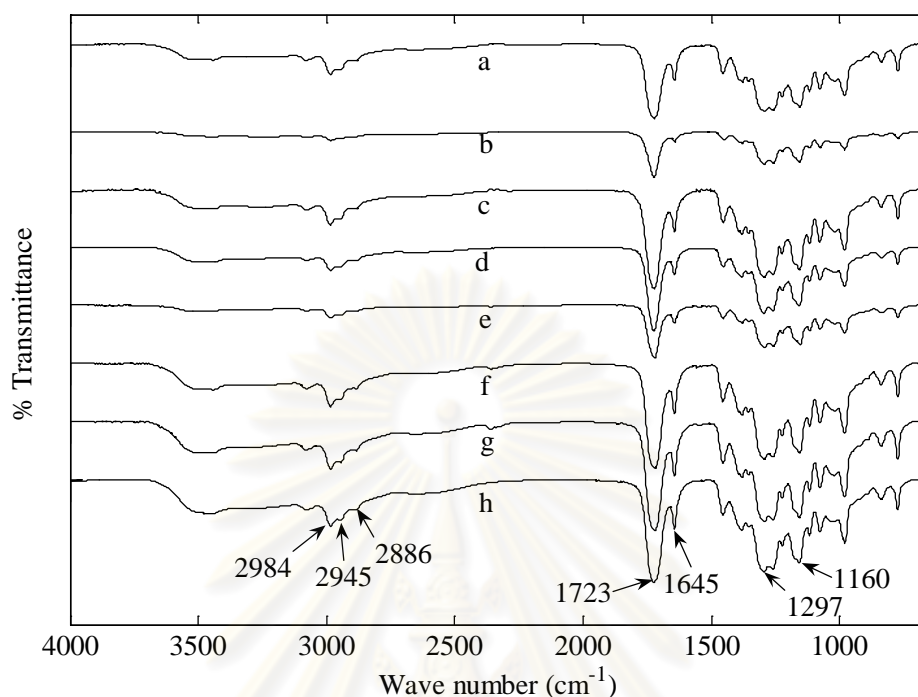


Figure 5.20 Representative FTIR spectra of synthesized unsaturated polyester: (a) UP9, (b) UP8, (c) UP7, (d) UP5, (e) UP4, (f) UP2, (g) UP2 and (h) UP1

Table 5.2 Functional group of unsaturated polyester resin and wave number (FTIR)

Functional group	Wave number (cm ⁻¹)
<i>Unsaturated polyester</i>	
Aliphatic C-H stretching	2984-2873
C=O stretching of C=O-O	1726-1717
Olefinic C=C stretching	1645-1636
C-O stretching of C=O-O	1297-1287
C-O stretching of O-CH ₂	1182-1121

5.7 Simulation results of process parameters

In this section, the inert gas flow rate and real temperature from experiments were used as input data in the simulation. The important parameters, the simulated results and their comparing to experimental data were presented and discussed.

5.7.1 Unsaturated polyester properties

The polymer properties from the simulation were plotted in Figure 5.21 as sample, operating at 220 °C and 600 ccm. These properties were increased when the polymerization progressed.

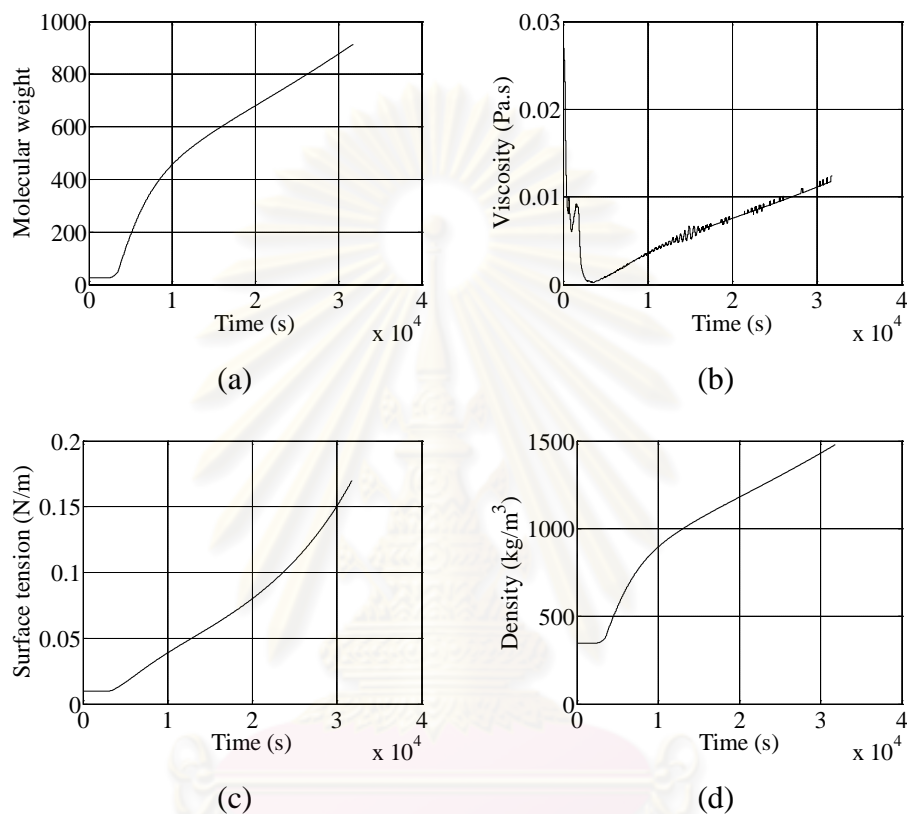


Figure 5.21 Unsaturated polyester properties from the simulation at reaction temperature 220 °C and inert gas flow 600 ccm: (a) molecular weight, (b) viscosity, (c) surface tension and (d) density

5.7.2 Energy dissipation

The plot of energy dissipation at constant reaction temperature 180 °C by varied inert gas flow was illustrated in Figure 5.22. Trend of these graph were slightly decreased as the reaction time progress cause of the liquid phase density increasing. When the inert gas flow rate increased, the energy dissipation was decreased cause of a bigger bubble was formed. This graph showed the trend of energy dissipation which concerned to the three dimensional plot in Figure 5.3. From figure 5.3 and 5.22, both two plots indicated significantly that continual increasing the inert gas flow rate

would obtain lower gain of energy dissipation. Hence, too high inert gas flow rate was more than enough and lost in process.

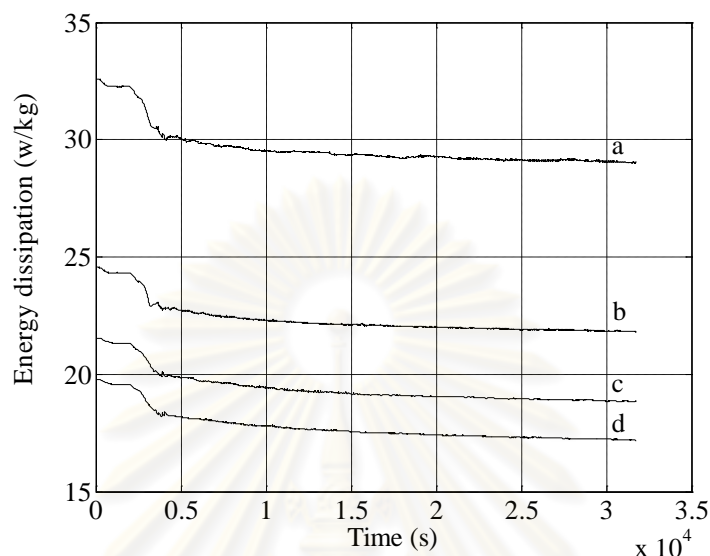


Figure 5.22 Energy dissipation at reaction temperature 180 °C: (a) 120 ccm, (b) 360 ccm, (c) 600 ccm, (d) and 840 ccm

5.7.3 Mass transfer coefficient

The mass coefficient was raised as step up when increased the reaction temperature at constant inert gas flow rate, Figure 5.23 presented this effectiveness. This occurrence can explain by equation 3.42), the mass transfer coefficient was proportional to the diffusivity which was the function of temperature (Comparing Figure 5.4a and 5.4b). Thus, reaction temperature seemed to have proportionally exact effect on mass transfer coefficient.

Meanwhile, the simulated results in case of increasing inert gas flow rate at constant reaction temperature were plotted in Figure 5.24. These plots illustrated that the higher inert gas flow rate induced mass transfer coefficient more declination. The decreasing of energy dissipation and increasing of viscosity as the polymerization progress caused of this declination, consider equation 3.42). Thus, inert gas flow rate seemed to have diverting effect on mass transfer coefficient, inverse proportion.

We can notice that, the declination in Figure 5.24 was clarity after reaction time around 7,500 s or at 75% conversion which concerned to Figure 5.19b. The simulated results in both Figure 5.23 and 5.24 were encouragement the three dimensional plot in Figure 5.5, 5.6 and 5.7.

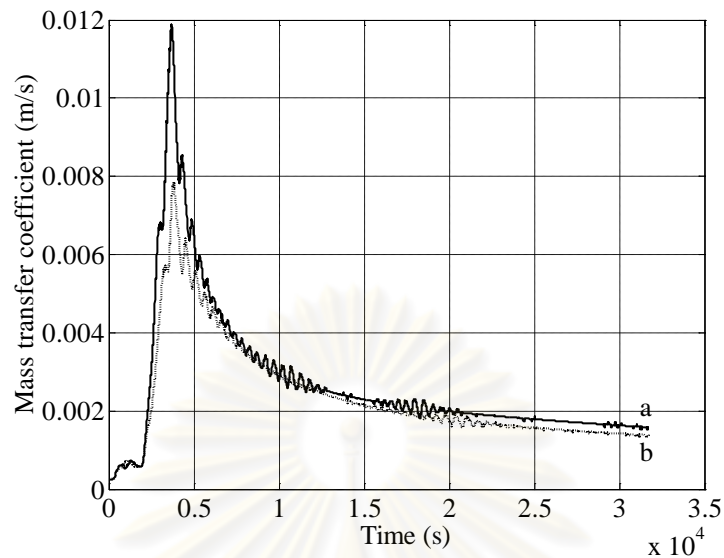


Figure 5.23 Effect of reaction temperature on mass transfer coefficient (H_2O), simulated at 600 ccm: (a) 200 °C and (b) 160 °C

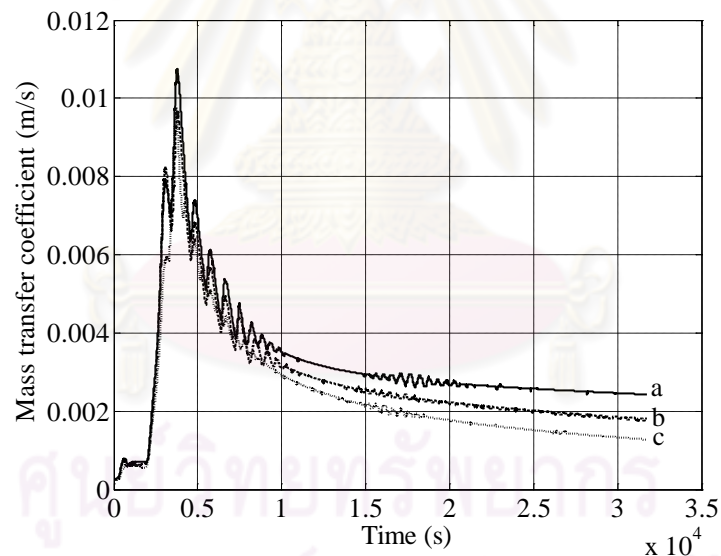


Figure 5.24 Effect of inert gas flow rate on mass transfer coefficient (H_2O), simulated at 180 °C: (a) 120 ccm, (b) 360 ccm, (c) and (d) 840 ccm

5.7.4 Gas hold-up and bubble size

The gas hold-up was more declination when the reaction temperature was increase as showed in Figure 5.25. The higher reaction temperature brought up the high reaction rate then both of viscosity and surface tension were increased faster, and the gas hold-up was more declined, see Figure 5.8c. Thus, reaction temperature seemed to have diverting effect on the gas hold-up, inverse proportion.

Figure 5.26 illustrated the step up rising of the gas hold-up when the inert gas flow rate was increased. From equation 3.46) and Figure 5.26, we could summarize that the inert gas flow rate seemed to have proportionally exact effect on the gas hold-up. Both Figure 5.25 and 5.26 confirmed the same results as the surface plot in Figure 5.9.

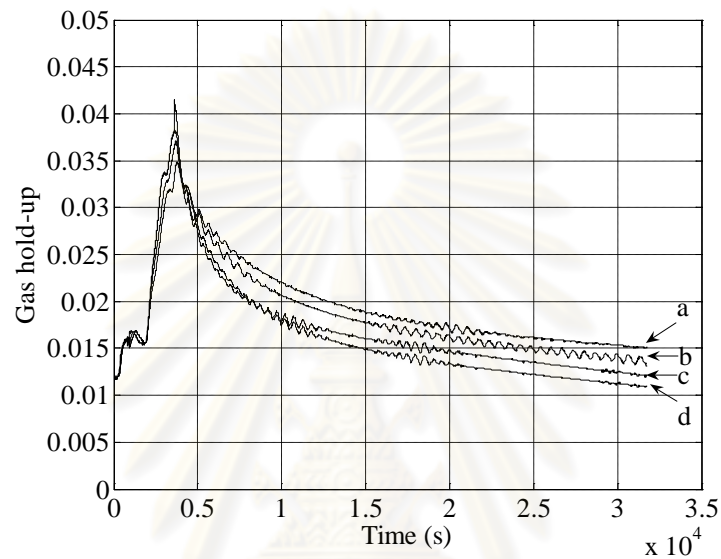


Figure 5.25 Effect of reaction temperature on gas hold-up, simulated at 600 ccm: (a) 160 °C, (b) 180 °C, (c) 200 °C and (d) 220 °C

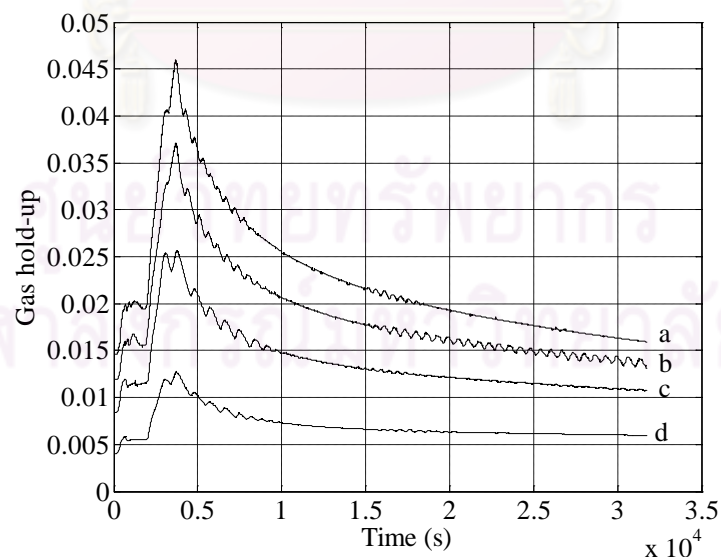


Figure 5.26 Effect of inert gas flow rate on gas hold-up, simulated at 180 °C: (a) 840 ccm, (b) 600 ccm, (c) 360 ccm and (d) 120 ccm

The bubble sizes from the simulations were plotted in Figures 5.27 and 5.28. The bubble became bigger as the polymerization progress caused of higher surface tension, see Figure 5.11. Figure 5.27 illustrated the inclination of the bubble size when increasing of reaction temperature, seemed to have proportionally diverting affectation. Meanwhile, the bubble sizes in Figure 5.28 were step up rising when increasing of insert gas flow rate, seemed to have proportionally exact affectation.

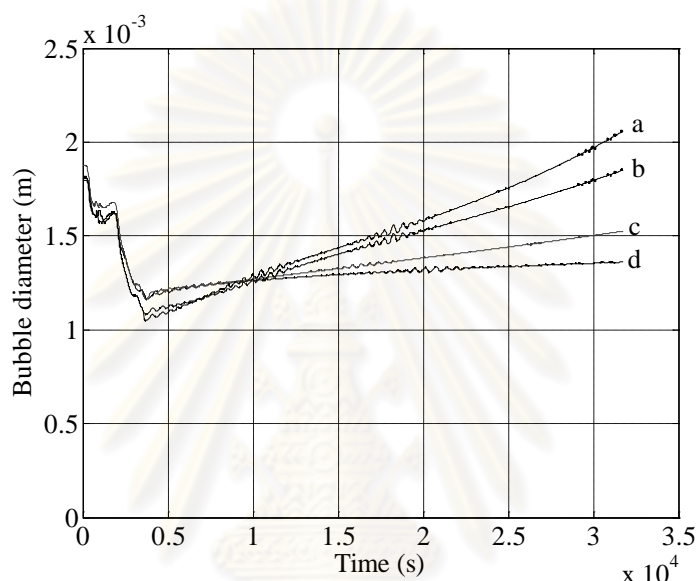


Figure 5.27 Effect of reaction temperature on bubble size, simulated at 600 ccm: (a) 220 °C, (b) 200 °C, (c) 180 °C and (d) 160 °C

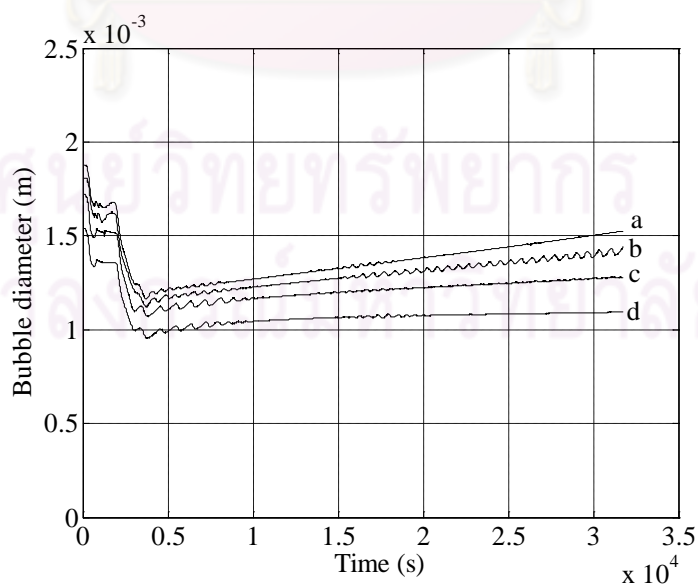


Figure 5.28 Effect of inert gas flow rate on bubble size, simulated at 180 °C: (a) 840 ccm, (b) 600 ccm, (c) 360 ccm and (d) 120 ccm

5.7.5 Specific interfacial area

The specific interfacial area was the ratio between the gas hold-up and bubble diameter. Both two parameters seemed to have diverting affectation from reaction temperature and seemed to have exact affectation from the inert gas flow rate. Also, the specific interfacial area seemed to have the same affectation from reaction temperature and the inert gas flow rate as the gas hold-up and the bubble diameter.

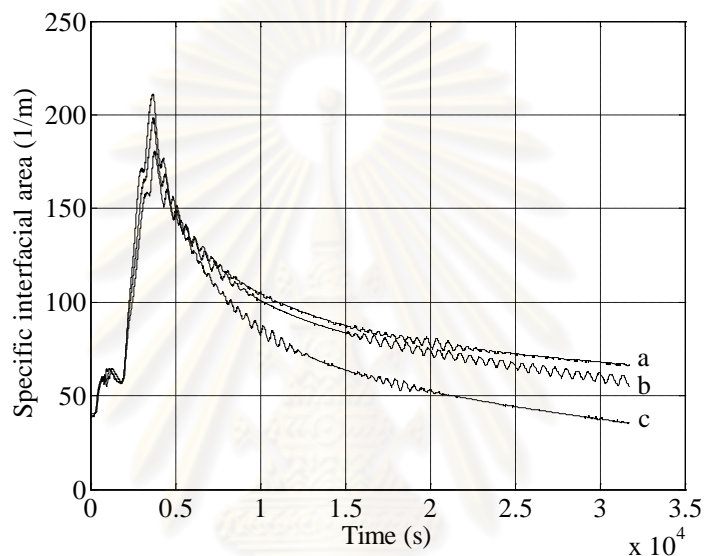


Figure 5.29 Effect of reaction temperature on specific interfacial area, simulated at 600 ccm: (a) 160 °C, (b) 180 °C and (c) 200 °C

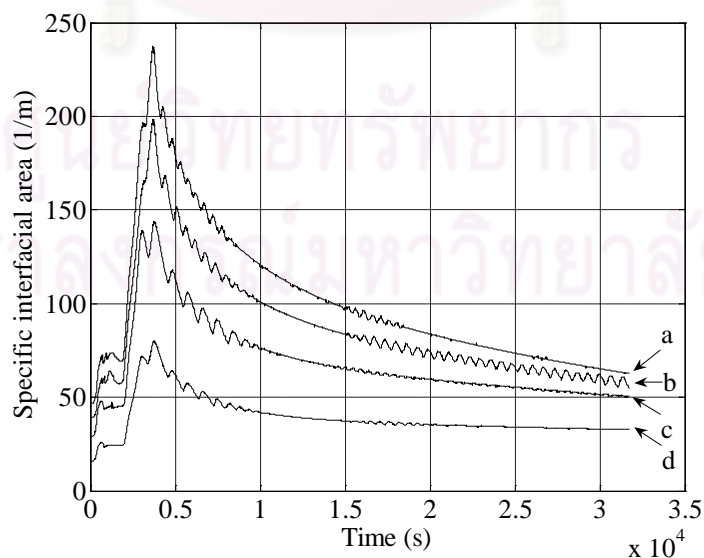


Figure 5.30 Effect of inert gas flow rate on specific interfacial area, simulated at 180 °C: (a) 840 ccm, (b) 600 ccm, (c) 360 ccm and (d) 120 ccm

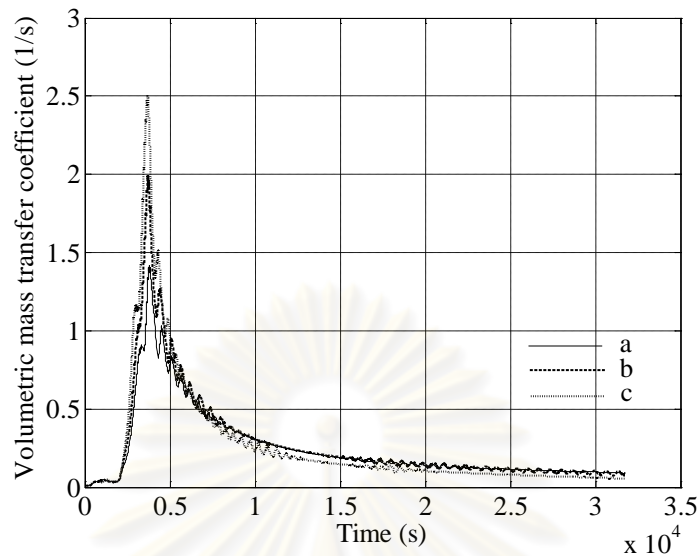


Figure 5.31 Effect of reaction temperature on volumetric mass transfer coefficient (H_2O), simulated at 600 ccm: (a) 160 °C, (b) 180 °C and (d) 200 °C

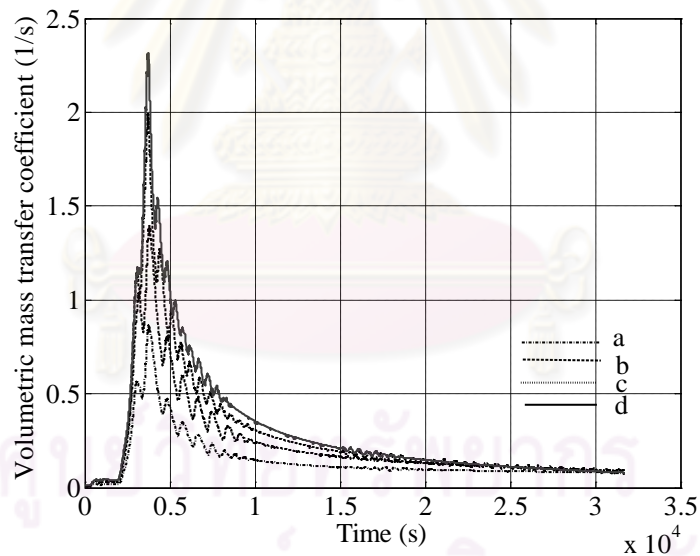


Figure 5.32 Effect of inert gas flow rate on volumetric mass transfer coefficient (H_2O), simulated at 180 °C: (a) 120 ccm, (b) 360 ccm, (c) 600 ccm and (d) 840 ccm

5.7.6 Volumetric mass transfer coefficient

Volumetric mass transfer coefficient was the multiple products between the mass transfer coefficient and the specific interfacial area. From section 5.6.3), the mass transfer seemed to have exact affectation from reaction temperature and seemed to have diverting affectation from inert gas flow rate. But from section 5.6.5), the

specific interfacial area seemed to have diverting affectation from reaction temperature and seemed to have exact affectation from the inert gas flow rate. Thus, it was rather difficult to identify the effect of both process conditions on volumetric mass transfer coefficient. The effect of temperature was illustrated in Figure 5.31 and the effect of the inert gas flow rate was illustrated in Figure 5.32. Increasing of both two process conditions had high influence on the volumetric mass transfer at the beginning of polymerization. Hence, the highest water removal rate should occur and induce to high polyesterification rate at this zone. Furthermore, for long reaction time the value of the volumetric mass transfer was convergent to a low and constant value. The simulated results in these two figures were concerned to the three dimensional plot in Figure 5.14 and 5.15.

5.8 Comparison of simulation results to experimental data

5.8.1 Acid number

The decreasing of acid number from the simulation was plotted and illustrated in Figure 5.33 and 5.34. Reaction temperature seemed to have exact effect on acid number, see Figure 5.33. Meanwhile, the inert gas flow rate seemed to have diverting effect on acid number as shown in Figure 5.34.

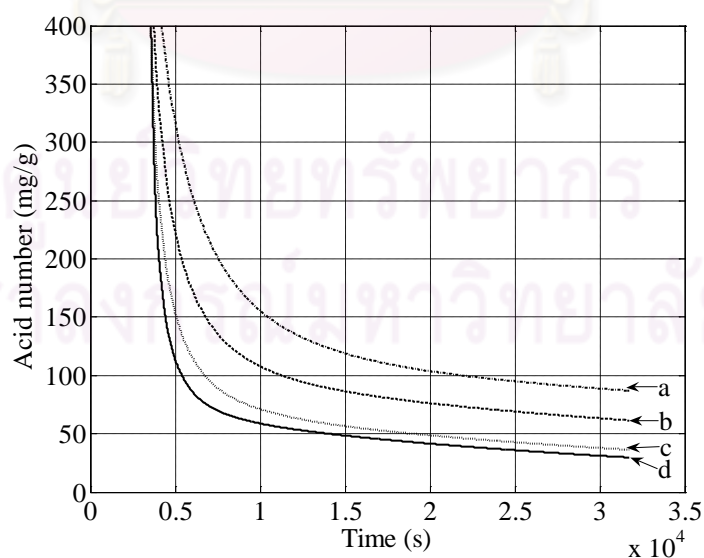


Figure 5.33 Acid number, simulated at inert gas flow rate 600 ccm: (a) 160 °C, (b) 180 °C, (c) 200 °C and (d) 220 °C

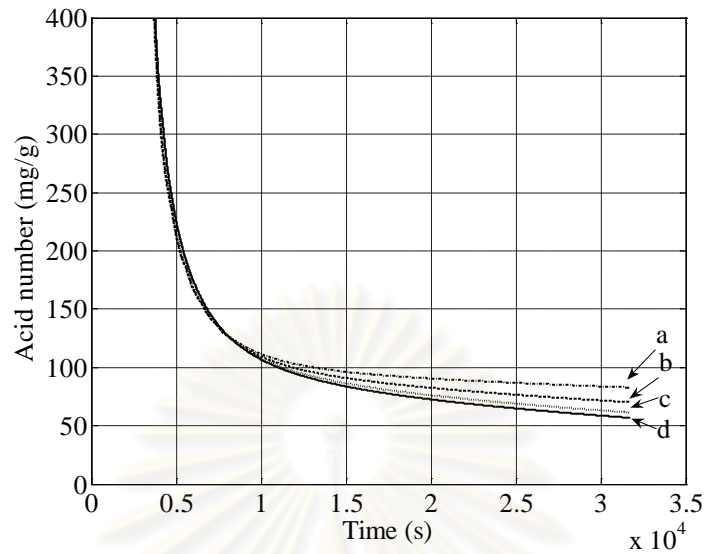


Figure 5.34 Acid number, simulated at 180 °C: (a) 160 ccm, (b) 360 ccm, (c) 600 ccm and (d) 840 ccm

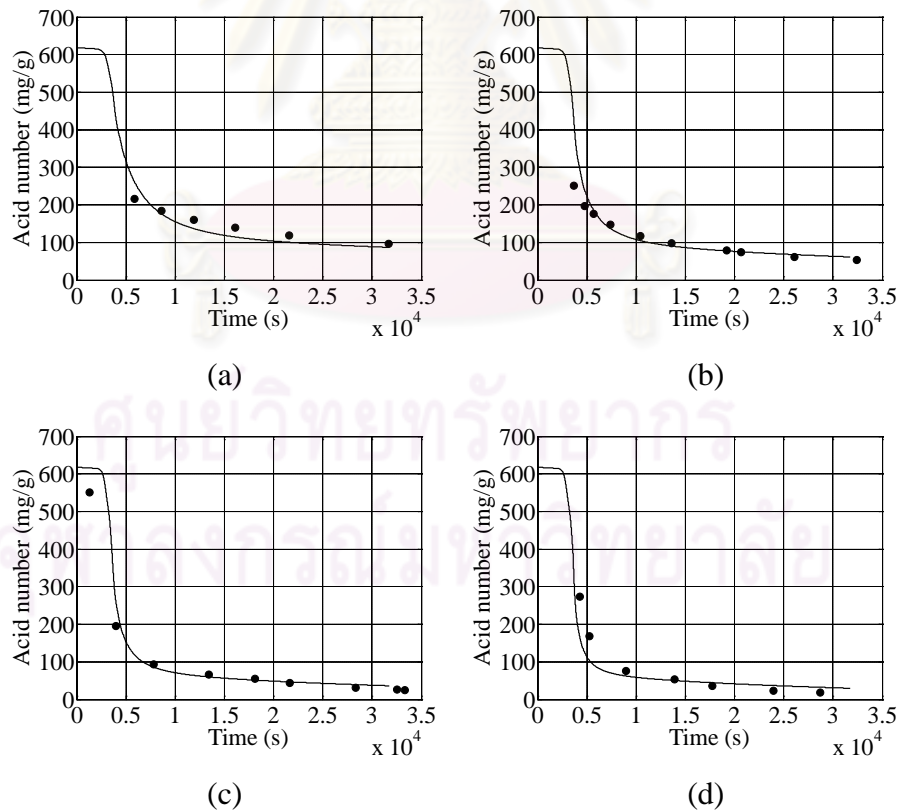


Figure 5.35 Comparison of acid number at constant N_2 flow 600 ccm, —simulation and • experiment: (a) 160 °C, (b) 180 °C, (c) 200 °C and (d) 240 °C

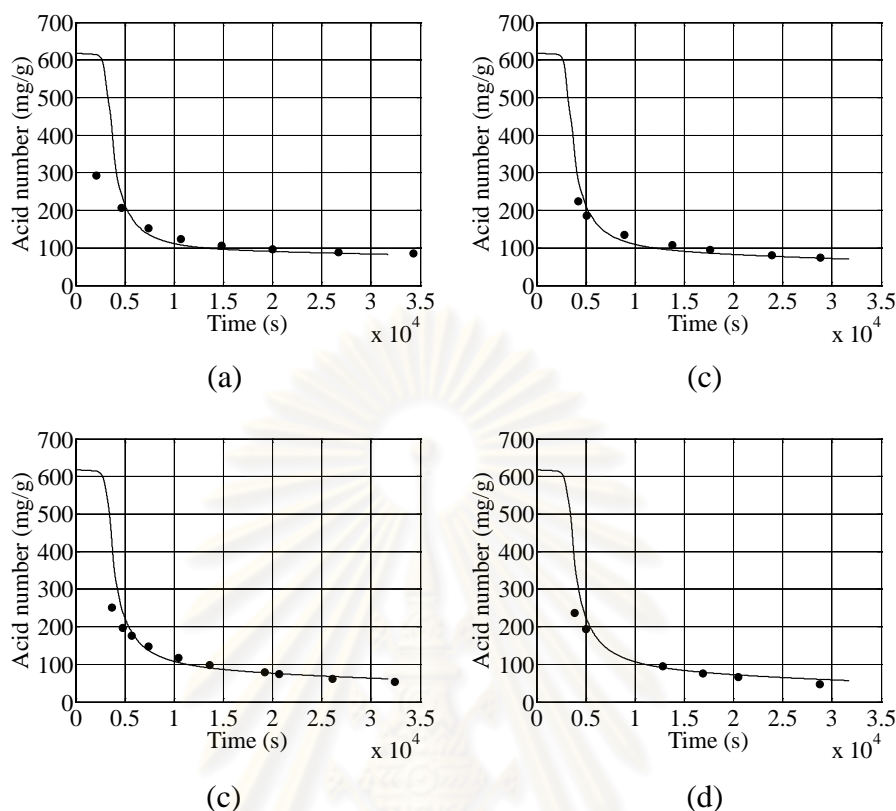


Figure 5.36 Comparison of acid number at reaction temperature 180 °C, —simulation and • experiment: (a) 120 ccm, (b) 360 ccm, (c) 600 ccm and (d) 800 ccm

From these simulated results, both of reaction temperature and the inert gas flow rate could increase the condensation polymerization rate. Generally of polyesterification, increasing of reaction temperature is directly effect to the polymerization rate via the higher rate constant. In case of the inert gas flow rate, the reaction was driven toward the production size because the higher water removal which caused from increasing of the volumetric mass transfer coefficient.

From Figure 5.34, we could notice that increasing of inert gas flow rate would have dominantly effect when the reaction conversion reached to around 75%, defining as effective point. These simulated results had same phenomenon as the experimental data in Figure 5.19 which had the same effective point around 75% conversion.

Figures 5.35 and 5.36 were the plot of acid number which compared the simulation result to the experimental data by varying the reaction temperature and inert gas flow rate, respectively. The simulation showed good agreement with the experiment.

5.8.2 Propylene glycol content in condensate

Figure 5.37 was the plot of propylene glycol content in condensate. Both simulation and experiment had small amount of propylene glycol, less than 0.5%. We could presume that almost of the condensate content was water.

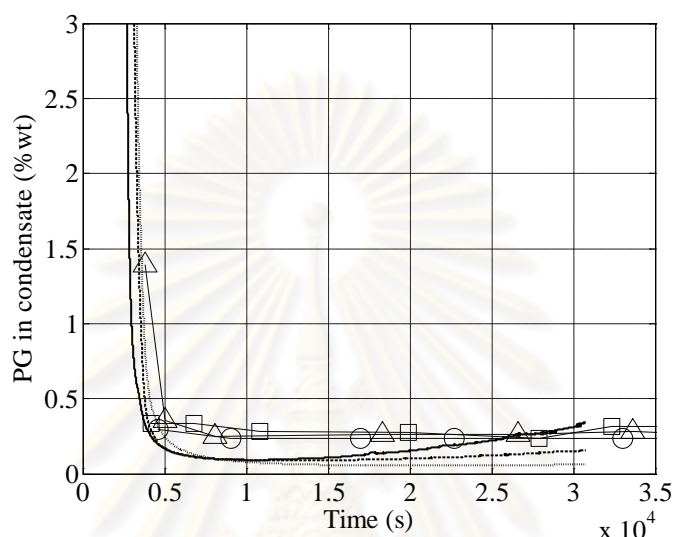


Figure 5.37 Propylene glycol content in condensate at N_2 flow rate 600 ccm: simulation 160 °C, - - 180 °C and — 200 °C, experiment o 160 °C, □ 180 °C and Δ 200 °C

5.8.3 Accumulative condensate

The condensate from the condenser which weighed and recorded as accumulation during the polymerization was plotted and compared to the simulated result. Figure 5.38 presented the effect of reaction temperature. The higher amount of condensate caused from the higher reaction rate as the reaction temperature increased. Figure 5.39 was the effect of inert gas flow rate. The higher water removal from inert gas flow rate increasing induced the higher amount of condensate. The simulation line in both two figures showed fair agreement with the experimental.

5.8.4 Water content in unsaturated polyester

Water content in synthesized unsaturated polyesters was measured during polyesterification and their plots were showed in Figure 5.40. At high reaction temperature 200 °C, the model gave good simulation result as show in Figure 5.40(a). In case of moderate and low reaction temperature, the water content was rather high if

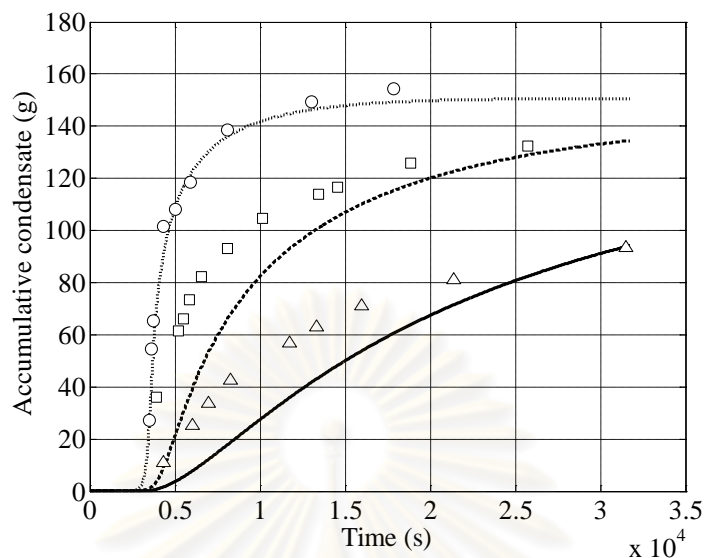


Figure 5.38 Comparison of accumulative condensate at constant N_2 flow rate 600 ccm: simulation — 160 °C, ---- 180 °C and 200 °C, experiment Δ 160 °C, \square 180 °C and \circ 200 °C

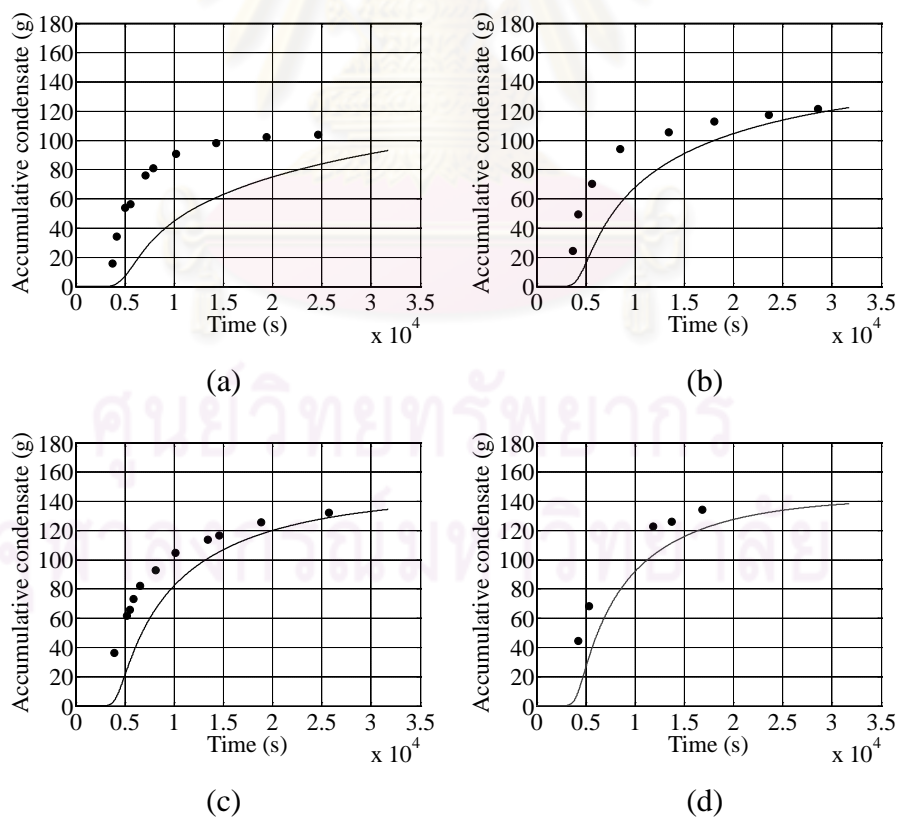
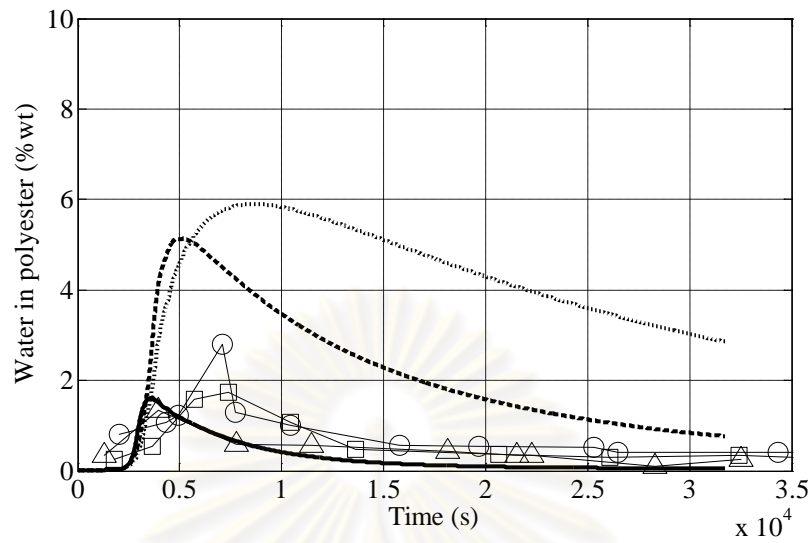
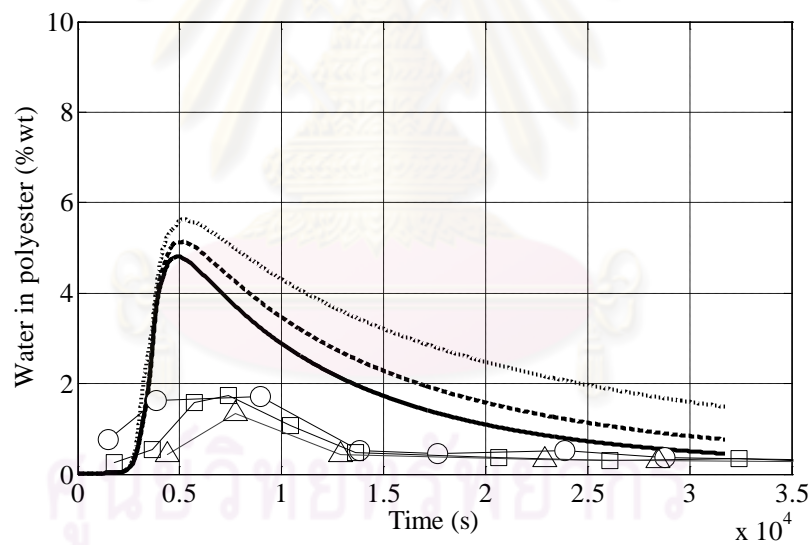


Figure 5.39 Comparison of accumulative condensate at reaction temperature 180 °C, — simulation and \bullet experiment: (a) 120 ccm, (b) 360 ccm, (c) 600 ccm and (d) 800 ccm



(a)



(b)

Figure 5.40 Water content in unsaturated polyester

(a) N_2 flow rate 600 ccm: simulate 160 °C, - -180 °C and — 200 °C,
 experiment o 160 °C, □ 180 °C and Δ 200 °C

(b) Reaction temperature 180 °C: simulation 360 ccm, - -600 ccm and — 840
 ccm, experiment o 360 ccm, □ 600 ccm and Δ 840 ccm

compare to the experimental data. Furthermore, higher amount of water in polyester indicated that the gas phase which transferred to the condenser had low water concentration. Thus, small amount of water was condensed and caused of lag prediction of accumulative condensate, see Figure 5.38 and 5.39.

The cause of lag prediction might come from too low value of vapor liquid equilibrium, too low of volumetric mass transfer coefficient and too high of polyesterification rate at the beginning of polymerization.

5.9 Concentration of each species in liquid phase

The concentrations proceeding of each species were plotted in Figure 5.41. The trans-ester was dominant product and follow by the saturated ester. This result indicated that more amount of excess propylene glycol was use in the Ordelt's saturation.

Figure 5.42 showed water concentration in bulk polymer during polyesterification at constant reaction temperature 180 °C. By increasing the inert gas flow rate, we found that water concentration in polyester was reduced. These simulation results confirmed that higher amount of water was transferred out from melt polymer.

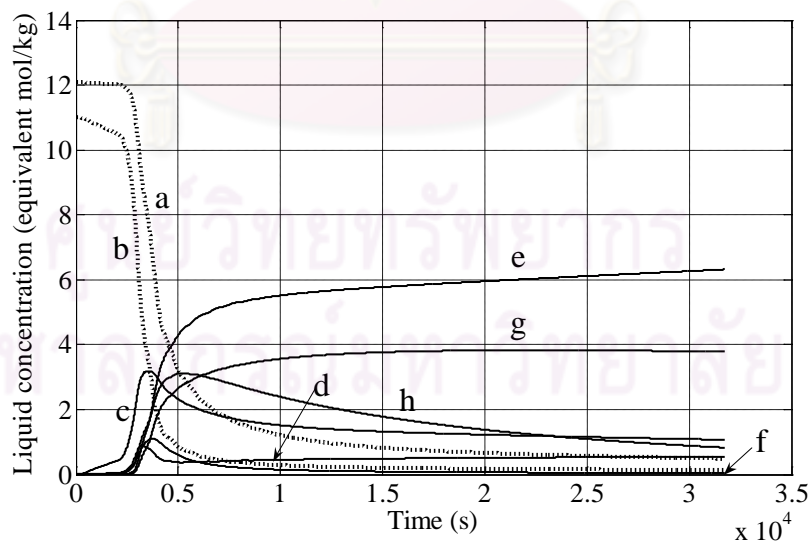


Figure 5.41 Liquid concentration of each species, reaction temperature 160 °C and inert gas flow rate 360ccm: (a) OH, (b) COOH1D, (c) COOH2D, (d) COOR1D, (e) COOR2D, (f) COOHS, (g) COORS and (h) H₂O

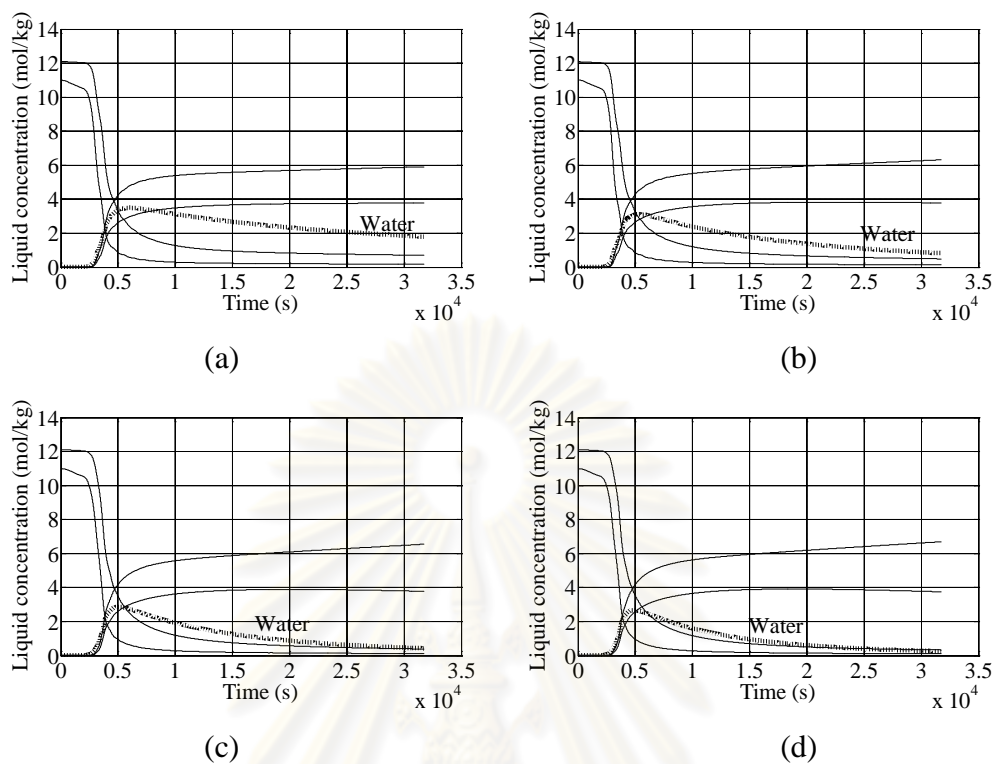


Figure 5.42 Water concentration in liquid phase at reaction temperature 180 °C: (a) 120 ccm, (b) 360 ccm, (c) 600 ccm and (d) 840 ccm

ศูนย์วิทยทรัพยากร
จุฬาลงกรณ์มหาวิทยาลัย

CHAPTER VI

CONCLUSIONS AND RECOMMENDATIONS

This work was carried out to predict the effect of operating conditions, reaction temperature and the inert gas flow rate, on polyesterification of unsaturated polyester. Because of Newtonian behavior of unsaturated polyester, then the complicate system could study by modeling and simulation. This research used the typical polymerized system between maleic anhydride and propylene glycol as a model reaction to rid of the kinetic complexity.

The developed dynamic model consisted of three parts, the reactor model, the kinetic model and the mass transfer model. The kinetic model was used to generate the ordinary differential equation in the reactor model meanwhile the mass transfer model was used to estimate needed parameters. The reactor model was core of the simulation and the answer of this simulation was done by the unsteady state solving during an interval time 1 second. The developed model could reasonable predict the effect of operating condition on the important parameters in the process, such as the energy dissipation, diffusivity, mass transfer coefficient, gas hold-up, mean bubble size, specific interfacial area and volumetric mass transfer coefficient. The predicted result conceived and brought about comprehensibility of both polyesterification and mass transfer which simultaneous occurrence. The simulation results indicated that the volumetric mass transfer coefficient was not constant during the polymerization, which quite differed from the previous research that used constant value in the model. This parameter was high at the beginning and decreased as the polymerization progress because of higher surface tension and viscosity. Increasing of reaction temperature and the inert gas flow rate had high influence on the volumetric mass transfer coefficient at the beginning of polymerization and enhanced the mass transfer.

From the simulation, the trans-ester and saturated-ester were the main products from polyesterification. Both of reaction temperature and the inert gas flow rate influenced the process parameters by exact and diverting effect. For reaction temperature, it seemed to have exact effect on mass transfer coefficient and diverting

effect on bubble size, gas hold-up and specific interfacial area. For the inert gas flow, it seemed exact effect on energy dissipation, bubble size, gas hold-up and specific interfacial area, but for mass transfer coefficient it seemed to have diverting effect. The effect of reaction temperature and the inert gas flow were more complicated to the volumetric mass transfer coefficient.

Generally, increasing of temperature would increase the rate of condensation polymerization by enhancement of rate constants, thus the reaction time should decrease. In case of increasing of inert gas flow at high turbulent regime, the polymerization system would obtain higher specific interfacial area for mass transfer. Hence, it can increase the rate of condensation polymerization and reduce the reaction time too. The inert gas flow rate dominantly affected the polymerization rate after the polyesterification reached the effective point which was around 75% conversion. Although the inert gas flow rate can enhance polyesterification rate, a too high increase would result in a drop in the gain and became loss of N₂ consumption in process.

To verify the simulated result, the polymerization reactor was set up for unsaturated polyester synthesis. Small amount of polyester was taken up as sampling to measure the process identification such as, acid number, water content and accumulative condensate. The comparison of the simulation and experiment gave a satisfaction and the developed model was valid.

Recommendations

To achieve a higher value of the specific interfacial area for mass transfer we can improve the process by adding of surfactant in melt polymer during polyesterification to obtain the smaller bubble and higher gas hold-up.

To reduce of the amount of inert gas using, the optimization of inert gas flow rate can be done by applying of effective point for inert gas feeding, the research can presume by using of the model.

REFERENCES

- [1] Lawrence, J. R. Polyester Resins. New York: Van Nostrand Reinhold, 1960.
- [2] Varma, I. K., and Gupta, V. B. Comprehensive Composite Materials [Online]. 2000. Available from: <https://www.ing.unimore.it> [2010, July]
- [3] Goodman, S. H. Handbook of Thermoset Plastics 2nd. New Jersey: Noyes publication, 1998.
- [4] Parkyn, B., Lamb, F., and Clifton, B.V. Polyesters. Vol. 2. London: London Life Books, 1967.
- [5] Irfan, M. H. Chemistry and Technology of Thermosetting Polymers in Construction Applications. Netherlands: Kluwer Academic Publishers, 1998.
- [6] King, M. Global Unsaturated Polyester Resin (UPR) 2010-2015: Trends, Forecast and Opportunity Analysis [Online]. 2010. Available from <http://www.pr-inside.com/global-unsaturated-polyester-resin-market-r1788314.htm> [2010, July]
- [7] Fradet, A., and Marechal, E. Study on models of double saturation during the synthesis of unsaturated polyester. Macromol. Chem. 118(1982b): 319-329.
- [8] Baehr, H. D.; Stehpan, K. Heat and mass transfer. Berlin: Springer, 1998.
- [9] Welty, J. R., Wicks, C. E., Wilson, R. E., and Rorrer, G. Fundamentals of momentum, heat and mass transfer 4th. Singapore: John Wiley & Sons, 2001.
- [10] Wilke, C. R., and Chang, P. Correlation of diffusion coefficients in dilute solutions. AIChE J., 1(1955), 264-274.
- [11] Whitman, W.G. Preliminary experimental confirmation of the two-film theory of gas absorption. Chem. Metall. Eng. 29(1923): 146-148.
- [12] Higbie, R. The rate of absorption of a pure gas into a still liquid during short periods of exposure. Trans. Amer. Inst. Chem. Eng. 31(1935): 365-389.
- [13] Danckwerts, P.V. Significance of liquid-film coefficients in gas absorption. Ind. Eng. Chem. 43(1951): 1460-1467.
- [14] Astarita, G., and Savage, D.W. Theory of chemical desorption. Chem. Eng. Sci. 35(1980): 649-656.
- [15] Astarita, G. Mass transfer with chemical reaction. Amsterdam: Elsevier, 1967.

- [16] Bakker, A. Komogoroff's theory-Applied computational fluid dynamics
[Online]. 2002. Available from: www.bakker.org/dartmouth06/engs150/09-kolm.ppt [2010, May]
- [17] Paatero, E., Narhi, K., Salmi, T., Still, M., Nyholm, P., and Immonen, K. Kinetic model for main and side reaction in the polyesterification of dicarboxylic with glycol. Chem. Eng. Sci. 49(1994): 3601-3616.
- [18] Salmi, T., Paatero, E., Nyholm, P., and Narhi, K. Kinetic of melt polymerization of maleic and phthalic acids with propylene glycol. Chem. Eng. Sci. 49(1994): 5053.
- [19] Lehtonen, J., Immonen, K., Salmi, T., Paatero, E., and Nyholm, P. Kinetic analysis of the reaction network in the catalyzed polyesterification of unsaturated carboxylic acids. Chem. Eng. Sci. 51(1996): 2799.
- [20] Salmi, T., Paatero, E., Lehtonen, J., Nyholm, P., and Harju, T. Polyesterification kinetics of complex mixtures in semibatch reactors. Chem. Eng. Sci. 56(2001): 1293.
- [21] Nalampang, K., and Johnson, A. F. Kinetics of polyesterification: modeling and simulation of unsaturated polyester synthesis involving 2-methyl-1,3-propanediol. Polymer 44(2003): 6130.
- [22] Zetterlund, P. B., Weaver, W., and Johnson, A. F. Kinetic of polyesterification: Modeling of the condensation of maleic anhydride, phthalic anhydride and 1,2-propylene glycol. Polym. React. Eng. 10(2002): 41.
- [23] Korbar, J., Golob, J., and Sebenik, A. Process of unsaturated polyester resin synthesis on a laboratory and industrial scale. Polym. Eng. Sci. 33(2004): 1212.
- [24] Salmi, T., Paatero, E., and Nyholm, P. Kinetic model for the increase of reaction order during polyesterification. Chem. Eng. Proc. 43(2004): 1487.
- [25] Dairanieh, I. S., and Rasoul, F. A. Bench-scale and pilot plant preparation of chemically modified polyester resins. J. App. Polym. Sci. 42(1991): 1623.
- [26] Boodhoo, K. V. K., and Jachuck, R. J. Process intensification: spinning disc reactor for condensation polymerization, Green Chemistry 2(2000): 235.

- [27] Lethonen, J., Salmi, T., Harju, T., Immonen, K., Pattero, E., and Nyholm, P. Dynamic modeling of simultaneous reaction and distillation in a semibatch reactor system. Chem. Eng. Sci. 53(1998): 113.
- [28] Flory, P. J. Kinetics of polyesterification: A study of the effects of molecular weight and viscosity on reaction rate. J. Am. Chem. Soc. 61(1939): 3334.
- [29] Lehtonen, J., Salmi, T., Immonen, K., Paatero, E., and Nyholm, P. Kinetic model for the homogeneously catalyzed polyesterification of dicarboxylic acids with diols. Ind. Eng. Chem. Res. 35(1996): 3951-3963.
- [30] Kawase, Y., Halard, B., and Moo-Young, M. Theoretical prediction of volumetric mass transfer coefficients in bubble columns for Newtonian and non-Newtonian fluids. Chem. Eng. Sci. 42(1987): 1609-1617.
- [31] Lamont, J. C., and Scott, D. S. An eddy cell model of mass transfer into the surface of a turbulent liquid. AIChE J. 16(1970): 513-519.
- [32] Prasher, B. D., and Wills, G. B. Mass transfer in agitated vessel. Ind. Eng. Chem. Process 12(1973): 351-354.
- [33] Thixotropic unsaturated polyester compositions and methods. United States Patent 4497918 [Online]. 1985. Available from: www.freepatentsonline.com/4497918.html [2010, September]
- [34] Kudrewizki, F., and Rabe, P. Model of the dissipation of mechanical energy in gassed stirred tanks. Chem. Eng. Sci. 41(1986): 2247-2252.
- [35] Kawase, Y., and Hashiguchi, N. Gas-liquid mass transfer in external-loop airlift columns with Newtonian and non-Newtonian fluids. Chem. Eng. J. 62(1996): 35-42.
- [36] Bhavaraju, S. M., Russell, T. W. F., and Blanch, H. W. The design of gas sparged devices for viscous liquid systems. AIChE J. 24(1978): 454-466.
- [37] Treybal, R. E. Mass-transfer operation 3rd. Singapore: McGraw-Hill, 1981.
- [38] Rushton, J.H., Costich, E.W., and Everett, H.J. Power characteristics of mixing impeller. Chem. Eng. Prog. 46(1950): 395-404.
- [39] Abrardi, V., Rover, G., Sicardi, S., Baldi, G., and Conti, R. Sparged vessels agitated by multiple turbines. Proc. Eur. Conf. Mix. 6(1988): 329-336.
- [40] Standard methods of testing urethane foam polyol raw materials. ASTM D2849-69(1980): 608-628.

- [41] Yan-Jyi, H., and Wen-Ching, J. Effect of chemical composition and structure of unsaturated polyester resins on the miscibility, cure sample morphology and mechanical properties for styrene/unsaturated polyester/low-profile additive ternary systems.1: Miscibility and cured sample morphology. Polymer 39(1998): 6631-6641.
- [42] Seader, J.D., and Henley, E. J. Seperation process principles 2nd. Singapore:John Wiley & Sons, Inc., 2005.
- [43] Billmeyer, F. W. Textbook of polymer science. Singapore: John Wiley & Sons, Inc., 1984.



ศูนย์วิทยทรัพยากร
จุฬาลงกรณ์มหาวิทยาลัย



APPENDICES

ศูนย์วิทยทรัพยากร
จุฬาลงกรณ์มหาวิทยาลัย

APPENDIX A

DEFINATION

Acid and hydroxyl number

The acid numbers and hydroxyl number serve as characteristic data for the identification of plastics. Both values apply predominantly to plastic that are esters. Determination is under the standard method ASTM D 2849 and DIN 53420.

Determination of acid number

Dissolve 1-5 g of the sample in 20 ml of titration solvent, acetone was use in this research. Titrate immediately with 0.1 N NaOH or KOH in the presence of phenolphthalein until a light pink color appears. A blank titration with 20 ml of solvent must also be run. The acid number is defined as the number of milligrams of KOH required to neutralize 1 g of the substance.

$$\text{Acid number} = 56.1 \left(\frac{(A-B)N}{W} \right)$$

Where A = ml NaOH (KOH) required to titrate sample

B = ml NaOH (KOH) required to titrate blank

N = normality of NaOH (KOH)

W = grams of sample used

Determination of hydroxyl number

For basic substance the hydroxyl number can determine by following the procedure below.

At the end point of acid number determination, add 0.1 N HCL to the mixture until the solution is colorless then add 1.0 ml excess. Back-titrate to end point with 0.1 N NaOH. A blank must also be titrated containing the same amount of 0.1 N HCl added. The hydroxyl number is defined as the number of milligrams of KOH equivalent to the hydroxyl content of 1 g of the substance.

$$\text{Hydroxyl number} = 56.1 \left(\frac{(B-A)N}{W} \right)$$

Where A = ml NaOH required to titrate sample

B = ml NaOH required to titrate blank

N = normality of NaOH

W = grams of sample used



ศูนย์วิทยทรัพยากร
จุฬาลงกรณ์มหาวิทยาลัย

APPENDIX B

Table B.1 Unsaturated polyester synthesized conditions and initial mass of each conditions

Synthesized No.	Reaction condition		Maleic anhydride (kg)	Propylene glycol (kg)
	Temp. (°C)	N ₂ Flow (ccm)		
UP5	160	600	0.9161	0.7819
UP1	180	120	0.9150	0.7810
UP2	180	360	0.9160	0.7818
UP3	180	600	0.9150	0.7810
UP4	180	840	0.9160	0.7818
UP8	200	360	0.9170	0.7827
UP6	200	600	0.9164	0.7821
UP7	200	840	0.9162	0.7820
UP9	220	600	0.9165	0.7819

ศูนย์วิทยทรัพยากร
จุฬาลงกรณ์มหาวิทยาลัย

APPENDIX C

DYNAMIC MODEL

Some part which necessary for simulation were written down here. All of these programs were programmed by MATLAB.

C.1 Overall model

C.1.1 Model for reaction temperature 180 °C and N₂ 360 ccm

```
function model9 %(Temperature180 °C and N2360 ccm)
%Import reaction temperature file
%Estimate of kLa
ndata1 = xlsread('Temp180N360.xls',1, 'B2:B4'); %initial weight
ndata2 = xlsread('Temp180N360.xls',1, 'C8:H31760'); %Actual temperature
n0 = [ndata1(1)/76.09*2; ndata1(2)/98.06*2; 0; 0; 0; 0; 0; 0; 0; 0];
% 1 mole of reactants = 2 functional group
%[OH; COOH1D; COOH2D; COOR1D; COOR2D; COOHS; COORS; H2O; VOH;
VH2O]
N2 = ndata1(3)/1000/60; %N2 standard cm3/min to lit/sec
times = ndata2(:,1);
maxtime = times(size(times,1),1);
TLdata = ndata2(:,6); %Liquid temp.
TVdata = ndata2(:,5); %Vapor temp.
TCdata = ndata2(:,2); %Top column temp.
TWIdata = ndata2(:,3); %Cooling water input temp.
TWOdata = ndata2(:,4); %Cooling water output temp.
%initial condition
KmA = [0; 0; 0; 0; 0; 0; 0; 0; 0];
P=1; %atm
nN2t = N2/22.4; %mol/sec
mL = (ndata1(1)+ndata1(2))/1000; %kilogram
%variable for integrate
tspan = [0 1];
n = zeros(maxtime,10);
concl = zeros(maxtime,10);
reactionrate = zeros(maxtime,10);
removalrate = zeros(maxtime,4);
%Flash condenser variable
PBelowDP = 0;
PAboveBP = 0;
Twophase = 0;
%weight loss variable
dmL = zeros(4,1);
```

```

condensate =zeros(1,2);
nGout = zeros(1,4);
%Properties variable-----
Acidno = zeros(maxtime,1);
OHno = zeros(maxtime,1);
MWn = zeros(maxtime,1);
Density = zeros(maxtime,1);
SurfTension = zeros(maxtime,1);
Viscosity = zeros(maxtime,1);
Diffusepg = zeros(maxtime,1);
Diffuseh2o = zeros(maxtime,1);
Renold = zeros(maxtime,1);
Powerconsume = zeros(maxtime,1);
Powerunareated = zeros(maxtime,1);
Powerdissipate = zeros(maxtime,1);
kLpg= zeros(maxtime,1);
kLh2o= zeros(maxtime,1);
Gasholdup = zeros(maxtime,1);
BBsize = zeros(maxtime,1);
InterArea = zeros(maxtime,1);
kLaPG = zeros(maxtime,1);
kLah2o = zeros(maxtime,1);
summassconden = zeros(maxtime,2);
totalconden = zeros(maxtime,1);
percentmassconden = zeros(maxtime,2);
waterpercent = zeros(maxtime,1);
%start up program-----
for i = 1:maxtime
    %TL=TLdata(i)+3;
    %TV=TVdata(i)+3;
    %TC=TCdata(i);
    %TWI=TWIdata(i);
    %TWO=TWOdata(i);
    if i < 3500
        TL=0;
        TV=0;
        TC=25;
        TWI=15;
        TWO=25;
    else
        TL=180;
        TV=180;
        TC=25;
        TWI=15;
        TWO=25;
    end
end
%-----

```

```

[t,y] = ode15s(@F,tspan,n0,[],mL,nN2t,KmA,TL,TV);
%-----
n(i,:) = y(size(y,1),:);
n0 = n(i,:);
%-----
[NA1,NA8,nGt1 nGt8] = Gasmolarflow (n0,mL,nN2t,KmA,TV);
%-----
Feed = nGt1+nGt8+nN2t;
z1=nGt1/(nGt1+nGt8+nN2t);
z2=nGt8/(nGt1+nGt8+nN2t);
z3=nN2t/(nGt1+nGt8+nN2t);
sumZ = z1+z2+z3;
%-----
[K1,K2,K3] = Vaporpressure (TC);
%-----
[V,L,x,y,PBelowDP,PAboveBP,TwoPhase] = flashcondenser4
(K1,K2,K3,(nGt1+nGt8+nN2t),z1,z2,z3,PBelowDP,PAboveBP,TwoPhase);
%-----
mL = mL - (V*y(1)*76.096/2 + V*y(2)*18 + L*x(1)*76.096/2 + L*x(2)*18)/1000;
%PG divide by 2 because only half molecule (1 functional group)
%removal rate PG-H2O both outlet gas and outlet condensate
removalrate(i,:) = [y(1)*V y(2)*V x(1)*L x(2)*L];
%find water percent in polymer
waterpercent(i,1)= n0(8)*18/1000/mL*100;
concl (i,:) = n(i:)/mL;
% find accumulate mole of condensate
% find reaction rate
if i == 1
    summassconden(i,:) = [x(1)*L*76.096/2 x(2)*L*18];
    reactionrate(i,:) = concl(i,:);
else
    summassconden(i,:) = [(summassconden(i-1,1)+x(1)*L*76.096/2
(summassconden(i-1,2)+x(2)*L*18)];
    reactionrate(i,:) = concl(i,:) - concl((i-1),:);
end
totalconden(i,1) = sum(summassconden(i,:));
percentmassconden(i,:)=[x(1)*L*76.096/2*100/(x(1)*L*76.096/2 +x(2)*L*18)
x(2)*L*18*100/(x(1)*L*76.096/2 +x(2)*L*18)];
%Loss weight from Vapor
dmL(1) = dmL(1) + V*y(1)*76.096/2/1000;
dmL(2) = dmL(2) + V*y(2)*18/1000;
%Loss weight from Condensate
dmL(3) = dmL(3) + L*x(1)*76.096/2/1000;
dmL(4) = dmL(4) + L*x(2)*18/1000;
%find mass of condensate
condensate(1) = condensate(1) + x(1)*L*76.096/2/1000;
condensate(2) = condensate(2) + x(2)*L*18/1000;

```

```

if mL < 0
    break
end
%Properties Estimation
OHno(i,1) = n0(1)*56.1*1000/(mL*1000);
Acidno(i,1) = (n0(2)+ n0(3)+n0(6))*56.1*1000/(mL*1000);
MWn(i,1) = 2*56100/(Acidno(i,1)+OHno(i,1))/2.45;
[Dense,SurfTen,Visco,Dpg,Dh2o] = UPproperty (MWn(i,1),TL);
Density(i,1) = Dense;
SurfTension(i,1) = SurfTen;
Viscosity(i,1) = Visco;
Diffusepg(i,1) = Dpg;
Diffuseh2o(i,1) = Dh2o;
[Re,Po,Power,E,kpg,kh2o]=Masstransfer(Density(i,1),Viscosity(i,1),N2,Diffusepg(i,1),Diffuseh2o(i,1),TV,mL);
Renold(i,1)=Re;
Powerunareated(i,1) = Po;
Powerconsume(i,1) = Power;
Powerdissipate(i,1)=E;
kLpg(i,1)=kpg;
kLh2o(i,1)=kh2o;
[Gashold,Bubble,Iarea] =
Gasholdup1(Density(i,1),SurfTension(i,1),Viscosity(i,1),Powerconsume(i,1),N2,TV,P,mL);
Gasholdup(i,1) = Gashold;
BBsize(i,1) = Bubble;
InterArea(i,1) = Iarea;
kLapg (i,1) = kLpg(i,1)*InterArea(i,1);
kLah2o(i,1) = kLh2o(i,1)*InterArea(i,1);
KmA(1) = kLapg (i,1);
KmA(8) = kLah2o(i,1);
end
mL
dmL
Lossweight = sum(dmL)
condensate
totalcondense = sum(condensate)
PBelowDP
PAboveBP
Twophase
t = times';
xlswrite('model999Temp180N360.xls',times,'Temp180N360','A2');
xlswrite('model999Temp180N360.xls',n,'Temp180N360','B2');
xlswrite('model999Temp180N360.xls',Acidno,'Temp180N360','Q2');
xlswrite('model999Temp180N360.xls',OHno,'Temp180N360','R2');
%-----
xlswrite('model999Temp180N360.xls',MWn,'Temp180N360','T2');

```

```

xlswrite('model999Temp180N360.xls',Density,'Temp180N360','W2');
xlswrite('model999Temp180N360.xls',SurfTension,'Temp180N360','X2');
xlswrite('model999Temp180N360.xls',Viscosity,'Temp180N360','Y2');
%-----
xlswrite('model999Temp180N360.xls',Renold,'Temp180N360','AA2');
xlswrite('model999Temp180N360.xls',Powerunareated,'Temp180N360','AB2');
xlswrite('model999Temp180N360.xls',Powerconsume,'Temp180N360','AC2');
xlswrite('model999Temp180N360.xls',Powerdissipate,'Temp180N360','AD2');
%-----
xlswrite('model999Temp180N360.xls',Diffusepg,'Temp180N360','AF2');
xlswrite('model999Temp180N360.xls',Diffuseh2o,'Temp180N360','AG2');
xlswrite('model999Temp180N360.xls',kLpg,'Temp180N360','AI2');
xlswrite('model999Temp180N360.xls',kLh2o,'Temp180N360','AJ2');
xlswrite('model999Temp180N360.xls',Gasholdup,'Temp180N360','AL2');
xlswrite('model999Temp180N360.xls',BBsize,'Temp180N360','AM2');
xlswrite('model999Temp180N360.xls',InterArea,'Temp180N360','AN2');
xlswrite('model999Temp180N360.xls',kLapg,'Temp180N360','AP2');
xlswrite('model999Temp180N360.xls',kLah2o,'Temp180N360','AQ2');
xlswrite('model999Temp180N360.xls',percentmassconden,'Temp180N360','AS2');
xlswrite('model999Temp180N360.xls',waterpercent,'Temp180N360','AV2');
xlswrite('model999Temp180N360.xls',summassconden,'Temp180N360','AX2');
xlswrite('model999Temp180N360.xls',totalconden,'Temp180N360','AZ2');
xlswrite('model999Temp180N360.xls',concL,'Temp180N360','BB2');
xlswrite('model999Temp180N360.xls',reactionrate,'Temp180N360','BM2');
xlswrite('model999Temp180N360.xls',removalrate,'Temp180N360','BX2');
%=====
function dn dt = F(t,n,mL,nN2t,KmA,tempL,tempV,Kv11,Kv18)
R = 0.0821; % liter.atm/(mol.K)
R1 = 8.314; %J/(K.mol)
kE = (120000/60*exp(-75*1000/(R1*(273+tempL))));
kI = (127000/60*exp(-56*1000/(R1*(273+tempL))));
kS5 = (476000e-4/60*exp(-48*1000/(R1*(273+tempL))));
kS6 = kS5;
kS7 = kS5;
%kS8 = 0;
KE = 25;
KI = 12.5;
KS5 = 0.87;
KS6 = 1e10000;
KS7 = KS5;
%KS8 = 1e10000;
%[OH; COOH1D; COOH2D; COOR1D; COOR2D; COOHS; COORS; H2O; VOH;
VH2O]
ri1 = -kE*(n(2)/mL*n(1)/mL - n(4)/mL*n(8)/mL/KE)...
-kE*(n(3)/mL*n(1)/mL - n(5)/mL*n(8)/mL/KE)...
-kE*(n(6)/mL*n(1)/mL - n(7)/mL*n(8)/mL/KE)...
-1/2*(kS5*(n(2)/mL*n(1)/mL - n(6)/mL/KS5) +...

```



```

    kS6*(n(3)/mL*n(1)/mL - n(6)/mL/KS6) +...
    kS7*(n(4)/mL*n(1)/mL - n(7)/mL/KS7));
ri2 = -kE*(n(2)/mL*n(1)/mL - n(4)/mL*n(8)/mL/KE)...
    -kI*(n(2)/mL - n(3)/mL/KI)...
    -kS5*(n(2)/mL*n(1)/mL - n(6)/mL/KS5);
ri3 = -kE*(n(3)/mL*n(1)/mL - n(5)/mL*n(8)/mL/KE)...
    +kI*(n(2)/mL - n(3)/mL/KI)...
    -kS6*(n(3)/mL*n(1)/mL - n(6)/mL/KS6);
ri4 = kE*(n(2)/mL*n(1)/mL - n(4)/mL*n(8)/mL/KE)...
    -kI*(n(4)/mL - n(5)/mL/KI)...
    -kS7*(n(4)/mL*n(1)/mL - n(7)/mL/KS7);
ri5 = kE*(n(3)/mL*n(1)/mL - n(5)/mL*n(8)/mL/KE)...
    +kI*(n(4)/mL - n(5)/mL/KI);
ri6 = -kE*(n(6)/mL*n(1)/mL - n(7)/mL*n(8)/mL/KE)...
    +kS5*(n(2)/mL*n(1)/mL - n(6)/mL/KS5)...
    +kS6*(n(3)/mL*n(1)/mL - n(6)/mL/KS6);
ri7 = kS7*(n(4)/mL*n(1)/mL - n(7)/mL/KS7)...
    +kE*(n(6)/mL*n(1)/mL - n(7)/mL*n(8)/mL/KE);
ri8 = 1/2*(kE*(n(2)/mL*n(1)/mL - n(4)/mL*n(8)/mL/KE) +...
    kE*(n(3)/mL*n(1)/mL - n(5)/mL*n(8)/mL/KE) +...
    kE*(n(6)/mL*n(1)/mL - n(7)/mL*n(8)/mL/KE));
%-----
[NA1,NA8,nGt1,nGt8] = Gasmolarflow (n,mL,nN2t,KmA,tempV);
%-----
%column vector
dndt = zeros(10,1);
    dndt(1) = ri1 *mL - NA1;
    dndt(2) = ri2*mL;
    dndt(3) = ri3*mL;
    dndt(4) = ri4*mL;
    dndt(5) = ri5*mL;
    dndt(6) = ri6*mL;
    dndt(7) = ri7*mL;
    dndt(8) = ri8*mL - NA8;
    dndt(9) = NA1 - nGt1;
    dndt(10) = NA8 - nGt8;
%=====
function [NA1,NA8,nGt1,nGt8] = Gasmolarflow (n,mL,nN2t,KmA,temp)
R = 0.0821; % liter.atm/(mol.K)
P=1; % atm
VreG=pi*13.05^2/4*9/1000;% lit
cGT = P/(R*(temp+273)); % total concentration of gas in Vapor phase
%nGT = n(9)+n(10)+nN2
nGT = P*VreG/(R*(273+temp)); % Total mol
    Kv11 = 1.46e-5 ;    % OH
    Kv18 = 1.4e-2;    % H2O
%Flux leaving the liquid phase

```

```

NA1 = (KmA(1)*mL*(n(1)/mL-n(9)/nGT*cGT/Kv11));
NA8 = (KmA(8)*mL*(n(8)/mL-n(10)/nGT*cGT/Kv18));
% gas phase molar flow
nGt1 = n(9)/(nGT)*(NA1+NA8+nN2t);
nGt8 = n(10)/(nGT)*(NA1+NA8+nN2t);
%=====
function [V,L,x,y,PBelowDP,PAboveBP,TwoPhase] = flashcondenser4
(K1,K2,K3,F,z1,z2,z3,PBelowDP,PAboveBP,TwoPhase)
% K1 = Pi/Pt => OH
% K2 = Water
% K3 = N2
% must specify Ki when temperature change
Psystem = 1; % 1 atm
% check outlet condition by Boiling and Dew point pressure
% Reference Distillation Principle and Practice Johann G. Stichmar and
% James R. Fair page 75 eq. 3.6 and 3.7 Figure 3.4
% Dew point pressure
% Ki=Pi/Pt ==> Pt=1atm then Pi=Ki
Pdew = 1/(z1/K1 + z2/K2 + z3/K3);
% Boiling point
Pboil = z1*K1 + z2*K2 + z3*K3;
if Psystem < Pdew
    % gas phase ==> un-condense
    PBelowDP = PBelowDP + 1;
    V = F;
    L = 0;
    x = zeros(1,3);
    y = zeros(1,3);
    y(1) = z1;
    y(2) = z2;
    y(3) = z3;
elseif Psystem > Pboil %
    % total condense
    PAboveBP = PAboveBP;
    L = F;
    V = 0;
    x = zeros(1,3);
    y = zeros(1,3);
    x(1) = z1;
    x(2) = z2;
    x(3) = z3;
else
    % 2 phase mixture
    %-----
    % rough estimate
    TwoPhase=TwoPhase+1
    minimum=1000000;

```

```

for a = 0.0004:0.0004:1
    VperF=a;
    sum = (z1*(1-K1)/(1+VperF*(K1-1)))+ ...
          (z2*(1-K2)/(1+VperF*(K2-1)))+ ...
          (z3*(1-K3)/(1+VperF*(K3-1)));
    derisum = -((z1*K1*(K1-1)/(1+VperF*(K1-1))^2)+ ...
               (z2*K2*(K2-1)/(1+VperF*(K2-1))^2)+ ...
               (z3*K3*(K3-1)/(1+VperF*(K3-1))^2));
    absVperF = abs(((VperF-(sum/derisum))-VperF)/VperF);
    if absVperF < minimum
        minimum=absVperF;
        BestVperF = VperF;
    end
end
end
%-----
%fine estimate
upperVF = BestVperF+0.0004;
lowerVF = BestVperF-0.0004;
minimum=1000000;
for a = lowerVF:0.000001:upperVF
    VperF=a;
    sum = (z1*(1-K1)/(1+VperF*(K1-1)))+ ...
          (z2*(1-K2)/(1+VperF*(K2-1)))+ ...
          (z3*(1-K3)/(1+VperF*(K3-1)));
    derisum = -((z1*K1*(K1-1)/(1+VperF*(K1-1))^2)+ ...
                (z2*K2*(K2-1)/(1+VperF*(K2-1))^2)+ ...
                (z3*K3*(K3-1)/(1+VperF*(K3-1))^2));
    absVperF = abs(((VperF-(sum/derisum))-VperF)/VperF);
    if absVperF < minimum
        minimum=absVperF;
        BestVperF = VperF;
    end
end
end
%-----
VperF = BestVperF;
V = F*VperF;
L = F-V;
x = zeros(1,3);
y = zeros(1,3);
% liquid composition
x(1) = z1/(1+VperF*(K1-1));
x(2) = z2/(1+VperF*(K2-1));
x(3) = z3/(1+VperF*(K3-1));
% vapor composition
y(1) = x(1)*K1;
y(2) = x(2)*K2;
y(3) = x(3)*K3;

```

```

end
%=====
function [K1,K2,K3] = Vaporpressure (TC)
% VP for OH H2O N2 use data from PERRY table
T = (TC + 273);
C = [212.8 -15420 -28.109 2.1564e-5 2];
VPpg = 9.869233e-6*(exp(C(1) + C(2)/T + C(3)*log(T) + C(4)*T^C(5)));
C = [73.649 -7258.2 -7.3037 4.1653e-6 2];
VPh2o = 9.869233e-6*(exp(C(1) + C(2)/T + C(3)*log(T) + C(4)*T^C(5)));
C = [58.282 -1084.1 -8.3144 4.4127e-2 1];
VPn2 = 9.869233e-6*(exp(C(1) + C(2)/T + C(3)*log(T) + C(4)*T^C(5)));
K1= VPpg;
K2= VPh2o;
K3= VPn2;
%=====
function [Dense, SurfTen, Visco, Dpg, Dh2o] = UPproperty (MW,TL)
%Density = g/cm3
Dense = (0.003*MW + 1.037)/3.3;
%Linear model Poly1:
% f(x) = p1*x + p2
%Coefficients (with 95% confidence bounds):
% p1 = 0.003 (0.002906, 0.003094)
% p2 = 1.037 (0.9331, 1.141)
%Surface tension = dyne/cm (g.cm/s^2 / cm)
MW1 = (MW-988)/509;
%SurfTen1 =(187.8*MW1^4 + 924.9*MW1^3 + 3280*MW1^2 + 6143*MW1 +
4166);
SurfTen1 = (2*4361*exp(1.169*MW1))/100;
SurfTen = SurfTen1 -0.1/100*(TL-20);
%Protect minus value of SurfTen ==> set to minimum value
%if SurfTen < 0
% SurfTen = 50;
%end
%Protect over SurfTen
%SurfTen = SurfTen;
%Linear model Poly4:
% f(x) = p1*x^4 + p2*x^3 + p3*x^2 + p4*x + p5
% where x is normalized by mean 988 and std 509
%Coefficients (with 95% confidence bounds):
% p1 = 187.8 (-327.3, 702.9)
% p2 = 924.9 (501.3, 1348)
% p3 = 3280 (1986, 4574)
% p4 = 6143 (5357, 6930)
% p5 = 4166 (3594, 4739)
%Viscosity = centiPoises, estimation Orrick and Erbar (1974) method
%A parameter
A = -0.01489*MW - 11.07;

```

```

%Linear model Poly1:
%   f(x) = p1*x + p2
%Coefficients (with 95% confidence bounds):
%   p1 = -0.01489 (-0.01599, -0.01379)
%   p2 = -11.07 (-12.42, -9.71)
%B parameter
B = 6.283*MW+2763;
%Linear model Poly1:
%   f(x) = p1*x + p2
%Coefficients (with 95% confidence bounds):
%   p1 = 6.283 (5.83, 6.735)
%   p2 = 2763 (2204, 3322)
Visco = (exp(A+(B/(TL+273-60))))*Dense*MW;
%Visco = centi-Poises %T = Kelvin %Dense = g/cm^3
%Coverse to poises(g/cm.s)
Visco =Visco/100;
%-----
%Estimate of Diffusion coefficient
%Wilke-Chang equation, 1955
%Molar volume at normal boiling point of H2O and PG, cm^3/mol
Vpg = 87.89625;
Vh2o = 18.79763;
Dpg = 7.4e-8*MW^(1/2)*(TL+273)/(Visco*100)/Vpg^0.6;
Dh2o = 7.4e-8*MW^(1/2)*(TL+273)/(Visco*100)/Vh2o^0.6;
%D=cm^2/s, T=Kelvin, Visco = centi-Poises, V=cm^3/mol
%converse D to m^2/s
Dpg = Dpg/100^2;
Dh2o = Dh2o/100^2;
%converse Dense to kg/m^3 %ViscoL to Pa.s %SurfTen to N/m
Dense = Dense*100^3/1000;
Visco = Visco/10;
SurfTen = SurfTen/100000*100;
%=====
% Volumetric mass transfer coefficient estimation
%Assumption
% 1)interfacial area and mean bubble size estimate from Nitrogen
% 2)Diffusivity of PG and H2O are not interact
% 3)kL of PG and H2O esimate from paper
%=====
function [Re,Po,Power,E,kpg,kh2o] =
Masstransfer(DenseL,ViscoL,N2,Dpg,Dh2o,TV,mL)
%Q=m^3/sec
Q=N2/1000;
Q=Q*(TV+273)/(25+273);
%Impeller diameter, T, for 4 flat blade turbine, H=liquid level
T = 5/100; %meter
H = 10/100; %meter

```

```

rpm = 15; %round per sec.
% Impeller Renolds number,  $Re = T^2 * N * DenseL / ViscoL$ 
%cross check for Renold number
 $Re = (T * 100)^2 * rpm * (DenseL / 100^3 * 1000) / (ViscoL * 10)$ ;
%at  $Re > 20000$  Power number( $Np$ )is constant = 5
 $Np = 5$ ;
% $Np = Po / (Dense * N^3 * T^5)$ 
% $Po = PowNo * (DenseL * N^3 / T^5)$ 
%  $Po =$ Power consumption in un-areated system
 $Po = Np * DenseL * (rpm)^3 * T^5$ ;
%For Rusthon turbine
 $Power = 0.783 * ((Po^2 * (rpm) * T^3) / (Q^0.56))^{0.459}$ ;
% $E =$ Energy dissipation
 $E = Power / (DenseL * pi / 4 * T^2 * H)$ ;
% $E =$ Power/mL;
%Mass transfer coefficient
 $kpg = 2 / pi^{1/2} * Dpg^{1/2} * (E * DenseL / ViscoL)^{1/4}$ ;
 $kh2o = 2 / pi^{1/2} * Dh2o^{1/2} * (E * DenseL / ViscoL)^{1/4}$ ;
%=====
function [Gashold,Bubble,Iarea] =
Gasholdup1(DenseL,SurfTen,ViscoL,Power,N2,T,P,mL)
ViscoN2 = 0.016493*T^0 + 4.9286e-005*T^1 + (-3.1215e-008)*T^2 + 1.4419e-
011*T^3;
% ViscoN2=cP %T=Celcius
%converse ViscoN2 to Pa.s
ViscoN2 = ViscoN2/10;
%N2 Density calculate from ideal gas law
 $DenseN2 = P * 28 / 0.08205 / (T + 273)$ ; % g/lit or kg/m^3
%Superficial velocity m/s
% Reactor diameter = 0.13 meter
%  $Q = m^3 / sec$ 
 $Q = N2 / 1000$ ;
 $Vs = Q / (pi * 0.13^2 / 4)$ ; % m/s
 $T = 5 / 100$ ; % meter
rpm = 15; %round per sec.
PreGashold =
0.819*Vs^(2/3)*rpm^(2/5)*T^(4/15)/9.81^(1/3)*(DenseL/SurfTen)^(1/5)*(DenseL/(
DenseL-DenseN2))*(DenseL/DenseN2)^(-1/15)*(ViscoL/ViscoN2)^(-1/4);
%Gas hold up in viscous liquid
Gashold = PreGashold/(1+PreGashold);
Bubble =
0.7*SurfTen^0.6/(Power/(mL/DenseL))^0.4/DenseL^0.2*(ViscoL/ViscoN2)^0.1;
Iarea = 6*Gashold/Bubble;
%=====

```

C.1.2 Model for reaction temperature 180 °C and N₂ 600 ccm

```

function model9 % (Temperature 180 °C and N2 600 ccm)
% Import reaction temperature file
% Estimate of kLa
ndata1 = xlsread('Temp180N600.xls',1, 'B2:B4'); % initial weight
ndata2 = xlsread('Temp180N600.xls',1, 'C8:H31760'); % Actual temperature
n0 = [ndata1(1)/76.09*2; ndata1(2)/98.06*2; 0; 0; 0; 0; 0; 0; 0; 0; 0];
% 1 mole of reactants = 2 functional group
% [OH; COOH1D; COOH2D; COOR1D; COOR2D; COOHS; COORS; H2O; VOH;
VH2O]
N2 = ndata1(3)/1000/60; % N2 standard cm3/min to lit/sec
times = ndata2(:,1);
maxtime = times(size(times,1),1);
TLdata = ndata2(:,6); % Liquid temp.
TVdata = ndata2(:,5); % Vapor temp.
TCdata = ndata2(:,2); % Top column temp.
TWIdata = ndata2(:,3); % Cooling water input temp.
TWOdata = ndata2(:,4); % Cooling water output temp.
% initial condition
KmA = [0; 0; 0; 0; 0; 0; 0; 0; 0];
P=1; % atm
nN2t = N2/22.4; % mol/sec
mL = (ndata1(1)+ndata1(2))/1000; % kilogram
% variable for integrate
tspan = [0 1];
n = zeros(maxtime,10);
concl = zeros(maxtime,10);
reactionrate = zeros(maxtime,10);
removalrate = zeros(maxtime,4);
% Flash condenser variable
PBelowDP = 0;
PAboveBP = 0;
Twophase = 0;
% weight loss variable
dmL = zeros(4,1);
condensate = zeros(1,2);
nGout = zeros(1,4);
% Properties variable-----
Acidno = zeros(maxtime,1);
OHno = zeros(maxtime,1);
MWn = zeros(maxtime,1);
Density = zeros(maxtime,1);
SurfTension = zeros(maxtime,1);
Viscosity = zeros(maxtime,1);
Diffusepg = zeros(maxtime,1);
Diffuseh2o = zeros(maxtime,1);

```

```

Renold = zeros(maxtime,1);
Powerconsume = zeros(maxtime,1);
Powerunareated = zeros(maxtime,1);
Powerdissipate = zeros(maxtime,1);
kLpg= zeros(maxtime,1);
kLh2o= zeros(maxtime,1);
Gasholdup = zeros(maxtime,1);
BBsize = zeros(maxtime,1);
InterArea = zeros(maxtime,1);
kLaPG = zeros(maxtime,1);
kLah2o = zeros(maxtime,1);
summassconden = zeros(maxtime,2);
totalconden = zeros(maxtime,1);
percentmassconden = zeros(maxtime,2);
waterpercent = zeros(maxtime,1);
%start up program-----
for i = 1:maxtime
    %TL=TLdata(i)+3;
    %TV=TVdata(i)+3;
    %TC=TCdata(i);
    %TWI=TWIdata(i);
    %TWO=TWOdata(i);
    if i < 3500
        TL=0;
        TV=0;
        TC=25;
        TWI=15;
        TWO=25;
    else
        TL=180;
        TV=180;
        TC=25;
        TWI=15;
        TWO=25;
    end
    %-----
    [t,y] = ode15s(@F,tspan,n0,[],mL,nN2t,KmA,TL,TV);
    %-----
    n(i,:) = y(size(y,1),:);
    n0 = n(i,:);
    %-----
    [NA1,NA8,nGt1 nGt8] = Gasmolarflow (n0,mL,nN2t,KmA,TV);
    %-----
    Feed = nGt1+nGt8+nN2t;
    z1=nGt1/(nGt1+nGt8+nN2t);
    z2=nGt8/(nGt1+nGt8+nN2t);
    z3=nN2t/(nGt1+nGt8+nN2t);

```



```

sumZ = z1+z2+z3;
%-----
[K1,K2,K3] = Vaporpressure (TC);
%-----
[V,L,x,y,PBelowDP,PAboveBP,TwoPhase] = flashcondenser4
(K1,K2,K3,(nGt1+nGt8+nN2t),z1,z2,z3,PBelowDP,PAboveBP,TwoPhase);
%-----
mL = mL - (V*y(1)*76.096/2 + V*y(2)*18 + L*x(1)*76.096/2 + L*x(2)*18)/1000;
%PG devide by 2 because only half molecule (1 functional group)
%removal rate PG-H2O both outlet gas and outlet condensate
removalrate(i,:) = [y(1)*V y(2)*V x(1)*L x(2)*L];
%find water percent in polymer
waterpercent(i,1)= n0(8)*18/1000/mL*100;
concl (i,:) = n(i:)/mL;
% find accumulate mole of condensate
% find reaction rate
if i == 1
    summassconden(i,:) = [x(1)*L*76.096/2 x(2)*L*18];
    reactionrate(i,:) = concl(i,:);
else
    summassconden(i,:) = [(summassconden(i-1,1)+x(1)*L*76.096/2)
(summassconden(i-1,2)+x(2)*L*18)];
    reactionrate(i,:) = concl(i,:) - concl((i-1),:);
end
totalconden(i,1) = sum(summassconden(i,:));
percentmassconden(i,:)=[x(1)*L*76.096/2*100/(x(1)*L*76.096/2 +x(2)*L*18)
x(2)*L*18*100/(x(1)*L*76.096/2 +x(2)*L*18)];
%Loss weight from Vapor
dmL(1) = dmL(1) + V*y(1)*76.096/2/1000;
dmL(2) = dmL(2) + V*y(2)*18/1000;
%Loss weight from Condensate
dmL(3) = dmL(3) + L*x(1)*76.096/2/1000;
dmL(4) = dmL(4) + L*x(2)*18/1000;
%find mass of condensate
condensate(1) = condensate(1) + x(1)*L*76.096/2/1000;
condensate(2) = condensate(2) + x(2)*L*18/1000;
if mL < 0
    break
end
%Properties Estimation
OHno(i,1) = n0(1)*56.1*1000/(mL*1000);
Acidno(i,1) = (n0(2)+ n0(3)+n0(6))*56.1*1000/(mL*1000);
MWn(i,1) = 2*56100/(Acidno(i,1)+OHno(i,1))/2.45;
[Dense,SurfTen,Visco,Dpg,Dh2o] = UPproperty (MWn(i,1),TL);
Density(i,1) = Dense;
SurfTension(i,1) = SurfTen;
Viscosity(i,1) = Visco;

```

```

Diffusepg(i,1) = Dpg;
Diffuseh2o(i,1) = Dh2o;
[Re,Po,Power,E,kpg,kh2o]=Masstransfer(Density(i,1),Viscosity(i,1),N2,Diffusepg(i,1),Diffuseh2o(i,1),TV,mL);
Renold(i,1)=Re;
Powerunareated(i,1) = Po;
Powerconsume(i,1) = Power;
Powerdissipate(i,1)=E;
kLpg(i,1)=kpg;
kLh2o(i,1)=kh2o;
[Gashold,Bubble,Iarea] =
Gasholdup1(Density(i,1),SurfTension(i,1),Viscosity(i,1),Powerconsume(i,1),N2,TV,P,mL);
Gasholdup(i,1) = Gashold;
BBsize(i,1) = Bubble;
InterArea(i,1) = Iarea;
kLapg(i,1) = kLpg(i,1)*InterArea(i,1);
kLah2o(i,1) = kLh2o(i,1)*InterArea(i,1);
KmA(1) = kLapg(i,1);
KmA(8) = kLah2o(i,1);
end
mL
dmL
Lossweight = sum(dmL)
condensate
totalcondense = sum(condensate)
PBelowDP
PAboveBP
Twophase
t = times';
xlswrite('model999Temp180N600.xls',times,'Temp180N600','A2');
xlswrite('model999Temp180N600.xls',n,'Temp180N600','B2');
xlswrite('model999Temp180N600.xls',Acidno,'Temp180N600','Q2');
xlswrite('model999Temp180N600.xls',OHno,'Temp180N600','R2');
%-----
xlswrite('model999Temp180N600.xls',MWn,'Temp180N600','T2');
xlswrite('model999Temp180N600.xls',Density,'Temp180N600','W2');
xlswrite('model999Temp180N600.xls',SurfTension,'Temp180N600','X2');
xlswrite('model999Temp180N600.xls',Viscosity,'Temp180N600','Y2');
%-----
xlswrite('model999Temp180N600.xls',Renold,'Temp180N600','AA2');
xlswrite('model999Temp180N600.xls',Powerunareated,'Temp180N600','AB2');
xlswrite('model999Temp180N600.xls',Powerconsume,'Temp180N600','AC2');
xlswrite('model999Temp180N600.xls',Powerdissipate,'Temp180N600','AD2');
%-----
xlswrite('model999Temp180N600.xls',Diffusepg,'Temp180N600','AF2');
xlswrite('model999Temp180N600.xls',Diffuseh2o,'Temp180N600','AG2');

```

```

xlswrite('model999Temp180N600.xls',kLpg,'Temp180N600','AI2');
xlswrite('model999Temp180N600.xls',kLh2o,'Temp180N600','AJ2');
xlswrite('model999Temp180N600.xls',Gasholdup,'Temp180N600','AL2');
xlswrite('model999Temp180N600.xls',BBsize,'Temp180N600','AM2');
xlswrite('model999Temp180N600.xls',InterArea,'Temp180N600','AN2');
xlswrite('model999Temp180N600.xls',kLapg,'Temp180N600','AP2');
xlswrite('model999Temp180N600.xls',kLah2o,'Temp180N600','AQ2');
xlswrite('model999Temp180N600.xls',percentmassconden,'Temp180N600','AS2');
xlswrite('model999Temp180N600.xls',waterpercent,'Temp180N600','AV2');
xlswrite('model999Temp180N600.xls',summassconden,'Temp180N600','AX2');
xlswrite('model999Temp180N600.xls',totalconden,'Temp180N600','AZ2');
xlswrite('model999Temp180N600.xls',concL,'Temp180N600','BB2');
xlswrite('model999Temp180N600.xls',reactionrate,'Temp180N600','BM2');
xlswrite('model999Temp180N600.xls',removalrate,'Temp180N600','BX2');
%=====
function dn dt = F(t,n,mL,nN2t,KmA,tempL,tempV,Kvl1,Kvl8)
R = 0.0821; % liter.atm/(mol.K)
R1 = 8.314; %J/(K.mol)
kE = (1200000/60*exp(-75*1000/(R1*(273+tempL))));
kI = (127000/60*exp(-56*1000/(R1*(273+tempL))));
kS5 = (476000e-4/60*exp(-48*1000/(R1*(273+tempL))));
kS6 = kS5;
kS7 = kS5;
%kS8 = 0;
KE = 25;
KI = 12.5;
KS5 = 0.87;
KS6 = 1e10000;
KS7 = KS5;
%KS8 = 1e10000;
%[OH; COOH1D; COOH2D; COOR1D; COOR2D; COOHS; COORS; H2O; VOH;
VH2O]
ri1 = -kE*(n(2)/mL*n(1)/mL - n(4)/mL*n(8)/mL/KE)...
      -kE*(n(3)/mL*n(1)/mL - n(5)/mL*n(8)/mL/KE)...
      -kE*(n(6)/mL*n(1)/mL - n(7)/mL*n(8)/mL/KE)...
      -1/2*(kS5*(n(2)/mL*n(1)/mL - n(6)/mL/KS5) +...
           kS6*(n(3)/mL*n(1)/mL - n(6)/mL/KS6) +...
           kS7*(n(4)/mL*n(1)/mL - n(7)/mL/KS7));
ri2 = -kE*(n(2)/mL*n(1)/mL - n(4)/mL*n(8)/mL/KE)...
      -kI*(n(2)/mL - n(3)/mL/KI)...
      -kS5*(n(2)/mL*n(1)/mL - n(6)/mL/KS5);
ri3 = -kE*(n(3)/mL*n(1)/mL - n(5)/mL*n(8)/mL/KE)...
      +kI*(n(2)/mL - n(3)/mL/KI)...
      -kS6*(n(3)/mL*n(1)/mL - n(6)/mL/KS6);
ri4 = kE*(n(2)/mL*n(1)/mL - n(4)/mL*n(8)/mL/KE)...
      -kI*(n(4)/mL - n(5)/mL/KI)...
      -kS7*(n(4)/mL*n(1)/mL - n(7)/mL/KS7);

```

```

ri5 = kE*(n(3)/mL*n(1)/mL - n(5)/mL*n(8)/mL/KE)...
      +kI*(n(4)/mL - n(5)/mL/KI);
ri6 = -kE*(n(6)/mL*n(1)/mL - n(7)/mL*n(8)/mL/KE)...
      +kS5*(n(2)/mL*n(1)/mL - n(6)/mL/KS5)...
      +kS6*(n(3)/mL*n(1)/mL - n(6)/mL/KS6);
ri7 = kS7*(n(4)/mL*n(1)/mL - n(7)/mL/KS7)...
      +kE*(n(6)/mL*n(1)/mL - n(7)/mL*n(8)/mL/KE);
ri8 = 1/2*(kE*(n(2)/mL*n(1)/mL - n(4)/mL*n(8)/mL/KE) +...
      kE*(n(3)/mL*n(1)/mL - n(5)/mL*n(8)/mL/KE) +...
      kE*(n(6)/mL*n(1)/mL - n(7)/mL*n(8)/mL/KE));
%-----
[NA1,NA8,nGt1,nGt8] = Gasmolarflow (n,mL,nN2t,KmA,tempV);
%-----
%column vector
dndt = zeros(10,1);
dndt(1) = ri1*mL - NA1;
dndt(2) = ri2*mL;
dndt(3) = ri3*mL;
dndt(4) = ri4*mL;
dndt(5) = ri5*mL;
dndt(6) = ri6*mL;
dndt(7) = ri7*mL;
dndt(8) = ri8*mL - NA8;
dndt(9) = NA1 - nGt1;
dndt(10) = NA8 - nGt8;
%=====
function [NA1,NA8,nGt1,nGt8] = Gasmolarflow (n,mL,nN2t,KmA,temp)
R = 0.0821; % liter.atm/(mol.K)
P=1; % atm
VreG=pi*13.05^2/4*9/1000;% lit
cGT = P/(R*(temp+273)); % total concentration of gas in Vapor phase
%nGT = n(9)+n(10)+nN2
nGT = P*VreG/(R*(273+temp)); % Total mol
Kv11 = 1.46e-5 ; % OH
Kv18 = 1.4e-2; % H2O
%Flux leaving the liquid phase
NA1 = (KmA(1)*mL*(n(1)/mL-n(9)/nGT*cGT/Kv11));
NA8 = (KmA(8)*mL*(n(8)/mL-n(10)/nGT*cGT/Kv18));
%gas phase molar flow
nGt1 = n(9)/(nGT)*(NA1+NA8+nN2t);
nGt8 = n(10)/(nGT)*(NA1+NA8+nN2t);
%=====
function [V,L,x,y,PBelowDP,PAboveBP,TwoPhase] = flashcondenser4
(K1,K2,K3,F,z1,z2,z3,PBelowDP,PAboveBP,TwoPhase)
%K1 = Pi/Pt => OH
%K2 = Water
%K3 = N2

```

```

% must specify Ki when temperature change
Psystem = 1; % 1 atm
% check outlet condition by Boiling and Dew point pressure
% Reference Distillation Principle and Practice Johann G. Stichlmair and
% James R. Fair page 75 eq. 3.6 and 3.7 Figure 3.4
% Dew point pressure
%  $K_i = P_i/P_t \implies P_t = 1 \text{ atm then } P_i = K_i$ 
Pdew = 1/(z1/K1 + z2/K2 + z3/K3);
% Boiling point
Pboil = z1*K1 + z2*K2 + z3*K3;
if Psystem < Pdew
    % gas phase  $\implies$  un-condense
    PBelowDP = PBelowDP + 1;
    V = F;
    L = 0;
    x = zeros(1,3);
    y = zeros(1,3);
    y(1) = z1;
    y(2) = z2;
    y(3) = z3;
elseif Psystem > Pboil %
    % total condense
    PAboveBP = PAboveBP;
    L = F;
    V = 0;
    x = zeros(1,3);
    y = zeros(1,3);
    x(1) = z1;
    x(2) = z2;
    x(3) = z3;
else
    % 2 phase mixture
    % -----
    % rough estimate
    Twophase = Twophase + 1
    minimum = 1000000;
    for a = 0.0004:0.0004:1
        VperF = a;
        sum = (z1*(1-K1)/(1+VperF*(K1-1))) + ...
            (z2*(1-K2)/(1+VperF*(K2-1))) + ...
            (z3*(1-K3)/(1+VperF*(K3-1)));
        derisum = -((z1*K1*(K1-1)/(1+VperF*(K1-1))^2) + ...
            (z2*K2*(K2-1)/(1+VperF*(K2-1))^2) + ...
            (z3*K3*(K3-1)/(1+VperF*(K3-1))^2));
        absVperF = abs(((VperF - (sum/derisum)) - VperF)/VperF);
        if absVperF < minimum
            minimum = absVperF;
    end
end

```

```

        BestVperF = VperF;
    end
end
%-----
%fine estimate
upperVF = BestVperF+0.0004;
lowerVF = BestVperF-0.0004;
minimum=1000000;
for a = lowerVF:0.000001:upperVF
    VperF=a;
    sum = (z1*(1-K1)/(1+VperF*(K1-1)))+ ...
          (z2*(1-K2)/(1+VperF*(K2-1)))+ ...
          (z3*(1-K3)/(1+VperF*(K3-1)));
    derisum = -((z1*K1*(K1-1)/(1+VperF*(K1-1))^2)+ ...
              (z2*K2*(K2-1)/(1+VperF*(K2-1))^2)+ ...
              (z3*K3*(K3-1)/(1+VperF*(K3-1))^2));
    absVperF = abs(((VperF-(sum/derisum))-VperF)/VperF);
    if absVperF < minimum
        minimum=absVperF;
        BestVperF = VperF;
    end
end
%-----
VperF = BestVperF;
V = F*VperF;
L = F-V;
x = zeros(1,3);
y = zeros(1,3);
% liquid composition
x(1) = z1/(1+VperF*(K1-1));
x(2) = z2/(1+VperF*(K2-1));
x(3) = z3/(1+VperF*(K3-1));
% vapor composition
y(1) = x(1)*K1;
y(2) = x(2)*K2;
y(3) = x(3)*K3;
end
%=====
function [K1,K2,K3] = Vaporpressure (TC)
% VP for OH H2O N2 use data from PERRY table
T = (TC + 273);
C = [212.8 -15420 -28.109 2.1564e-5 2];
VPpg = 9.869233e-6*(exp(C(1) + C(2)/T + C(3)*log(T) + C(4)*T^C(5)));
C = [73.649 -7258.2 -7.3037 4.1653e-6 2];
VPh2o = 9.869233e-6*(exp(C(1) + C(2)/T + C(3)*log(T) + C(4)*T^C(5)));
C = [58.282 -1084.1 -8.3144 4.4127e-2 1];
VPn2 = 9.869233e-6*(exp(C(1) + C(2)/T + C(3)*log(T) + C(4)*T^C(5)));

```

```

K1= VPpg;
K2= VPh2o;
K3= VPn2;
%=====
function [Dense, SurfTen, Visco, Dpg, Dh2o] = UPproperty (MW,TL)
%Density = g/cm3
Dense = (0.003*MW + 1.037)/3.3;
%Linear model Poly1:
% f(x) = p1*x + p2
%Coefficients (with 95% confidence bounds):
% p1 = 0.003 (0.002906, 0.003094)
% p2 = 1.037 (0.9331, 1.141)
%Surface tension = dyne/cm (g.cm/s^2 / cm)
MW1 = (MW-988)/509;
%SurfTen1 =(187.8*MW1^4 + 924.9*MW1^3 + 3280*MW1^2 + 6143*MW1 +
4166);
SurfTen1 = (2*4361*exp(1.169*MW1))/100;
SurfTen = SurfTen1 -0.1/100*(TL-20);
%Protect minus value of SurfTen ==> set to minimum value
%if SurfTen < 0
% SurfTen = 50;
%end
%Protect over SurfTen
%SurfTen = SurfTen;
%Linear model Poly4:
% f(x) = p1*x^4 + p2*x^3 + p3*x^2 + p4*x + p5
% where x is normalized by mean 988 and std 509
%Coefficients (with 95% confidence bounds):
% p1 = 187.8 (-327.3, 702.9)
% p2 = 924.9 (501.3, 1348)
% p3 = 3280 (1986, 4574)
% p4 = 6143 (5357, 6930)
% p5 = 4166 (3594, 4739)
%Viscosity = centiPoises, estimation Orrick and Erbar (1974) method
%A parameter
A = -0.01489*MW - 11.07;
%Linear model Poly1:
% f(x) = p1*x + p2
%Coefficients (with 95% confidence bounds):
% p1 = -0.01489 (-0.01599, -0.01379)
% p2 = -11.07 (-12.42, -9.71)
%B parameter
B = 6.283*MW+2763;
%Linear model Poly1:
% f(x) = p1*x + p2
%Coefficients (with 95% confidence bounds):
% p1 = 6.283 (5.83, 6.735)

```

```

% p2 = 2763 (2204, 3322)
Visco = (exp(A+(B/(TL+273-60))))*Dense*MW;
% Visco = centi-Poises %T = Kelvin %Dense = g/cm^3
% Coverse to poises(g/cm.s)
Visco =Visco/100;
%-----
% Estimate of Diffusion coefficient
% Wilke-Chang equation, 1955
% Molar volume at normal boiling point of H2O and PG, cm^3/mol
Vpg = 87.89625;
Vh2o = 18.79763;
Dpg = 7.4e-8*MW^(1/2)*(TL+273)/(Visco*100)/Vpg^0.6;
Dh2o = 7.4e-8*MW^(1/2)*(TL+273)/(Visco*100)/Vh2o^0.6;
%D=cm^2/s, T=Kelvin, Visco = centi-Poises, V=cm^3/mol
%converse D to m^2/s
Dpg = Dpg/100^2;
Dh2o = Dh2o/100^2;
%converse Dense to kg/m^3 %ViscoL to Pa.s %SurfTen to N/m
Dense = Dense*100^3/1000;
Visco = Visco/10;
SurfTen = SurfTen/100000*100;
%=====
% Volumetric mass transfer coefficient estimation
% Assumption
% 1)interfacial area and mean bubble size estimate from Nitrogen
% 2)Diffusivity of PG and H2O are not interact
% 3)kL of PG and H2O esimate from paper
%=====f
unction [Re,Po,Power,E,kpg,kh2o] =
Masstransfer(DenseL,ViscoL,N2,Dpg,Dh2o,TV,mL)
% Q=m^3/sec
Q=N2/1000;
Q=Q*(TV+273)/(25+273);
% Impeller diameter, T, for 4 flat blade turbine, H=liquid level
T = 5/100; % meter
H = 10/100; % meter
rpm = 15; % round per sec.
% Impeller Renolds number, Re = T^2*N*DenseL/ViscoL
% cross check for Renold number
Re = (T*100)^2*rpm*(DenseL/100^3*1000)/(ViscoL*10);
% at Re > 20000 Power number(Np)is constant = 5
Np=5;
% Np=Po/(Dense*N^3*T^5)
% Po = PowNo*(DenseL*N^3/T^5)
% Po=Power consumption in un-areated system
Po=Np*DenseL*(rpm)^3*T^5;
% For Rusthon turbine

```



```

Power=0.783*((Po^2*(rpm)*T^3)/(Q^0.56))^0.459;
%E=Energy dissipation
E=Power/(DenseL*pi/4*T^2*H);
%E=Power/mL;
%Mass transfer coefficient
kpg = 2/pi^(1/2)*Dpg^(1/2)*(E*DenseL/ViscoL)^(1/4);
kh2o = 2/pi^(1/2)*Dh2o^(1/2)*(E*DenseL/ViscoL)^(1/4);
%=====f
unction [Gashold,Bubble,Iarea] =
Gasholdup1(DenseL,SurfTen,ViscoL,Power,N2,T,P,mL)
ViscoN2 = 0.016493*T^0 + 4.9286e-005*T^1 + (-3.1215e-008)*T^2 + 1.4419e-
011*T^3;
% ViscoN2=cP %T=Celcius
%converse ViscoN2 to Pa.s
ViscoN2 = ViscoN2/10;
%N2 Density calculate from ideal gas law
DenseN2 = P*28/0.08205/(T+273); % g/lit or kg/m^3
%Superficial velocity m/s
% Reactor diameter = 0.13 meter
%Q=m^3/sec
Q=N2/1000;
Vs = Q/(pi*0.13^2/4); % m/s
T = 5/100; % meter
rpm = 15; % round per sec.
PreGashold =
0.819*Vs^(2/3)*rpm^(2/5)*T^(4/15)/9.81^(1/3)*(DenseL/SurfTen)^(1/5)*(DenseL/(
DenseL-DenseN2))*(DenseL/DenseN2)^(-1/15)*(ViscoL/ViscoN2)^(-1/4);
% Gas hold up in viscous liquid
Gashold = PreGashold/(1+PreGashold);
Bubble =
0.7*SurfTen^0.6/(Power/(mL/DenseL))^0.4/DenseL^0.2*(ViscoL/ViscoN2)^0.1;
Iarea = 6*Gashold/Bubble;
%=====

```

C.1.3 Model for reaction temperature 180 °C and N₂ 840 ccm

```

function model9 %( temperature 180 °C and N2 840 ccm)
% Import reaction temperature file
% Estimate of kLa
ndata1 = xlsread('Temp180N840.xls',1, 'B2:B4'); % initial weight
ndata2 = xlsread('Temp180N840.xls',1, 'C8:H31760'); % Actual temperature
n0 = [ndata1(1)/76.09*2; ndata1(2)/98.06*2; 0; 0; 0; 0; 0; 0; 0; 0; 0];
% 1 mole of reactants = 2 functional group
% [OH; COOH1D; COOH2D; COOR1D; COOR2D; COOHS; COORS; H2O; VOH;
VH2O]
N2 = ndata1(3)/1000/60; % N2 standard cm3/min to lit/sec
times = ndata2(:,1);
maxtime = times(size(times,1),1);
TLdata = ndata2(:,6); % Liquid temp.
TVdata = ndata2(:,5); % Vapor temp.
TCdata = ndata2(:,2); % Top column temp.
TWIdata = ndata2(:,3); % Cooling water input temp.
TWOdata = ndata2(:,4); % Cooling water output temp.
% initial condition
KmA = [0; 0; 0; 0; 0; 0; 0; 0; 0];
P=1; % atm
nN2t = N2/22.4; % mol/sec
mL = (ndata1(1)+ndata1(2))/1000; % kilogram
% variable for integrate
tspan = [0 1];
n = zeros(maxtime,10);
concl = zeros(maxtime,10);
reactionrate = zeros(maxtime,10);
removalrate = zeros(maxtime,4);
% Flash condenser variable
PBelowDP = 0;
PAboveBP = 0;
Twophase = 0;
% weight loss variable
dmL = zeros(4,1);
condensate = zeros(1,2);
nGout = zeros(1,4);
% Properties variable-----
Acidno = zeros(maxtime,1);
OHno = zeros(maxtime,1);
MWn = zeros(maxtime,1);
Density = zeros(maxtime,1);
SurfTension = zeros(maxtime,1);
Viscosity = zeros(maxtime,1);
Diffusepg = zeros(maxtime,1);
Diffuseh2o = zeros(maxtime,1);

```

```

Renold = zeros(maxtime,1);
Powerconsume = zeros(maxtime,1);
Powerunareated = zeros(maxtime,1);
Powerdissipate = zeros(maxtime,1);
kLpg= zeros(maxtime,1);
kLh2o= zeros(maxtime,1);
Gasholdup = zeros(maxtime,1);
BBsize = zeros(maxtime,1);
InterArea = zeros(maxtime,1);
kLaPG = zeros(maxtime,1);
kLah2o = zeros(maxtime,1);
summassconden = zeros(maxtime,2);
totalconden = zeros(maxtime,1);
percentmassconden = zeros(maxtime,2);
waterpercent = zeros(maxtime,1);
%start up program-----
for i = 1:maxtime
    TL=TLdata(i);
    TV=TVdata(i);
    TC=TCdata(i);
    TWI=TWIdata(i);
    TWO=TWOdata(i);
    %-----
    [t,y] = ode15s(@F,tspan,n0,[],mL,nN2t,KmA,TL,TV);
    %-----
    n(i,:) = y(size(y,1),:);
    n0 = n(i,:);
    %-----
    [NA1,NA8,nGt1 nGt8] = Gasmolarflow (n0,mL,nN2t,KmA,TV);
    %-----
    Feed = nGt1+nGt8+nN2t;
    z1=nGt1/(nGt1+nGt8+nN2t);
    z2=nGt8/(nGt1+nGt8+nN2t);
    z3=nN2t/(nGt1+nGt8+nN2t);
    sumZ = z1+z2+z3;
    %-----
    [K1,K2,K3] = Vaporpressure (TC);
    %-----
    [V,L,x,y,PBelowDP,PAboveBP,TwoPhase] = flashcondenser4
(K1,K2,K3,(nGt1+nGt8+nN2t),z1,z2,z3,PBelowDP,PAboveBP,TwoPhase);
    %-----
    mL = mL - (V*y(1)*76.096/2 + V*y(2)*18 + L*x(1)*76.096/2 + L*x(2)*18)/1000;
    %PG devide by 2 because only half molecule (1 functional group)
    %removal rate PG-H2O both outlet gas and outlet condensate
    removalrate(i,:) = [y(1)*V y(2)*V x(1)*L x(2)*L];
    %find water percent in polymer
    waterpercent(i,1)= n0(8)*18/1000/mL*100;

```

```

concl (i,:) = n(i:)/mL;
% find accumulate mole of condensate
% find reaction rate
if i == 1
    summassconden(i,:) = [x(1)*L*76.096/2 x(2)*L*18];
    reactionrate(i,:) = concl(i,:);
else
    summassconden(i,:) = [(summassconden(i-1,1)+x(1)*L*76.096/2)
(summassconden(i-1,2)+x(2)*L*18)];
    reactionrate(i,:) = concl(i,:) - concl((i-1),:);
end
totalconden(i,1) = sum(summassconden(i,:));
percentmassconden(i,:)=[x(1)*L*76.096/2*100/(x(1)*L*76.096/2 +x(2)*L*18)
x(2)*L*18*100/(x(1)*L*76.096/2 +x(2)*L*18)];
%Loss weight from Vapor
dmL(1) = dmL(1) + V*y(1)*76.096/2/1000;
dmL(2) = dmL(2) + V*y(2)*18/1000;
%Loss weight from Condensate
dmL(3) = dmL(3) + L*x(1)*76.096/2/1000;
dmL(4) = dmL(4) + L*x(2)*18/1000;
%find mass of condensate
condensate(1) = condensate(1) + x(1)*L*76.096/2/1000;
condensate(2) = condensate(2) + x(2)*L*18/1000;
if mL < 0
    break
end
% Properties Estimation
OHno(i,1) = n0(1)*56.1*1000/(mL*1000);
Acidno(i,1) = (n0(2)+ n0(3)+n0(6))*56.1*1000/(mL*1000);
MWn(i,1) = 2*56100/(Acidno(i,1)+OHno(i,1))/2.45;
[Dense,SurfTen,Visco,Dpg,Dh2o] = UPproperty (MWn(i,1),TL);
Density(i,1) = Dense;
SurfTension(i,1) = SurfTen;
Viscosity(i,1) = Visco;
Diffusepg(i,1) = Dpg;
Diffuseh2o(i,1) = Dh2o;
[Re,Po,Power,E,kpg,kh2o]=Masstransfer(Density(i,1),Viscosity(i,1),N2,Diffusepg(i,1),Diffuseh2o(i,1),TV,mL);
Renold(i,1)=Re;
Powerunareated(i,1) = Po;
Powerconsume(i,1) = Power;
Powerdissipate(i,1)=E;
kLpg(i,1)=kpg;
kLh2o(i,1)=kh2o;

```

```

[Gashold,Bubble,Iarea] =
Gasholdup1(Density(i,1),SurfTension(i,1),Viscosity(i,1),Powerconsume(i,1),N2,TV,P
,mL);
  Gasholdup(i,1) = Gashold;
  BBsize(i,1) = Bubble;
  InterArea(i,1) = Iarea;
  kLapg (i,1) = kLpg(i,1)*InterArea(i,1);
  kLah2o(i,1) = kLh2o(i,1)*InterArea(i,1);
  KmA(1) = kLapg (i,1);
  KmA(8) = kLah2o(i,1);
end
mL
dmL
Lossweight = sum(dmL)
condensate
totalcondense = sum(condensate)
PBelowDP
PAboveBP
Twophase
t = times';
xlswrite('model999Temp180N840.xls',times,'Temp180N840','A2');
xlswrite('model999Temp180N840.xls',n,'Temp180N840','B2');
xlswrite('model999Temp180N840.xls',Acidno,'Temp180N840','Q2');
xlswrite('model999Temp180N840.xls',OHno,'Temp180N840','R2');
%-----
xlswrite('model999Temp180N840.xls',MWn,'Temp180N840','T2');
xlswrite('model999Temp180N840.xls',Density,'Temp180N840','W2');
xlswrite('model999Temp180N840.xls',SurfTension,'Temp180N840','X2');
xlswrite('model999Temp180N840.xls',Viscosity,'Temp180N840','Y2');
%-----
xlswrite('model999Temp180N840.xls',Renold,'Temp180N840','AA2');
xlswrite('model999Temp180N840.xls',Powerunareated,'Temp180N840','AB2');
xlswrite('model999Temp180N840.xls',Powerconsume,'Temp180N840','AC2');
xlswrite('model999Temp180N840.xls',Powerdissipate,'Temp180N840','AD2');
%-----
xlswrite('model999Temp180N840.xls',Diffusepg,'Temp180N840','AF2');
xlswrite('model999Temp180N840.xls',Diffuseh2o,'Temp180N840','AG2');
xlswrite('model999Temp180N840.xls',kLpg,'Temp180N840','AI2');
xlswrite('model999Temp180N840.xls',kLh2o,'Temp180N840','AJ2');
xlswrite('model999Temp180N840.xls',Gasholdup,'Temp180N840','AL2');
xlswrite('model999Temp180N840.xls',BBsize,'Temp180N840','AM2');
xlswrite('model999Temp180N840.xls',InterArea,'Temp180N840','AN2');
xlswrite('model999Temp180N840.xls',kLapg,'Temp180N840','AP2');
xlswrite('model999Temp180N840.xls',kLah2o,'Temp180N840','AQ2');
xlswrite('model999Temp180N840.xls',percentmassconden,'Temp180N840','AS2');
xlswrite('model999Temp180N840.xls',waterpercent,'Temp180N840','AV2');
xlswrite('model999Temp180N840.xls',summassconden,'Temp180N840','AX2');

```

```

xlswrite('model999Temp180N840.xls',totalconden,'Temp180N840','AZ2');
xlswrite('model999Temp180N840.xls',concL,'Temp180N840','BB2');
xlswrite('model999Temp180N840.xls',reactionrate,'Temp180N840','BM2');
xlswrite('model999Temp180N840.xls',removalrate,'Temp180N840','BX2');
%=====
function dndt = F(t,n,mL,nN2t,KmA,tempL,tempV)
R = 0.0821; % liter.atm/(mol.K)
R1 = 8.314; %J/(K.mol)
kE = (23100/60*exp(-58.2*1000/(R1*(273+tempL))));
kI = (6210/60*exp(-41.5*1000/(R1*(273+tempL))));
kS5 = (1.76e-4/60*exp(-10.2*1000/(R1*(273+tempL))));
kS6 = (5.90/60*exp(-24.9*1000/(R1*(273+tempL))));
kS7 = (15800/60*exp(-52.9*1000/(R1*(273+tempL))));
%kS8 = 0;
KE = (19.7*exp(-0/(R1*(273+tempL))));
KI = (2860*exp(-21.2*1000/(R1*(273+tempL))));
KS5 = (9.46e-5*exp(-0*1000/(R1*(273+tempL))));
KS6 = 1e10000;
KS7 = (2.63e6*exp(-46.5*1000/(R1*(273+tempL))));
%KS8 = 1e10000;
%[OH; COOH1D; COOH2D; COOR1D; COOR2D; COOHS; COORS; H2O; VOH;
VH2O]
ri1 = -kE*(n(2)/mL*n(1)/mL - n(4)/mL*n(8)/mL/KE)...
      -kE*(n(3)/mL*n(1)/mL - n(5)/mL*n(8)/mL/KE)...
      -kE*(n(6)/mL*n(1)/mL - n(7)/mL*n(8)/mL/KE)...
      -1/2*(kS5*(n(2)/mL*n(1)/mL - n(6)/mL/KS5) +...
            kS6*(n(3)/mL*n(1)/mL - n(6)/mL/KS6) +...
            kS7*(n(4)/mL*n(1)/mL - n(7)/mL/KS7));
ri2 = -kE*(n(2)/mL*n(1)/mL - n(4)/mL*n(8)/mL/KE)...
      -kI*(n(2)/mL - n(3)/mL/KI)...
      -kS5*(n(2)/mL*n(1)/mL - n(6)/mL/KS5);
ri3 = -kE*(n(3)/mL*n(1)/mL - n(5)/mL*n(8)/mL/KE)...
      +kI*(n(2)/mL - n(3)/mL/KI)...
      -kS6*(n(3)/mL*n(1)/mL - n(6)/mL/KS6);
ri4 = kE*(n(2)/mL*n(1)/mL - n(4)/mL*n(8)/mL/KE)...
      -kI*(n(4)/mL - n(5)/mL/KI)...
      -kS7*(n(4)/mL*n(1)/mL - n(7)/mL/KS7);
ri5 = kE*(n(3)/mL*n(1)/mL - n(5)/mL*n(8)/mL/KE)...
      +kI*(n(4)/mL - n(5)/mL/KI);
ri6 = -kE*(n(6)/mL*n(1)/mL - n(7)/mL*n(8)/mL/KE)...
      +kS5*(n(2)/mL*n(1)/mL - n(6)/mL/KS5)...
      +kS6*(n(3)/mL*n(1)/mL - n(6)/mL/KS6);
ri7 = kS7*(n(4)/mL*n(1)/mL - n(7)/mL/KS7)...
      +kE*(n(6)/mL*n(1)/mL - n(7)/mL*n(8)/mL/KE);
ri8 = 1/2*(kE*(n(2)/mL*n(1)/mL - n(4)/mL*n(8)/mL/KE) +...
          kE*(n(3)/mL*n(1)/mL - n(5)/mL*n(8)/mL/KE) +...
          kE*(n(6)/mL*n(1)/mL - n(7)/mL*n(8)/mL/KE));

```

```

%-----
[NA1,NA8,nGt1,nGt8] = Gasmolarflow (n,mL,nN2t,KmA,tempV);
%-----
%column vector
dndt = zeros(10,1);
dndt(1) = ri1*mL - NA1;
dndt(2) = ri2*mL;
dndt(3) = ri3*mL;
dndt(4) = ri4*mL;
dndt(5) = ri5*mL;
dndt(6) = ri6*mL;
dndt(7) = ri7*mL;
dndt(8) = ri8*mL - NA8;
dndt(9) = NA1 - nGt1;
dndt(10) = NA8 - nGt8;

%=====
function [NA1,NA8,nGt1,nGt8] = Gasmolarflow (n,mL,nN2t,KmA,temp)
R = 0.0821; %liter.atm/(mol.K)
P=1; % atm
VreG=pi*13.05^2/4*9/1000;% lit
cGT = P/(R*(temp+273)); %total concentration of gas in Vapor phase
%nGT = n(9)+n(10)+nN2
nGT = P*VreG/(R*(273+temp)); %Total mol
Kv11 = 5.12e-6 ; % OH
Kv18 = 0.77e-2; %H2O
%Flux leaving the liquid phase
NA1 = (KmA(1)*mL*(n(1)/mL-n(9)/nGT*cGT/Kv11));
NA8 = (KmA(8)*mL*(n(8)/mL-n(10)/nGT*cGT/Kv18));
%gas phase molar flow
nGt1 = n(9)/(nGT)*(NA1+NA8+nN2t);
nGt8 = n(10)/(nGT)*(NA1+NA8+nN2t);

%=====
function [V,L,x,y,PBelowDP,PAboveBP,Twophase] = flashcondenser4
(K1,K2,K3,F,z1,z2,z3,PBelowDP,PAboveBP,Twophase)
%K1 = Pi/Pt => OH
%K2 = Water
%K3 = N2
% must specify Ki when temperature change
Psystem = 1; % 1 atm
%check outlet condition by Boiling and Dew point pressure
%Reference Distillation Principle and Practice Johann G. Stichmar and
%James R. Fair page75 eq. 3.6 and 3.7 Figure 3.4
%Dew point pressure
%Ki=Pi/Pt ==> Pt=1atm then Pi=Ki
Pdew = 1/(z1/K1 + z2/K2 + z3/K3);
%Boiling point
Pboil = z1*K1 + z2*K2 + z3*K3;

```

```

if Psystem < Pdew
    %gasphase ==> un-condense
    PBelowDP = PBelowDP + 1;
    V = F;
    L = 0;
    x = zeros(1,3);
    y = zeros(1,3);
    y(1) = z1;
    y(2) = z2;
    y(3) = z3;
elseif Psystem > Pboil %
    %total condense
    PAboveBP = PAboveBP;
    L = F;
    V = 0;
    x = zeros(1,3);
    y = zeros(1,3);
    x(1) = z1;
    x(2) = z2;
    x(3) = z3;
else
    %2 phase mixture
    %-----
    %rough estimate
    Twophase=Twophase+1
    minimum=1000000;
    for a = 0.0004:0.0004:1
        VperF=a;
        sum = (z1*(1-K1)/(1+VperF*(K1-1)))+ ...
            (z2*(1-K2)/(1+VperF*(K2-1)))+ ...
            (z3*(1-K3)/(1+VperF*(K3-1)));
        derisum = -((z1*K1*(K1-1)/(1+VperF*(K1-1))^2)+ ...
            (z2*K2*(K2-1)/(1+VperF*(K2-1))^2)+ ...
            (z3*K3*(K3-1)/(1+VperF*(K3-1))^2));
        absVperF = abs(((VperF-(sum/derisum))-VperF)/VperF);
        if absVperF < minimum
            minimum=absVperF;
            BestVperF = VperF;
        end
    end
end
%-----
%fine estimate
upperVF = BestVperF+0.0004;
lowerVF = BestVperF-0.0004;
minimum=1000000;
for a = lowerVF:0.000001:upperVF
    VperF=a;

```



```

sum = (z1*(1-K1)/(1+VperF*(K1-1)))+ ...
      (z2*(1-K2)/(1+VperF*(K2-1)))+ ...
      (z3*(1-K3)/(1+VperF*(K3-1)));
derisum = -((z1*K1*(K1-1)/(1+VperF*(K1-1))^2)+ ...
           (z2*K2*(K2-1)/(1+VperF*(K2-1))^2)+ ...
           (z3*K3*(K3-1)/(1+VperF*(K3-1))^2));
absVperF = abs(((VperF-(sum/derisum))-VperF)/VperF);
if absVperF < minimum
    minimum=absVperF;
    BestVperF = VperF;
end
end
%-----
VperF = BestVperF;
V = F*VperF;
L = F-V;
x = zeros(1,3);
y = zeros(1,3);
% liquid composition
x(1) = z1/(1+VperF*(K1-1));
x(2) = z2/(1+VperF*(K2-1));
x(3) = z3/(1+VperF*(K3-1));
% vapor composition
y(1) = x(1)*K1;
y(2) = x(2)*K2;
y(3) = x(3)*K3;
end
%=====
function [K1,K2,K3] = Vaporpressure (TC)
% VP for OH H2O N2 use data from PERRY table
T = (TC + 273);
C = [212.8 -15420 -28.109 2.1564e-5 2];
VPpg = 9.869233e-6*(exp(C(1) + C(2)/T + C(3)*log(T) + C(4)*T^C(5)));
C = [73.649 -7258.2 -7.3037 4.1653e-6 2];
VPh2o = 9.869233e-6*(exp(C(1) + C(2)/T + C(3)*log(T) + C(4)*T^C(5)));
C = [58.282 -1084.1 -8.3144 4.4127e-2 1];
VPn2 = 9.869233e-6*(exp(C(1) + C(2)/T + C(3)*log(T) + C(4)*T^C(5)));
K1= VPpg;
K2= VPh2o;
K3= VPn2;
%=====
function [Dense, SurfTen, Visco, Dpg, Dh2o] = UPproperty (MW,TL)
%Density = g/cm3
Dense = (0.003*MW + 1.037)/3.3;
%Linear model Poly1:
% f(x) = p1*x + p2
%Coefficients (with 95% confidence bounds):

```

```

% p1 = 0.003 (0.002906, 0.003094)
% p2 = 1.037 (0.9331, 1.141)
%Surface tension = dyne/cm (g.cm/s^2 / cm)
MW1 = (MW-988)/509;
%SurfTen1 =(187.8*MW1^4 + 924.9*MW1^3 + 3280*MW1^2 + 6143*MW1 +
4166);
SurfTen1 = (2*4361*exp(1.169*MW1))/100;
SurfTen = SurfTen1 -0.1/100*(TL-20);
%Protect minus value of SurfTen ==> set to minimum value
%if SurfTen < 0
% SurfTen = 50;
%end
%Protect over SurfTen
%SurfTen = SurfTen;
%Linear model Poly4:
% f(x) = p1*x^4 + p2*x^3 + p3*x^2 + p4*x + p5
% where x is normalized by mean 988 and std 509
%Coefficients (with 95% confidence bounds):
% p1 = 187.8 (-327.3, 702.9)
% p2 = 924.9 (501.3, 1348)
% p3 = 3280 (1986, 4574)
% p4 = 6143 (5357, 6930)
% p5 = 4166 (3594, 4739)
%Viscosity = centiPoises, estimation Orrick and Erbar (1974) method
%A parameter
A = -0.01489*MW - 11.07;
%Linear model Poly1:
% f(x) = p1*x + p2
%Coefficients (with 95% confidence bounds):
% p1 = -0.01489 (-0.01599, -0.01379)
% p2 = -11.07 (-12.42, -9.71)
%B parameter
B = 6.283*MW+2763;
%Linear model Poly1:
% f(x) = p1*x + p2
%Coefficients (with 95% confidence bounds):
% p1 = 6.283 (5.83, 6.735)
% p2 = 2763 (2204, 3322)
Visco = (exp(A+(B/(TL+273-60))))*Dense*MW;
%Visco = centi-Poises %T = Kelvin %Dense = g/cm^3
%Coverse to poises(g/cm.s)
Visco =Visco/100;
%-----
%Estimate of Diffusion coefficient
%Wilke-Chang equation, 1955
%Molar volume at normal boiling point of H2O and PG, cm^3/mol
Vpg = 87.89625;

```

```

Vh2o = 18.79763;
Dpg = 7.4e-8*MW^(1/2)*(TL+273)/(Visco*100)/Vpg^0.6;
Dh2o = 7.4e-8*MW^(1/2)*(TL+273)/(Visco*100)/Vh2o^0.6;
%D=cm^2/s, T=Kelvin, Visco = centi-Poises, V=cm^3/mol
%convert D to m^2/s
Dpg = Dpg/100^2;
Dh2o = Dh2o/100^2;
%convert Dense to kg/m^3 %ViscoL to Pa.s %SurfTen to N/m
Dense = Dense*100^3/1000;
Visco = Visco/10;
SurfTen = SurfTen/100000*100;
%=====
% Volumetric mass transfer coefficient estimation
% Assumption
% 1)interfacial area and mean bubble size estimate from Nitrogen
% 2)Diffusivity of PG and H2O are not interact
% 3)kL of PG and H2O estimate from paper
%=====
function [Re,Po,Power,E,kpg,kh2o] =
Masstransfer(DenseL,ViscoL,N2,Dpg,Dh2o,TV,mL)
%Q=m^3/sec
Q=N2/1000;
Q=Q*(TV+273)/(25+273);
% Impeller diameter, T, for 4 flat blade turbine, H=liquid level
T = 5/100; % meter
H = 10/100; % meter
rpm = 15; % round per sec.
% Impeller Renolds number, Re = T^2*N*DenseL/ViscoL
% cross check for Renold number
Re = (T*100)^2*rpm*(DenseL/100^3*1000)/(ViscoL*10);
% at Re > 20000 Power number(Np)is constant = 5
Np=5;
% Np=Po/(Dense*N^3*T^5)
% Po = PowNo*(DenseL*N^3/T^5)
% Po=Power consumption in un-areated system
Po=Np*DenseL*(rpm)^3*T^5;
% For Rusthon turbine
Power=0.783*((Po^2*(rpm)*T^3)/(Q^0.56))^0.459;
%E=Energy dissipation
E=Power/(DenseL*pi/4*T^2*H);
%E=Power/mL;
% Mass transfer coefficient
kpg = 2/pi^(1/2)*Dpg^(1/2)*(E*DenseL/ViscoL)^(1/4);
kh2o = 2/pi^(1/2)*Dh2o^(1/2)*(E*DenseL/ViscoL)^(1/4);
%=====
function [Gashold,Bubble,Iarea] =
Gasholdup1(DenseL,SurfTen,ViscoL,Power,N2,T,P,mL)

```

```

ViscoN2 = 0.016493*T^0 + 4.9286e-005*T^1 + (-3.1215e-008)*T^2 + 1.4419e-
011*T^3;
% ViscoN2=cP %T=Celcius
%convert ViscoN2 to Pa.s
ViscoN2 = ViscoN2/10;
%N2 Density calculate from ideal gas law
DenseN2 = P*28/0.08205/(T+273); % g/lit or kg/m^3
%Superficial velocity m/s
% Reactor diameter = 0.13 meter
%Q=m^3/sec
Q=N2/1000;
Vs = Q/(pi*0.13^2/4); % m/s
T = 5/100; % meter
rpm = 15; % round per sec.
PreGashold =
0.819*Vs^(2/3)*rpm^(2/5)*T^(4/15)/9.81^(1/3)*(DenseL/SurfTen)^(1/5)*(DenseL/(
DenseL-DenseN2))*(DenseL/DenseN2)^(-1/15)*(ViscoL/ViscoN2)^(-1/4);
% Gas hold up in viscous liquid
Gashold = PreGashold/(1+PreGashold);
Bubble =
0.7*SurfTen^0.6/(Power/(mL/DenseL))^0.4/DenseL^0.2*(ViscoL/ViscoN2)^0.1;
Iarea = 6*Gashold/Bubble;
%=====

```

ศูนย์วิทยทรัพยากร
จุฬาลงกรณ์มหาวิทยาลัย

C.2 Estimation of vapor liquid equilibrium ratio

function model9 % (temperature 180 °C and N₂ 600 ccm)

```

% Import reaction temperature file
ndata1 = xlsread('Temp180N600.xls',1, 'B2:B4'); % initial weight
ndata2 = xlsread('Temp180N600.xls',1, 'C8:H44785'); % Actual temperature
%n0 = [ndata1(1)/76.09*2; ndata1(2)/98.06*2; 0; 0; 0; 0; 0; 0; 0; 0];
% 1 mole of reactants = 2 functional group
% [OH; COOH1D; COOH2D; COOR1D; COOR2D; COOHS; COORS; H2O; VOH;
VH2O]
N2 = ndata1(3)/1000/60; % N2 standard cm3/min to lit/sec
times = ndata2(:,1);
maxtime = times(size(times,1),1);
TLdata = ndata2(:,6)+2; % Liquid temp.
TVdata = ndata2(:,5)+2; % Vapor temp.
TCdata = ndata2(:,2); % Top column temp.
TWIdata = ndata2(:,3); % Cooling water input temp.
TWOdata = ndata2(:,4); % Cooling water output temp.
% data for estimate KVL
% percent PG in condensate data
t1 = [4200 6780 10800 19920 27900 32340 43380];
PGdata = [0.33668 0.33363 0.28502 0.27659 0.23487
0.31502 0.30526];
% total Condensate data
t2 = [5400 6520 6920 7380 8140 8900 10840 13440 14580 18840
25740 31420];
Condendata = [36.12 61.57 65.99 73.33 82.36 92.9 104.75 113.84 116.73
125.68 131.31 134.62];
% plot
figure
subplot(1,2,1)
plot(t1,PGdata);
title('percentmasscondenPG')
hold on
subplot(1,2,2)
plot(t2,Condendata);
title('masscondensate')
hold on
c1=1; % amount of cycle for clculation
c2=1;
maxtime = maxtime;
temp = [180 117 25 15 25];
Kv11 = 5.12e-6; % OH
Kv18 = 1.47e-2; % H2O
Kv18first = 1.47e-2; % H2O use nearest value for estimate Kv11
Kv11step=0.00e-6;
Kv18step=0.00e-2;

```

```

%=====
[RsquarePG] = EstimateKv11
(c1,maxtime,ndata1,N2,temp,Kv11,Kv18first,Kv11step,t1,PGdata);
for d=1:1:c1
    if RsquarePG(d) == min(RsquarePG);
        Kv11Estimate = Kv11-d*Kv11step;
    end
end
[RsquareConden] = EstimateKv18
(c2,maxtime,ndata1,N2,temp,Kv11Estimate,Kv18,Kv18step,t2,Condendata);
for d=1:1:c2
    if RsquareConden(d) == min(RsquareConden);
        Kv18Estimate = Kv18-d*Kv18step;
    end
end
RsquarePG
MinRsquarePG=min(RsquarePG)
Kv11Estimate
RsquareConden
MinRsquareConden=min(RsquareConden)
Kv18Estimate
hold off
hold off
%=====
function [RsquarePG] = EstimateKv11
(c,maxtime,ndata1,N2,temp,Kv11,Kv18,Kv11step,t1,PGdata)
%Properties variable-----
    Acidno = zeros(maxtime,1,c);
    OHno = zeros(maxtime,1,c);
    MWn = zeros(maxtime,1,c);
    Density = zeros(maxtime,1,c);
    SurfTension = zeros(maxtime,1,c);
    Viscosity = zeros(maxtime,1,c);
    Diffusepg = zeros(maxtime,1,c);
    Diffuseh2o = zeros(maxtime,1,c);
    Renold = zeros(maxtime,1,c);
    Powerconsume = zeros(maxtime,1,c);
    Powerunareated = zeros(maxtime,1,c);
    Powerdissipate = zeros(maxtime,1,c);
    kLpg= zeros(maxtime,1,c);
    kLh2o= zeros(maxtime,1,c);
    Gasholdup = zeros(maxtime,1,c);
    BBsize = zeros(maxtime,1,c);
    InterArea = zeros(maxtime,1,c);
    kLaPG = zeros(maxtime,1,c);
    kLah2o = zeros(maxtime,1,c);
    summassconden = zeros(maxtime,2,c);

```

```

totalconden = zeros(maxtime,1,c);
percentmassconden = zeros(maxtime,2,c);
waterpercent = zeros(maxtime,1,c);
PBelowDP = zeros(1,1,c);
PAboveBP = zeros(1,1,c);
Twophase = zeros(1,1,c);
%initial condition
n00 = [ndata1(1)/76.09*2; ndata1(2)/98.06*2; 0; 0; 0; 0; 0; 0; 0; 0];
P=1; % atm
nN2t = N2/22.4; % mol/sec
mL0 = (ndata1(1)+ndata1(2))/1000; %kilogram
%variable for integrate
tspan = [0 1];
n = zeros(maxtime,10,c);
concl = zeros(maxtime,10,c);
reactionrate = zeros(maxtime,10,c);
removalrate = zeros(maxtime,4,c);
%weight loss variable
dmL = zeros(4,1,c);
condensate =zeros(1,2,c);
nGout = zeros(1,4,c);
%start up program-----
for a = 1:c
    Kv11 = Kv11-Kv11step; % OH
    Kv18 = Kv18; %H2O
    for b = 1:1:maxtime
        a
        if b < 3500
            TL=0;TV=0;TC=temp(3);TWI=temp(4);TWO=temp(5);
        else
            TL=temp(1);TV=temp(2);TC=temp(3);TWI=temp(4);TWO=temp(5);
        end
        if b == 1
            mL=mL0;n0=n00;KmA=zeros(1,8);
        end
        if b==t1(7)
            RsquarePG(a) = ((percentmassconden(t1(1),1,a)-PGdata(1))^2)^(1/2) + ...
                ((percentmassconden(t1(2),1,a)-PGdata(2))^2)^(1/2) + ...
                ((percentmassconden(t1(3),1,a)-PGdata(3))^2)^(1/2) + ...
                ((percentmassconden(t1(4),1,a)-PGdata(4))^2)^(1/2) + ...
                ((percentmassconden(t1(5),1,a)-PGdata(5))^2)^(1/2) + ...
                ((percentmassconden(t1(6),1,a)-PGdata(6))^2)^(1/2) + ...
                ((percentmassconden(t1(7),1,a)-PGdata(7))^2)^(1/2);
        end
    end
%-----
[t,y] = ode15s(@F,tspan,n0,[],mL,nN2t,KmA,TL,TV,Kv11,Kv18);
%-----

```

```

n(b,:,a) = y(size(y,1),:);
n0 = n(b,:,a);
%-----
[NA1,NA8,nGt1 nGt8] = Gasmolarflow
(n0,mL,nN2t,KmA,TV,Kv11,Kv18);
%-----
Feed = nGt1+nGt8+nN2t;
z1=nGt1/(nGt1+nGt8+nN2t);
z2=nGt8/(nGt1+nGt8+nN2t);
z3=nN2t/(nGt1+nGt8+nN2t);
sumZ = z1+z2+z3;
%-----
[K1,K2,K3] = Vaporpressure (TC);
%-----
[V,L,x,y,PBelowDP1,PAboveBP1,TwoPhase1] = flashcondenser4
(K1,K2,K3,(nGt1+nGt8+nN2t),z1,z2,z3,PBelowDP(:,a),PAboveBP(:,a),TwoPhase(
(:,a)));
PBelowDP(:,a)=PBelowDP1;
PAboveBP(:,a)=PAboveBP1;
TwoPhase(:,a)=TwoPhase1;
%-----
mL = mL - (V*y(1)*76.096/2 + V*y(2)*18 + L*x(1)*76.096/2 +
L*x(2)*18)/1000;
% PG divide by 2 because only half molecule (1 functional group)
%removal rate PG-H2O both outlet gas and outlet condensate
removalrate(b,:,a) = [y(1)*V y(2)*V x(1)*L x(2)*L];
% find water percent in polymer
waterpercent(b,:,a)= n0(8)*18/1000/mL*100;
concl (b,:,a) = n(b,:,a)/mL;
% find accumulate mole of condensate
% find reaction rate
if b == 1
    summassconden(b,:,a) = [x(1)*L*76.096/2 x(2)*L*18];
    reactionrate(b,:,a) = concl(b,:,a);
else
    summassconden(b,:,a) = [(summassconden(b-1,1,a)+x(1)*L*76.096/2
(summassconden(b-1,2,a)+x(2)*L*18)];
    reactionrate(b,:,a) = concl(b,:,a) - concl(b-1,:,a);
end
totalconden(b,:,a) = sum(summassconden(b,:,a));
percentmassconden(b,:,a)=[x(1)*L*76.096/2*100/(x(1)*L*76.096/2
+x(2)*L*18) x(2)*L*18*100/(x(1)*L*76.096/2 +x(2)*L*18)];
%Loss weight from Vapor
dmL(1,1,a) = dmL(1,1,a) + V*y(1)*76.096/2/1000;
dmL(2,1,a) = dmL(2,1,a) + V*y(2)*18/1000;
%Loss weight from Condensate
dmL(3,1,a) = dmL(3,1,a) + L*x(1)*76.096/2/1000;

```



```

    dmL(4,1,a) = dmL(4,1,a) + L*x(2)*18/1000;
%find mass of condensate
    condensate(1,1,a) = condensate(1) + x(1)*L*76.096/2/1000;
    condensate(1,2,a) = condensate(2) + x(2)*L*18/1000;
    if mL < 0
        mL
        break
    end
%Properties Estimation
    OHno(b,:,a) = n0(1)*56.1*1000/(mL*1000);
    Acidno(b,:,a) = (n0(2)+ n0(3)+n0(6))*56.1*1000/(mL*1000);
    MWn(b,:,a) = 2*56100/(Acidno(b,:,a)+OHno(b,:,a))/2.45;
%=====
    [Dense,SurfTen,Visco,Dpg,Dh2o] = UPproperty (MWn(b,:,a),TL);
    Density(b,:,a) = Dense;
    SurfTension(b,:,a) = SurfTen;
    Viscosity(b,:,a) = Visco;
    Diffusepg(b,:,a) = Dpg;
    Diffuseh2o(b,:,a) = Dh2o;
%=====
    [Re,Po,Power,E,kpg,kh2o]=Masstransfer(Density(b,:,a),Viscosity(b,:,a),N2,Diffusepg
(b,:,a),Diffuseh2o(b,:,a),TV,mL);
    Renold(b,:,a)=Re;
    Powerunareated(b,:,a) = Po;
    Powerconsume(b,:,a) = Power;
    Powerdissipate(b,:,a)=E;
    kLpg(b,:,a)=kpg;
    kLh2o(b,:,a)=kh2o;
%=====
    [Gashold,Bubble,Iarea] =
Gasholdup1(Density(b,:,a),SurfTension(b,:,a),Viscosity(b,:,a),Powerconsume(b,:,a),N
2,TV,P,mL);
    Gasholdup(b,:,a) = Gashold;
    BBSize(b,:,a) = Bubble;
    InterArea(b,:,a) = Iarea;
    kLapg (b,:,a) = kLpg(b,:,a)*InterArea(b,:,a);
    kLah2o(b,:,a) = kLh2o(b,:,a)*InterArea(b,:,a);
    KmA(1) = kLapg (b,:,a);
    KmA(8) = kLah2o(b,:,a);
end
t=linspace(1,(maxtime),maxtime);
t=t';
subplot(1,2,1)
plot(t,percentmassconden(:,1,a));
%subplot(1,2,2)
%plot(t,totalconden(:,a));
end

```

```

dmL
condensate
PBelowDP
PAboveBP
Twophase
%=====
function [RsquareConden] = EstimateKvl8
(c,maxtime,ndata1,N2,temp,Kvl1Estimate,Kvl8,Kvl8step,t2,Condenata)
%Properties variable-----
    Acidno = zeros(maxtime,1,c);
    OHno = zeros(maxtime,1,c);
    MWn = zeros(maxtime,1,c);
    Density = zeros(maxtime,1,c);
    SurfTension = zeros(maxtime,1,c);
    Viscosity = zeros(maxtime,1,c);
    Diffusepg = zeros(maxtime,1,c);
    Diffuseh2o = zeros(maxtime,1,c);
    Renold = zeros(maxtime,1,c);
    Powerconsume = zeros(maxtime,1,c);
    Powerunareated = zeros(maxtime,1,c);
    Powerdissipate = zeros(maxtime,1,c);
    kLpg= zeros(maxtime,1,c);
    kLh2o= zeros(maxtime,1,c);
    Gasholdup = zeros(maxtime,1,c);
    BBsize = zeros(maxtime,1,c);
    InterArea = zeros(maxtime,1,c);
    kLaPG = zeros(maxtime,1,c);
    kLah2o = zeros(maxtime,1,c);
    summassconden = zeros(maxtime,2,c);
    totalconden = zeros(maxtime,1,c);
    percentmassconden = zeros(maxtime,2,c);
    waterpercent = zeros(maxtime,1,c);
    PBelowDP = zeros(1,1,c);
    PAboveBP = zeros(1,1,c);
    Twophase = zeros(1,1,c);
%initial condition
    n00 = [ndata1(1)/76.09*2; ndata1(2)/98.06*2; 0; 0; 0; 0; 0; 0; 0; 0];
    P=1; % atm
    nN2t = N2/22.4; % mol/sec
    mL0 = (ndata1(1)+ndata1(2))/1000; %kilogram
%variable for integrate
    tspan = [0 1];
    n = zeros(maxtime,10,c);
    concL = zeros(maxtime,10,c);
    reactionrate = zeros(maxtime,10,c);
    removalrate = zeros(maxtime,4,c);
%weight loss variable

```

```

dmL = zeros(4,1,c);
condensate = zeros(1,2,c);
nGout = zeros(1,4,c);
%start up program-----
for a = 1:c
    Kv11 = Kv11Estimate;    %OH
    Kv18 = Kv18-Kv18step;  %H2O
    for b = 1:1:maxtime
        if b < 3500
            TL=0;TV=0;TC=temp(3);TWI=temp(4);TWO=temp(5);
        else
            TL=temp(1);TV=temp(2);TC=temp(3);TWI=temp(4);TWO=temp(5);
        end
        if b == 1
            mL=mL0;n0=n00;KmA=zeros(1,8)';
        end
        if b==t2(12)
            RsquareConden(a) = ((totalconden(t2(1),1,a)-Condendata(1))^2)^(1/2) +
...
            ((totalconden(t2(2),1,a)-Condendata(2))^2)^(1/2) + ...
            ((totalconden(t2(3),1,a)-Condendata(3))^2)^(1/2) + ...
            ((totalconden(t2(4),1,a)-Condendata(4))^2)^(1/2) + ...
            ((totalconden(t2(5),1,a)-Condendata(5))^2)^(1/2) + ...
            ((totalconden(t2(6),1,a)-Condendata(6))^2)^(1/2) + ...
            ((totalconden(t2(7),1,a)-Condendata(7))^2)^(1/2) + ...
            ((totalconden(t2(8),1,a)-Condendata(8))^2)^(1/2) + ...
            ((totalconden(t2(9),1,a)-Condendata(9))^2)^(1/2) + ...
            ((totalconden(t2(10),1,a)-Condendata(10))^2)^(1/2) + ...
            ((totalconden(t2(11),1,a)-Condendata(11))^2)^(1/2) + ...
            ((totalconden(t2(12),1,a)-Condendata(12))^2)^(1/2);
        end
    %-----
    [t,y] = ode15s(@F,tspan,n0,[],mL,nN2t,KmA,TL,TV,Kv11,Kv18);
    %-----
    n(b,:,a) = y(size(y,1),:);
    n0 = n(b,:,a);
    %-----
    [NA1,NA8,nGt1 nGt8] = Gasmolarflow
(n0,mL,nN2t,KmA,TV,Kv11,Kv18);
    %-----
    Feed = nGt1+nGt8+nN2t;
    z1=nGt1/(nGt1+nGt8+nN2t);
    z2=nGt8/(nGt1+nGt8+nN2t);
    z3=nN2t/(nGt1+nGt8+nN2t);
    sumZ = z1+z2+z3;
    %-----
    [K1,K2,K3] = Vaporpressure (TC);

```

```

%-----
[V,L,x,y,PBelowDP1,PAboveBP1,TwoPhase1] = flashcondenser4
(K1,K2,K3,(nGt1+nGt8+nN2t),z1,z2,z3,PBelowDP(:, :, a),PAboveBP(:, :, a),TwoPhase(
(:, :, a)));
    PBelowDP(:, :, a)=PBelowDP1;
    PAboveBP(:, :, a)=PAboveBP1;
    TwoPhase(:, :, a)=TwoPhase1;
%-----
mL = mL - (V*y(1)*76.096/2 + V*y(2)*18 + L*x(1)*76.096/2 +
L*x(2)*18)/1000;
%PG divide by 2 because only half molecule (1 functional group)
%removal rate PG-H2O both outlet gas and outlet condensate
removalrate(b, :, a) = [y(1)*V y(2)*V x(1)*L x(2)*L];
%find water percent in polymer
waterpercent(b, :, a)= n0(8)*18/1000/mL*100;
concl (b, :, a) = n(b, :, a)/mL;
% find accumulate mole of condensate
% find reaction rate
if b == 1
    summassconden(b, :, a) = [x(1)*L*76.096/2 x(2)*L*18];
    reactionrate(b, :, a) = concl(b, :, a);
else
    summassconden(b, :, a) = [(summassconden(b-1, 1, a)+x(1)*L*76.096/2
(summassconden(b-1, 2, a)+x(2)*L*18)];
    reactionrate(b, :, a) = concl(b, :, a) - concl(b-1, :, a);
end
    totalconden(b, :, a) = sum(summassconden(b, :, a));
    percentmassconden(b, :, a)=[x(1)*L*76.096/2*100/(x(1)*L*76.096/2
+x(2)*L*18) x(2)*L*18*100/(x(1)*L*76.096/2 +x(2)*L*18)];
%Loss weight from Vapor
dmL(1, 1, a) = dmL(1, 1, a) + V*y(1)*76.096/2/1000;
dmL(2, 1, a) = dmL(2, 1, a) + V*y(2)*18/1000;
%Loss weight from Condensate
dmL(3, 1, a) = dmL(3, 1, a) + L*x(1)*76.096/2/1000;
dmL(4, 1, a) = dmL(4, 1, a) + L*x(2)*18/1000;
%find mass of condensate
condensate(1, 1, a) = condensate(1) + x(1)*L*76.096/2/1000;
condensate(1, 2, a) = condensate(2) + x(2)*L*18/1000;
if mL < 0
    ml
    break
end
%Properties Estimation
OHno(b, :, a) = n0(1)*56.1*1000/(mL*1000);
Acidno(b, :, a) = (n0(2)+ n0(3)+n0(6))*56.1*1000/(mL*1000);
MWn(b, :, a) = 2*56100/(Acidno(b, :, a)+OHno(b, :, a))/2.45;
%=====

```

```

[Dense, SurfTen, Visco, Dpg, Dh2o] = UPproperty (MWn(b, :, a), TL);
Density(b, :, a) = Dense;
SurfTension(b, :, a) = SurfTen;
Viscosity(b, :, a) = Visco;
Diffusepg(b, :, a) = Dpg;
Diffuseh2o(b, :, a) = Dh2o;
%=====
[Re, Po, Power, E, kpg, kh2o] = Masstransfer(Density(b, :, a), Viscosity(b, :, a), N2, Diffusepg
(b, :, a), Diffuseh2o(b, :, a), TV, mL);
Renold(b, :, a) = Re;
Powerunareated(b, :, a) = Po;
Powerconsume(b, :, a) = Power;
Powerdissipate(b, :, a) = E;
kLpg(b, :, a) = kpg;
kLh2o(b, :, a) = kh2o;
%=====
[Gashold, Bubble, Iarea] =
Gasholdup1(Density(b, :, a), SurfTension(b, :, a), Viscosity(b, :, a), Powerconsume(b, :, a), N
2, TV, P, mL);
Gasholdup(b, :, a) = Gashold;
BBsize(b, :, a) = Bubble;
InterArea(b, :, a) = Iarea;
kLapg(b, :, a) = kLpg(b, :, a) * InterArea(b, :, a);
kLah2o(b, :, a) = kLh2o(b, :, a) * InterArea(b, :, a);
KmA(1) = kLapg(b, :, a);
KmA(8) = kLah2o(b, :, a);
end
t = linspace(1, (maxtime), maxtime);
t = t';
subplot(1, 2, 2)
plot(t, totalconden(:, :, a));
end
dmL
condensate
PBelowDP
PAboveBP
Twophase
%=====
function dn dt = F(t, n, mL, nN2t, KmA, tempL, tempV, Kvl1, Kvl8)
R = 0.0821; % liter.atm/(mol.K)
R1 = 8.314; % J/(K.mol)
kE = (120000/60 * exp(-75 * 1000 / (R1 * (273 + tempL))));
% kE = (23100/60 * exp(-58.2 * 1000 / (R1 * (273 + tempL))));
kI = (127000/60 * exp(-56 * 1000 / (R1 * (273 + tempL))));
kS5 = (476000/60 * exp(-48 * 1000 / (R1 * (273 + tempL))));
kS6 = kS5;
kS7 = kS5;

```

```

%kS8 = 0;
KE = 19;
KI = 9.1;
KS5 = 2.3;
KS6 = 1e10000;
KS7 = KS5;
%KS8 = 1e10000;
%[OH; COOH1D; COOH2D; COOR1D; COOR2D; COOHS; COORS; H2O; VOH;
VH2O]
ri1 = -kE*(n(2)/mL*n(1)/mL - n(4)/mL*n(8)/mL/KE)...
      -kE*(n(3)/mL*n(1)/mL - n(5)/mL*n(8)/mL/KE)...
      -kE*(n(6)/mL*n(1)/mL - n(7)/mL*n(8)/mL/KE)...
      -1/2*(kS5*(n(2)/mL*n(1)/mL - n(6)/mL/KS5) +...
            kS6*(n(3)/mL*n(1)/mL - n(6)/mL/KS6) +...
            kS7*(n(4)/mL*n(1)/mL - n(7)/mL/KS7));
ri2 = -kE*(n(2)/mL*n(1)/mL - n(4)/mL*n(8)/mL/KE)...
      -kI*(n(2)/mL - n(3)/mL/KI)...
      -kS5*(n(2)/mL*n(1)/mL - n(6)/mL/KS5);
ri3 = -kE*(n(3)/mL*n(1)/mL - n(5)/mL*n(8)/mL/KE)...
      +kI*(n(2)/mL - n(3)/mL/KI)...
      -kS6*(n(3)/mL*n(1)/mL - n(6)/mL/KS6);
ri4 = kE*(n(2)/mL*n(1)/mL - n(4)/mL*n(8)/mL/KE)...
      -kI*(n(4)/mL - n(5)/mL/KI)...
      -kS7*(n(4)/mL*n(1)/mL - n(7)/mL/KS7);
ri5 = kE*(n(3)/mL*n(1)/mL - n(5)/mL*n(8)/mL/KE)...
      +kI*(n(4)/mL - n(5)/mL/KI);
ri6 = -kE*(n(6)/mL*n(1)/mL - n(7)/mL*n(8)/mL/KE)...
      +kS5*(n(2)/mL*n(1)/mL - n(6)/mL/KS5)...
      +kS6*(n(3)/mL*n(1)/mL - n(6)/mL/KS6);
ri7 = kS7*(n(4)/mL*n(1)/mL - n(7)/mL/KS7)...
      +kE*(n(6)/mL*n(1)/mL - n(7)/mL*n(8)/mL/KE);
ri8 = 1/2*(kE*(n(2)/mL*n(1)/mL - n(4)/mL*n(8)/mL/KE) +...
        kE*(n(3)/mL*n(1)/mL - n(5)/mL*n(8)/mL/KE) +...
        kE*(n(6)/mL*n(1)/mL - n(7)/mL*n(8)/mL/KE));
%-----
[NA1,NA8,nGt1,nGt8] = Gasmolarflow (n,mL,nN2t,KmA,tempV,Kv11,Kv18);
%-----
%column vector
dndt = zeros(10,1);
dndt(1) = ri1*mL - NA1;
dndt(2) = ri2*mL;
dndt(3) = ri3*mL;
dndt(4) = ri4*mL;
dndt(5) = ri5*mL;
dndt(6) = ri6*mL;
dndt(7) = ri7*mL;
dndt(8) = ri8*mL - NA8;

```

```

dndt(9) = NA1 - nGt1;
dndt(10) = NA8 - nGt8;
%=====
function [NA1,NA8,nGt1,nGt8] = Gasmolarflow (n,mL,nN2t,KmA,temp, Kv11,Kv18)
R = 0.0821; %liter.atm/(mol.K)
P=1; % atm
VreG=pi*13.05^2/4*9/1000;% lit
cGT = P/(R*(temp+273)); %total concentration of gas in Vapor phase
%nGT = n(9)+n(10)+nN2
nN2t = nN2t/298*(temp+273);
nGT = P*VreG/(R*(273+temp)); % Total mol
%Kv11 = 1.6e-5 ; % OH
%Kv18 = 2.1e-2; % H2O
% Flux leaving the liquid phase
NA1 = (KmA(1)*mL*(n(1)/mL-n(9)/nGT*cGT/Kv11));
NA8 = (KmA(8)*mL*(n(8)/mL-n(10)/nGT*cGT/Kv18));
% gas phase molar flow
nGt1 = n(9)/(nGT)*(NA1+NA8+nN2t);
nGt8 = n(10)/(nGT)*(NA1+NA8+nN2t);
%=====
function [V,L,x,y,PBelowDP,PAboveBP,TwoPhase] = flashcondenser4
(K1,K2,K3,F,z1,z2,z3,PBelowDP,PAboveBP,TwoPhase)
%K1 = Pi/Pt => OH
%K2 = Water
%K3 = N2
% must specify Ki when temperature change
Psystem = 1; % 1 atm
%check outlet condition by Boiling and Dew point pressure
%Reference Distillation Principle and Practice Johann G. Stichmar and
%James R. Fair page75 eq. 3.6 and 3.7 Figure 3.4
%Dew point pressure
%Ki=Pi/Pt ==> Pt=1atm then Pi=Ki
Pdew = 1/(z1/K1 + z2/K2 + z3/K3);
% Boiling point
Pboil = z1*K1 + z2*K2 + z3*K3;
if Psystem < Pdew
% gasphase ==> un-condense
PBelowDP = PBelowDP + 1;
V = F;
L = 0;
x = zeros(1,3);
y = zeros(1,3);
y(1) = z1;
y(2) = z2;
y(3) = z3;
elseif Psystem > Pboil %
%total condense

```

```

PAboveBP = PAboveBP;
L = F;
V = 0;
x = zeros(1,3);
y = zeros(1,3);
x(1) = z1;
x(2) = z2;
x(3) = z3;
else
%2 phase mixture
%-----
%rough estimate
Twophase=Twophase+1
minimum=1000000;
for a = 0.0004:0.0004:1
    VperF=a;
    sum = (z1*(1-K1)/(1+VperF*(K1-1)))+ ...
          (z2*(1-K2)/(1+VperF*(K2-1)))+ ...
          (z3*(1-K3)/(1+VperF*(K3-1)));
    derisum = -((z1*K1*(K1-1)/(1+VperF*(K1-1))^2)+ ...
              (z2*K2*(K2-1)/(1+VperF*(K2-1))^2)+ ...
              (z3*K3*(K3-1)/(1+VperF*(K3-1))^2));
    absVperF = abs(((VperF-(sum/derisum))-VperF)/VperF);
    if absVperF < minimum
        minimum=absVperF;
        BestVperF = VperF;
    end
end
%-----
%fine estimate
upperVF = BestVperF+0.0004;
lowerVF = BestVperF-0.0004;
minimum=1000000;
for a = lowerVF:0.000001:upperVF
    VperF=a;
    sum = (z1*(1-K1)/(1+VperF*(K1-1)))+ ...
          (z2*(1-K2)/(1+VperF*(K2-1)))+ ...
          (z3*(1-K3)/(1+VperF*(K3-1)));
    derisum = -((z1*K1*(K1-1)/(1+VperF*(K1-1))^2)+ ...
              (z2*K2*(K2-1)/(1+VperF*(K2-1))^2)+ ...
              (z3*K3*(K3-1)/(1+VperF*(K3-1))^2));
    absVperF = abs(((VperF-(sum/derisum))-VperF)/VperF);
    if absVperF < minimum
        minimum=absVperF;
        BestVperF = VperF;
    end
end
end

```



```

%-----
VperF = BestVperF;
V = F*VperF;
L = F-V;
x = zeros(1,3);
y = zeros(1,3);
% liquid composition
x(1) = z1/(1+VperF*(K1-1));
x(2) = z2/(1+VperF*(K2-1));
x(3) = z3/(1+VperF*(K3-1));
% vapor composition
y(1) = x(1)*K1;
y(2) = x(2)*K2;
y(3) = x(3)*K3;
end
%=====
function [K1,K2,K3] = Vaporpressure (TC)
% VP for OH H2O N2 use data from PERRY table
T = (TC + 273);
C = [212.8 -15420 -28.109 2.1564e-5 2];
VPpg = 9.869233e-6*(exp(C(1) + C(2)/T + C(3)*log(T) + C(4)*T^C(5)));
C = [73.649 -7258.2 -7.3037 4.1653e-6 2];
VPh2o = 9.869233e-6*(exp(C(1) + C(2)/T + C(3)*log(T) + C(4)*T^C(5)));
C = [58.282 -1084.1 -8.3144 4.4127e-2 1];
VPn2 = 9.869233e-6*(exp(C(1) + C(2)/T + C(3)*log(T) + C(4)*T^C(5)));
K1= VPpg;
K2= VPh2o;
K3= VPn2;
%=====
function [Dense, SurfTen, Visco, Dpg, Dh2o] = UPproperty (MW,TL)
%Density = g/cm3
Dense = (0.003*MW + 1.037)/3.3;
%Linear model Poly1:
% f(x) = p1*x + p2
%Coefficients (with 95% confidence bounds):
% p1 = 0.003 (0.002906, 0.003094)
% p2 = 1.037 (0.9331, 1.141)
%Surface tension = dyne/cm (g.cm/s^2 / cm)
MW1 = (MW-988)/509;
%SurfTen1 =(187.8*MW1^4 + 924.9*MW1^3 + 3280*MW1^2 + 6143*MW1 +
4166);
SurfTen1 = (2*4361*exp(1.169*MW1))/100;
SurfTen = SurfTen1 -0.1/100*(TL-20);
%Protect minus value of SurfTen ==> set to minimum value
%if SurfTen < 0
% SurfTen = 50;
%end

```

```

%Protect over SurfTen
%SurfTen = SurfTen;
%Linear model Poly4:
%   f(x) = p1*x^4 + p2*x^3 + p3*x^2 + p4*x + p5
%   where x is normalized by mean 988 and std 509
%Coefficients (with 95% confidence bounds):
%   p1 =    187.8 (-327.3, 702.9)
%   p2 =    924.9 (501.3, 1348)
%   p3 =    3280 (1986, 4574)
%   p4 =    6143 (5357, 6930)
%   p5 =    4166 (3594, 4739)
%Viscosity = centiPoises, estimation Orrick and Erbar (1974) method
%A parameter
A = -0.01489*MW - 11.07;
%Linear model Poly1:
%   f(x) = p1*x + p2
%Coefficients (with 95% confidence bounds):
%   p1 =  -0.01489 (-0.01599, -0.01379)
%   p2 =  -11.07 (-12.42, -9.71)
%B parameter
B = 6.283*MW+2763;
%Linear model Poly1:
%   f(x) = p1*x + p2
%Coefficients (with 95% confidence bounds):
%   p1 =    6.283 (5.83, 6.735)
%   p2 =    2763 (2204, 3322)
Visco = (exp(A+(B/(TL+273-60))))*Dense*MW;
%Visco = centi-Poises %T = Kelvin %Dense = g/cm^3
%Coverse to poises(g/cm.s)
Visco =Visco/100;
%-----
%Estimate of Diffusion coefficient
%Wilke-Chang equation, 1955
%Molar volume at normal boiling point of H2O and PG, cm^3/mol
Vpg = 87.89625;
Vh2o = 18.79763;
Dpg = 7.4e-8*MW^(1/2)*(TL+273)/(Visco*100)/Vpg^0.6;
Dh2o = 7.4e-8*MW^(1/2)*(TL+273)/(Visco*100)/Vh2o^0.6;
%D=cm^2/s, T=Kelvin, Visco = centi-Poises, V=cm^3/mol
%converse D to m^2/s
Dpg = Dpg/100^2;
Dh2o = Dh2o/100^2;
%converse Dense to kg/m^3 %ViscoL to Pa.s %SurfTen to N/m
Dense = Dense*100^3/1000;
Visco = Visco/10;
SurfTen = SurfTen/100000*100;
%=====

```

```

% Volumetric mass transfer coefficient estimation
% Assumption
% 1) interfacial area and mean bubble size estimate from Nitrogen
% 2) Diffusivity of PG and H2O are not interact
% 3) kL of PG and H2O estimate from paper
% =====
function [Re,Po,Power,E,kpg,kh2o] =
Masstransfer(DenseL,ViscoL,N2,Dpg,Dh2o,TV,mL)
% Q=m^3/sec
Q=N2/1000;
Q=Q*(TV+273)/(25+273);
% Impeller diameter, T, for 4 flat blade turbine, H=liquid level
T = 5/100; % meter
H = 10/100; % meter
rpm = 15; % round per sec.
% Impeller Reynolds number, Re = T^2*N*DenseL/ViscoL
% cross check for Renold number
Re = (T*100)^2*rpm*(DenseL/100^3*1000)/(ViscoL*10);
% at Re > 20000 Power number(Np) is constant = 5
Np=5;
% Np=Po/(Dense*N^3*T^5)
% Po = PowNo*(DenseL*N^3/T^5)
% Po=Power consumption in un-aerated system
Po=Np*DenseL*(rpm)^3*T^5;
% For Rushton turbine
Power=0.783*((Po^2*(rpm)*T^3)/(Q^0.56))^0.459;
% E=Energy dissipation
E=Power/(DenseL*pi/4*T^2*H);
% E=Power/mL;
% Mass transfer coefficient
kpg = 2/pi^(1/2)*Dpg^(1/2)*(E*DenseL/ViscoL)^(1/4);
kh2o = 2/pi^(1/2)*Dh2o^(1/2)*(E*DenseL/ViscoL)^(1/4);
% =====f
unction [Gashold,Bubble,Iarea] =
Gasholdup1(DenseL,SurfTen,ViscoL,Power,N2,T,P,mL)
ViscoN2 = 0.016493*T^0 + 4.9286e-005*T^1 + (-3.1215e-008)*T^2 + 1.4419e-
011*T^3;
% ViscoN2=cP % T=Celcius
% converse ViscoN2 to Pa.s
ViscoN2 = ViscoN2/10;
% N2 Density calculate from ideal gas law
DenseN2 = P*28/0.08205/(T+273); % g/lit or kg/m^3
% Superficial velocity m/s
% Reactor diameter = 0.13 meter
% Q=m^3/sec
Q=N2/1000;
Vs = Q/(pi*0.13^2/4); % m/s

```

```

T = 5/100; % meter
rpm = 15; % round per sec.
PreGashold =
0.819*Vs^(2/3)*rpm^(2/5)*T^(4/15)/9.81^(1/3)*(DenseL/SurfTen)^(1/5)*(DenseL/(
DenseL-DenseN2))*(DenseL/DenseN2)^(-1/15)*(ViscoL/ViscoN2)^(-1/4);
% Gas hold up in viscous liquid
Gashold = PreGashold/(1+PreGashold);
Bubble =
0.7*SurfTen^0.6/(Power/(mL/DenseL))^0.4/DenseL^0.2*(ViscoL/ViscoN2)^0.1;
Iarea = 6*Gashold/Bubble;
%=====
function model9 %(Temp180 °C N2 840 ccm)
% Import reaction temperature file
% Estimate of kLa
ndata1 = xlsread('Temp180N840.xls',1, 'B2:B4'); % initial weight
ndata2 = xlsread('Temp180N840.xls',1, 'C8:H31760'); % Actual temperature
n0 = [ndata1(1)/76.09*2; ndata1(2)/98.06*2; 0; 0; 0; 0; 0; 0; 0; 0];
% 1 mole of reactants = 2 functional group
% [OH; COOH1D; COOH2D; COOR1D; COOR2D; COOHS; COORS; H2O; VOH;
VH2O]
N2 = ndata1(3)/1000/60; % N2 standard cm3/min to lit/sec
times = ndata2(:,1);
maxtime = times(size(times,1),1);
TLdata = ndata2(:,6); % Liquid temp.
TVdata = ndata2(:,5); % Vapor temp.
TCdata = ndata2(:,2); % Top column temp.
TWDdata = ndata2(:,3); % Cooling water input temp.
TWOdata = ndata2(:,4); % Cooling water output temp.
% initial condition
KmA = [0; 0; 0; 0; 0; 0; 0; 0];
P=1; % atm
nN2t = N2/22.4; % mol/sec
mL = (ndata1(1)+ndata1(2))/1000; % kilogram
% variable for integrate
tspan = [0 1];
n = zeros(maxtime,10);
concl = zeros(maxtime,10);
reactionrate = zeros(maxtime,10);
removalrate = zeros(maxtime,4);
% Flash condenser variable
PBelowDP = 0;
PAboveBP = 0;
Twophase = 0;
% weight loss variable
dmL = zeros(4,1);
condensate = zeros(1,2);
nGout = zeros(1,4);

```

```

%Properties variable-----
Acidno = zeros(maxtime,1);
OHno = zeros(maxtime,1);
MWn = zeros(maxtime,1);
Density = zeros(maxtime,1);
SurfTension = zeros(maxtime,1);
Viscosity = zeros(maxtime,1);
Diffusepg = zeros(maxtime,1);
Diffuseh2o = zeros(maxtime,1);
Renold = zeros(maxtime,1);
Powerconsume = zeros(maxtime,1);
Powerunareated = zeros(maxtime,1);
Powerdissipate = zeros(maxtime,1);
kLpg= zeros(maxtime,1);
kLh2o= zeros(maxtime,1);
Gasholdup = zeros(maxtime,1);
BBsize = zeros(maxtime,1);
InterArea = zeros(maxtime,1);
kLaPG = zeros(maxtime,1);
kLah2o = zeros(maxtime,1);
summassconden = zeros(maxtime,2);
totalconden = zeros(maxtime,1);
percentmassconden = zeros(maxtime,2);
waterpercent = zeros(maxtime,1);
%start up program-----
for i = 1:maxtime
    %TL=TLdata(i)+3;
    %TV=TVdata(i)+3;
    %TC=TCdata(i);
    %TWI=TWIdata(i);
    %TWO=TWOdata(i);
    if i < 3500
        TL=0;
        TV=0;
        TC=25;
        TWI=15;
        TWO=25;
    else
        TL=180;
        TV=180;
        TC=25;
        TWI=15;
        TWO=25;
    end
end
%-----
[t,y] = ode15s(@F,tspan,n0,[],mL,nN2t,KmA,TL,TV);
%-----

```

```

n(i,:) = y(size(y,1),:);
n0 = n(i,:);
%-----
[NA1,NA8,nGt1 nGt8] = Gasmolarflow (n0,mL,nN2t,KmA,TV);
%-----
Feed = nGt1+nGt8+nN2t;
z1=nGt1/(nGt1+nGt8+nN2t);
z2=nGt8/(nGt1+nGt8+nN2t);
z3=nN2t/(nGt1+nGt8+nN2t);
sumZ = z1+z2+z3;
%-----
[K1,K2,K3] = Vaporpressure (TC);
%-----
[V,L,x,y,PBelowDP,PAboveBP,TwoPhase] = flashcondenser4
(K1,K2,K3,(nGt1+nGt8+nN2t),z1,z2,z3,PBelowDP,PAboveBP,TwoPhase);
%-----
mL = mL - (V*y(1)*76.096/2 + V*y(2)*18 + L*x(1)*76.096/2 + L*x(2)*18)/1000;
%PG divide by 2 because only half molecule (1 functional group)
%removal rate PG-H2O both outlet gas and outlet condensate
removalrate(i,:) = [y(1)*V y(2)*V x(1)*L x(2)*L];
%find water percent in polymer
waterpercent(i,1)= n0(8)*18/1000/mL*100;
concl (i,:) = n(i:)/mL;
% find accumulate mole of condensate
% find reaction rate
if i == 1
    summassconden(i,:) = [x(1)*L*76.096/2 x(2)*L*18];
    reactionrate(i,:) = concl(i,:);
else
    summassconden(i,:) = [(summassconden(i-1,1)+x(1)*L*76.096/2)
(summassconden(i-1,2)+x(2)*L*18)];
    reactionrate(i,:) = concl(i,:) - concl((i-1),:);
end
totalconden(i,1) = sum(summassconden(i,:));
percentmassconden(i,:)=[x(1)*L*76.096/2*100/(x(1)*L*76.096/2 +x(2)*L*18)
x(2)*L*18*100/(x(1)*L*76.096/2 +x(2)*L*18)];
%Loss weight from Vapor
dmL(1) = dmL(1) + V*y(1)*76.096/2/1000;
dmL(2) = dmL(2) + V*y(2)*18/1000;
%Loss weight from Condensate
dmL(3) = dmL(3) + L*x(1)*76.096/2/1000;
dmL(4) = dmL(4) + L*x(2)*18/1000;
%find mass of condensate
condensate(1) = condensate(1) + x(1)*L*76.096/2/1000;
condensate(2) = condensate(2) + x(2)*L*18/1000;
if mL < 0
    break

```

```

end
%Properties Estimation
OHno(i,1) = n0(1)*56.1*1000/(mL*1000);
Acidno(i,1) = (n0(2)+ n0(3)+n0(6))*56.1*1000/(mL*1000);
MWn(i,1) = 2*56100/(Acidno(i,1)+OHno(i,1))/2.45;
[Dense,SurfTen,Visco,Dpg,Dh2o] = UPproperty (MWn(i,1),TL);
Density(i,1) = Dense;
SurfTension(i,1) = SurfTen;
Viscosity(i,1) = Visco;
Diffusepg(i,1) = Dpg;
Diffuseh2o(i,1) = Dh2o;

[Re,Po,Power,E,kpg,kh2o]=Masstransfer(Density(i,1),Viscosity(i,1),N2,Diffusepg(i,1),Diffuseh2o(i,1),TV,mL);
Renold(i,1)=Re;
Powerunareated(i,1) = Po;
Powerconsume(i,1) = Power;
Powerdissipate(i,1)=E;
kLpg(i,1)=kpg;
kLh2o(i,1)=kh2o;
[Gashold,Bubble,Iarea] =
Gasholdup1(Density(i,1),SurfTension(i,1),Viscosity(i,1),Powerconsume(i,1),N2,TV,P,mL);
Gasholdup(i,1) = Gashold;
BBsize(i,1) = Bubble;
InterArea(i,1) = Iarea;
kLapg (i,1) = kLpg(i,1)*InterArea(i,1);
kLah2o(i,1) = kLh2o(i,1)*InterArea(i,1);
KmA(1) = kLapg (i,1);
KmA(8) = kLah2o(i,1);
end
mL
dmL
Lossweight = sum(dmL)
condensate
totalcondense = sum(condensate)
PBelowDP
PAboveBP
Twophase
t = times';
xlswrite('model999Temp180N840.xls',times,'Temp180N840','A2');
xlswrite('model999Temp180N840.xls',n,'Temp180N840','B2');
xlswrite('model999Temp180N840.xls',Acidno,'Temp180N840','Q2');
xlswrite('model999Temp180N840.xls',OHno,'Temp180N840','R2');
%-----
xlswrite('model999Temp180N840.xls',MWn,'Temp180N840','T2');
xlswrite('model999Temp180N840.xls',Density,'Temp180N840','W2');

```

```

xlswrite('model999Temp180N840.xls',SurfTension,'Temp180N840','X2');
xlswrite('model999Temp180N840.xls',Viscosity,'Temp180N840','Y2');
%-----
xlswrite('model999Temp180N840.xls',Renold,'Temp180N840','AA2');
xlswrite('model999Temp180N840.xls',Powerunareated,'Temp180N840','AB2');
xlswrite('model999Temp180N840.xls',Powerconsume,'Temp180N840','AC2');
xlswrite('model999Temp180N840.xls',Powerdissipate,'Temp180N840','AD2');
%-----
xlswrite('model999Temp180N840.xls',Diffusepg,'Temp180N840','AF2');
xlswrite('model999Temp180N840.xls',Diffuseh2o,'Temp180N840','AG2');
xlswrite('model999Temp180N840.xls',kLpg,'Temp180N840','AI2');
xlswrite('model999Temp180N840.xls',kLh2o,'Temp180N840','AJ2');
xlswrite('model999Temp180N840.xls',Gasholdup,'Temp180N840','AL2');
xlswrite('model999Temp180N840.xls',BBsize,'Temp180N840','AM2');
xlswrite('model999Temp180N840.xls',InterArea,'Temp180N840','AN2');
xlswrite('model999Temp180N840.xls',kLapg,'Temp180N840','AP2');
xlswrite('model999Temp180N840.xls',kLah2o,'Temp180N840','AQ2');
xlswrite('model999Temp180N840.xls',percentmassconden,'Temp180N840','AS2');
xlswrite('model999Temp180N840.xls',waterpercent,'Temp180N840','AV2');
xlswrite('model999Temp180N840.xls',summassconden,'Temp180N840','AX2');
xlswrite('model999Temp180N840.xls',totalconden,'Temp180N840','AZ2');
xlswrite('model999Temp180N840.xls',concL,'Temp180N840','BB2');
xlswrite('model999Temp180N840.xls',reactionrate,'Temp180N840','BM2');
xlswrite('model999Temp180N840.xls',removalrate,'Temp180N840','BX2');
%=====
function dn dt = F(t,n,mL,nN2t,KmA,tempL,tempV,Kvl1,Kvl8)
R = 0.0821; % liter.atm/(mol.K)
R1 = 8.314; %J/(K.mol)
kE = (1200000/60*exp(-75*1000/(R1*(273+tempL))));
kI = (127000/60*exp(-56*1000/(R1*(273+tempL))));
kS5 = (476000e-4/60*exp(-48*1000/(R1*(273+tempL))));
kS6 = kS5;
kS7 = kS5;
%kS8 = 0;
KE = 25;
KI = 12.5;
KS5 = 0.87;
KS6 = 1e10000;
KS7 = KS5;
%KS8 = 1e10000;
%[OH; COOH1D; COOH2D; COOR1D; COOR2D; COOHS; COORS; H2O; VOH;
VH2O]
ri1 = -kE*(n(2)/mL*n(1)/mL - n(4)/mL*n(8)/mL/KE)...
-kE*(n(3)/mL*n(1)/mL - n(5)/mL*n(8)/mL/KE)...
-kE*(n(6)/mL*n(1)/mL - n(7)/mL*n(8)/mL/KE)...
-1/2*(kS5*(n(2)/mL*n(1)/mL - n(6)/mL/KS5) +...
kS6*(n(3)/mL*n(1)/mL - n(6)/mL/KS6) +...

```



```

    kS7*(n(4)/mL*n(1)/mL - n(7)/mL/KS7));
ri2 = -kE*(n(2)/mL*n(1)/mL - n(4)/mL*n(8)/mL/KE)...
    -kI*(n(2)/mL - n(3)/mL/KI)...
    -kS5*(n(2)/mL*n(1)/mL - n(6)/mL/KS5);
ri3 = -kE*(n(3)/mL*n(1)/mL - n(5)/mL*n(8)/mL/KE)...
    +kI*(n(2)/mL - n(3)/mL/KI)...
    -kS6*(n(3)/mL*n(1)/mL - n(6)/mL/KS6);
ri4 = kE*(n(2)/mL*n(1)/mL - n(4)/mL*n(8)/mL/KE)...
    -kI*(n(4)/mL - n(5)/mL/KI)...
    -kS7*(n(4)/mL*n(1)/mL - n(7)/mL/KS7);
ri5 = kE*(n(3)/mL*n(1)/mL - n(5)/mL*n(8)/mL/KE)...
    +kI*(n(4)/mL - n(5)/mL/KI);
ri6 = -kE*(n(6)/mL*n(1)/mL - n(7)/mL*n(8)/mL/KE)...
    +kS5*(n(2)/mL*n(1)/mL - n(6)/mL/KS5)...
    +kS6*(n(3)/mL*n(1)/mL - n(6)/mL/KS6);
ri7 = kS7*(n(4)/mL*n(1)/mL - n(7)/mL/KS7)...
    +kE*(n(6)/mL*n(1)/mL - n(7)/mL*n(8)/mL/KE);
ri8 = 1/2*(kE*(n(2)/mL*n(1)/mL - n(4)/mL*n(8)/mL/KE) +...
    kE*(n(3)/mL*n(1)/mL - n(5)/mL*n(8)/mL/KE) +...
    kE*(n(6)/mL*n(1)/mL - n(7)/mL*n(8)/mL/KE));
%-----
[NA1,NA8,nGt1,nGt8] = Gasmolarflow (n,mL,nN2t,KmA,tempV);
%-----
%column vector
dndt = zeros(10,1);
dndt(1) = ri1*mL - NA1;
dndt(2) = ri2*mL;
dndt(3) = ri3*mL;
dndt(4) = ri4*mL;
dndt(5) = ri5*mL;
dndt(6) = ri6*mL;
dndt(7) = ri7*mL;
dndt(8) = ri8*mL - NA8;
dndt(9) = NA1 - nGt1;
dndt(10) = NA8 - nGt8;
%=====
function [NA1,NA8,nGt1,nGt8] = Gasmolarflow (n,mL,nN2t,KmA,temp)
R = 0.0821; % liter.atm/(mol.K)
P=1; % atm
VreG=pi*13.05^2/4*9/1000;% lit
cGT = P/(R*(temp+273)); % total concentration of gas in Vapor phase
%nGT = n(9)+n(10)+nN2
nGT = P*VreG/(R*(273+temp)); % Total mol
Kv11 = 1.46e-5 ; % OH
Kv18 = 1.4e-2; % H2O
%Flux leaving the liquid phase
NA1 = (KmA(1)*mL*(n(1)/mL-n(9)/nGT*cGT/Kv11));

```

```

NA8 = (KmA(8)*mL*(n(8)/mL-n(10)/nGT*cGT/Kv18));
% gas phase molar flow
nGt1 = n(9)/(nGT)*(NA1+NA8+nN2t);
nGt8 = n(10)/(nGT)*(NA1+NA8+nN2t);
%=====
function [V,L,x,y,PBelowDP,PAboveBP,TwoPhase] = flashCondenser4
(K1,K2,K3,F,z1,z2,z3,PBelowDP,PAboveBP,TwoPhase)
% K1 = Pi/Pt => OH
% K2 = Water
% K3 = N2
% must specify Ki when temperature change
Psystem = 1; % 1 atm
% check outlet condition by Boiling and Dew point pressure
% Reference Distillation Principle and Practice Johann G. Stichmar and
% James R. Fair page 75 eq. 3.6 and 3.7 Figure 3.4
% Dew point pressure
% Ki=Pi/Pt ==> Pt=1atm then Pi=Ki
Pdew = 1/(z1/K1 + z2/K2 + z3/K3);
% Boiling point
Pboil = z1*K1 + z2*K2 + z3*K3;
if Psystem < Pdew
    % gas phase ==> un-condense
    PBelowDP = PBelowDP + 1;
    V = F;
    L = 0;
    x = zeros(1,3);
    y = zeros(1,3);
    y(1) = z1;
    y(2) = z2;
    y(3) = z3;
elseif Psystem > Pboil %
    % total condense
    PAboveBP = PAboveBP;
    L = F;
    V = 0;
    x = zeros(1,3);
    y = zeros(1,3);
    x(1) = z1;
    x(2) = z2;
    x(3) = z3;
else
    % 2 phase mixture
    %-----
    % rough estimate
    TwoPhase = TwoPhase + 1
    minimum = 1000000;
    for a = 0.0004:0.0004:1

```

```

VperF=a;
sum = (z1*(1-K1)/(1+VperF*(K1-1)))+ ...
      (z2*(1-K2)/(1+VperF*(K2-1)))+ ...
      (z3*(1-K3)/(1+VperF*(K3-1)));
derisum = -((z1*K1*(K1-1)/(1+VperF*(K1-1))^2)+ ...
           (z2*K2*(K2-1)/(1+VperF*(K2-1))^2)+ ...
           (z3*K3*(K3-1)/(1+VperF*(K3-1))^2));
absVperF = abs(((VperF-(sum/derisum))-VperF)/VperF);
if absVperF < minimum
    minimum=absVperF;
    BestVperF = VperF;
end
end
%-----
%fine estimate
upperVF = BestVperF+0.0004;
lowerVF = BestVperF-0.0004;
minimum=1000000;
for a = lowerVF:0.000001:upperVF
    VperF=a;
    sum = (z1*(1-K1)/(1+VperF*(K1-1)))+ ...
          (z2*(1-K2)/(1+VperF*(K2-1)))+ ...
          (z3*(1-K3)/(1+VperF*(K3-1)));
    derisum = -((z1*K1*(K1-1)/(1+VperF*(K1-1))^2)+ ...
               (z2*K2*(K2-1)/(1+VperF*(K2-1))^2)+ ...
               (z3*K3*(K3-1)/(1+VperF*(K3-1))^2));
    absVperF = abs(((VperF-(sum/derisum))-VperF)/VperF);
    if absVperF < minimum
        minimum=absVperF;
        BestVperF = VperF;
    end
end
end
%-----
VperF = BestVperF;
V = F*VperF;
L = F-V;
x = zeros(1,3);
y = zeros(1,3);
% liquid composition
x(1) = z1/(1+VperF*(K1-1));
x(2) = z2/(1+VperF*(K2-1));
x(3) = z3/(1+VperF*(K3-1));
% vapor composition
y(1) = x(1)*K1;
y(2) = x(2)*K2;
y(3) = x(3)*K3;
end

```

```

%=====
function [K1,K2,K3] = Vaporpressure (TC)
% VP for OH H2O N2 use data from PERRY table
T = (TC + 273);
C = [212.8 -15420 -28.109 2.1564e-5 2];
VPpg = 9.869233e-6*(exp(C(1) + C(2)/T + C(3)*log(T) + C(4)*T^C(5)));
C = [73.649 -7258.2 -7.3037 4.1653e-6 2];
VPh2o = 9.869233e-6*(exp(C(1) + C(2)/T + C(3)*log(T) + C(4)*T^C(5)));
C = [58.282 -1084.1 -8.3144 4.4127e-2 1];
VPn2 = 9.869233e-6*(exp(C(1) + C(2)/T + C(3)*log(T) + C(4)*T^C(5)));
K1= VPpg;
K2= VPh2o;
K3= VPn2;
%=====
function [Dense, SurfTen, Visco, Dpg, Dh2o] = UPproperty (MW,TL)
%Density = g/cm3
Dense = (0.003*MW + 1.037)/3.3;
%Linear model Poly1:
% f(x) = p1*x + p2
%Coefficients (with 95% confidence bounds):
% p1 = 0.003 (0.002906, 0.003094)
% p2 = 1.037 (0.9331, 1.141)
%Surface tension = dyne/cm (g.cm/s^2 / cm)
MW1 = (MW-988)/509;
%SurfTen1 =(187.8*MW1^4 + 924.9*MW1^3 + 3280*MW1^2 + 6143*MW1 +
4166);
SurfTen1 = (2*4361*exp(1.169*MW1))/100;
SurfTen = SurfTen1 -0.1/100*(TL-20);
%Protect minus value of SurfTen ==> set to minimum value
%if SurfTen < 0
% SurfTen = 50;
%end
%Protect over SurfTen
%SurfTen = SurfTen;
%Linear model Poly4:
% f(x) = p1*x^4 + p2*x^3 + p3*x^2 + p4*x + p5
% where x is normalized by mean 988 and std 509
%Coefficients (with 95% confidence bounds):
% p1 = 187.8 (-327.3, 702.9)
% p2 = 924.9 (501.3, 1348)
% p3 = 3280 (1986, 4574)
% p4 = 6143 (5357, 6930)
% p5 = 4166 (3594, 4739)
% Viscosity = centiPoises, estimation Orrick and Erbar (1974) method
%A parameter
A = -0.01489*MW - 11.07;
%Linear model Poly1:

```

```

% f(x) = p1*x + p2
%Coefficients (with 95% confidence bounds):
% p1 = -0.01489 (-0.01599, -0.01379)
% p2 = -11.07 (-12.42, -9.71)
%B parameter
B = 6.283*MW+2763;
%Linear model Poly1:
% f(x) = p1*x + p2
%Coefficients (with 95% confidence bounds):
% p1 = 6.283 (5.83, 6.735)
% p2 = 2763 (2204, 3322)
Visco = (exp(A+(B/(TL+273-60))))*Dense*MW;
%Visco = centi-Poises %T = Kelvin %Dense = g/cm^3
%Coverse to poises(g/cm.s)
Visco =Visco/100;
%-----
%Estimate of Diffusion coefficient
%Wilke-Chang equation, 1955
%Molar volume at normal boiling point of H2O and PG, cm^3/mol
Vpg = 87.89625;
Vh2o = 18.79763;
Dpg = 7.4e-8*MW^(1/2)*(TL+273)/(Visco*100)/Vpg^0.6;
Dh2o = 7.4e-8*MW^(1/2)*(TL+273)/(Visco*100)/Vh2o^0.6;
%D=cm^2/s, T=Kelvin, Visco = centi-Poises, V=cm^3/mol
%converse D to m^2/s
Dpg = Dpg/100^2;
Dh2o = Dh2o/100^2;
%converse Dense to kg/m^3 %ViscoL to Pa.s %SurfTen to N/m
Dense = Dense*100^3/1000;
Visco = Visco/10;
SurfTen = SurfTen/100000*100;
%=====
% Volumetric mass transfer coefficient estimation
%Assumption
% 1)interfacial area and mean bubble size estimate from Nitrogen
% 2)Diffusivity of PG and H2O are not interact
% 3)kL of PG and H2O esimate from paper
%=====f
unction [Re,Po,Power,E,kpg,kh2o] =
Masstransfer(DenseL,ViscoL,N2,Dpg,Dh2o,TV,mL)
%Q=m^3/sec
Q=N2/1000;
Q=Q*(TV+273)/(25+273);
%Impeller diameter, T, for 4 flat blade turbine, H=liquid level
T = 5/100; %meter
H = 10/100; %meter
rpm = 15; %round per sec.

```

```

% Impeller Renolds number,  $Re = T^2 * N * DenseL / ViscoL$ 
% cross check for Renold number
 $Re = (T * 100)^2 * rpm * (DenseL / 100^3 * 1000) / (ViscoL * 10)$ ;
% at  $Re > 20000$  Power number(Np) is constant = 5
Np=5;
%  $Np = Po / (Dense * N^3 * T^5)$ 
%  $Po = PowNo * (DenseL * N^3 / T^5)$ 
%  $Po =$  Power consumption in un-aerated system
 $Po = Np * DenseL * (rpm)^3 * T^5$ ;
% For Rushton turbine
 $Power = 0.783 * ((Po^2 * (rpm) * T^3) / (Q^{0.56}))^{0.459}$ ;
% E=Energy dissipation
 $E = Power / (DenseL * pi / 4 * T^2 * H)$ ;
% E=Power/mL;
% Mass transfer coefficient
 $kpg = 2 / pi^{(1/2)} * Dpg^{(1/2)} * (E * DenseL / ViscoL)^{(1/4)}$ ;
 $kh2o = 2 / pi^{(1/2)} * Dh2o^{(1/2)} * (E * DenseL / ViscoL)^{(1/4)}$ ;
%=====
function [Gashold,Bubble,Iarea] =
Gasholdup1(DenseL,SurfTen,ViscoL,Power,N2,T,P,mL)
ViscoN2 = 0.016493*T^0 + 4.9286e-005*T^1 + (-3.1215e-008)*T^2 + 1.4419e-
011*T^3;
% ViscoN2=cP %T=Celcius
% converse ViscoN2 to Pa.s
ViscoN2 = ViscoN2/10;
% N2 Density calculate from ideal gas law
 $DenseN2 = P * 28 / 0.08205 / (T + 273)$ ; % g/lit or kg/m^3
% Superficial velocity m/s
% Reactor diameter = 0.13 meter
%  $Q = m^3/sec$ 
 $Q = N2 / 1000$ ;
 $Vs = Q / (pi * 0.13^2 / 4)$ ; % m/s
T = 5/100; % meter
rpm = 15; % round per sec.
PreGashold =
0.819 * Vs^(2/3) * rpm^(2/5) * T^(4/15) / 9.81^(1/3) * (DenseL / SurfTen)^(1/5) * (DenseL / (
DenseL - DenseN2)) * (DenseL / DenseN2)^(-1/15) * (ViscoL / ViscoN2)^(-1/4);
% Gas hold up in viscous liquid
Gashold = PreGashold / (1 + PreGashold);
Bubble =
0.7 * SurfTen^0.6 / (Power / (mL / DenseL))^0.4 / DenseL^0.2 * (ViscoL / ViscoN2)^0.1;
Iarea = 6 * Gashold / Bubble;
%=====

```

C.3 Model for three dimensional plot

Use for predicting the sensitivity of process parameter.

C.3.1 Model for prediction of specific interfacial area characterization

function SpecificInterfacialarea3D

```

D = linspace(0.004e-9,4e-9,40); %Diffusivity
ViscosL = linspace(0.0005,0.02,40); %Pa.s
DenseL = linspace(100,1000,40); %kg/m^3
E = linspace(0,5,40); %energy dissipation
Q = linspace(0e-6,1.4e-5,40); %N2 flow m^3/s
Temp = linspace(50,250,40);
SurfTen = linspace(0.01,0.1,40);
%QN2=m^3/sec
%Q=Q*(TV+273)/(25+273);
%Vs = Q/(pi*0.13^2/4); %m/s
T = 5/100; %meter
H = 10/100; %meter
rpm = 15; %round per sec.
Np=5;
mL = 1.6; %kg
mL1 = linspace(1.7,1.5,20);
Di = 0.13; %vessel diameter meter
Mw = linspace(50,1000,40);
%Bubble = 0.7/0.8856/(5^2*rpm^7*T^13)^0.1836*0.1^4 .*SurfTen.^0.6 *
Q'.^0.1028.*(1./DenseL).^0.1672.*(ViscosL./1.5e-3).^0.1
%=====
%vary density
PreGashold1 = 0.819*(6e-6/(pi*0.13^2/4)).^(2/3)
*(1./SurfTen').^(1/5)*rpm^(2/5)*T^(4/15)/9.81^(1/3)*(250)^(1/5)*(250/(250-
0.9))*(250/0.9)^(-1/15) *(ViscosL/1.5e-3).^(-1/4);
PreGashold2 = 0.819*(6e-6/(pi*0.13^2/4)).^(2/3)
*(1./SurfTen').^(1/5)*rpm^(2/5)*T^(4/15)/9.81^(1/3)*(500)^(1/5)*(500/(500-
0.9))*(500/0.9)^(-1/15) *(ViscosL/1.5e-3).^(-1/4);
PreGashold3 = 0.819*(6e-6/(pi*0.13^2/4)).^(2/3)
*(1./SurfTen').^(1/5)*rpm^(2/5)*T^(4/15)/9.81^(1/3)*(750)^(1/5)*(750/(750-
0.9))*(750/0.9)^(-1/15) *(ViscosL/1.5e-3).^(-1/4);
PreGashold4 = 0.819*(6e-6/(pi*0.13^2/4)).^(2/3)
*(1./SurfTen').^(1/5)*rpm^(2/5)*T^(4/15)/9.81^(1/3)*(1000)^(1/5)*(1000/(1000-
0.9))*(1000/0.9)^(-1/15) *(ViscosL/1.5e-3).^(-1/4);
Gashold1 = PreGashold1.*(1./(1+PreGashold1));
Gashold2 = PreGashold2.*(1./(1+PreGashold2));
Gashold3 = PreGashold3.*(1./(1+PreGashold3));
Gashold4 = PreGashold4.*(1./(1+PreGashold4));

%Bubble = 0.7/0.8856/(5^2*rpm^7*T^13)^0.1836*0.1^4 .*SurfTen.^0.6 *
Q'.^0.1028.*(1./DenseL).^0.1672.*(ViscosL./1.5e-3).^0.1

```

```

Bubble1 = 0.7/0.8856/(5^2*rpm^7*T^13)^0.1836*0.1^4 .*SurfTen'.^0.6 * 6e-
6.^0.1028.*(1./250).^0.1672 *(ViscosL./1.5e-3).^0.1;
Bubble2 = 0.7/0.8856/(5^2*rpm^7*T^13)^0.1836*0.1^4 .*SurfTen'.^0.6 * 6e-
6.^0.1028.*(1./500).^0.1672 *(ViscosL./1.5e-3).^0.1;
Bubble3 = 0.7/0.8856/(5^2*rpm^7*T^13)^0.1836*0.1^4 .*SurfTen'.^0.6 * 6e-
6.^0.1028.*(1./750).^0.1672 *(ViscosL./1.5e-3).^0.1;
Bubble4 = 0.7/0.8856/(5^2*rpm^7*T^13)^0.1836*0.1^4 .*SurfTen'.^0.6 * 6e-
6.^0.1028.*(1./1000).^0.1672 *(ViscosL./1.5e-3).^0.1;
Iarea1 = 6*Gashold1./Bubble1;
Iarea2 = 6*Gashold2./Bubble2;
Iarea3 = 6*Gashold3./Bubble3;
Iarea4 = 6*Gashold4./Bubble4;
figure
hold on
view(3)
grid on
mesh(ViscosL,SurfTen,Iarea1);
mesh(ViscosL,SurfTen,Iarea2);
mesh(ViscosL,SurfTen,Iarea3);
mesh(ViscosL,SurfTen,Iarea4);
hold off
title('Interfacial area Viscosity vs Surfacentension vary density')
%=====
%vary inert gas flow
PreGashold5 = 0.819*(2e-6/(pi*0.13^2/4)).^(2/3)
*(1./SurfTen').^(1/5)*rpm^(2/5)*T^(4/15)/9.81^(1/3)*(500)^(1/5)*(500/(500-
0.9))*(500/0.9)^(-1/15) *(ViscosL/1.5e-3).^(-1/4);
PreGashold6 = 0.819*(6e-6/(pi*0.13^2/4)).^(2/3)
*(1./SurfTen').^(1/5)*rpm^(2/5)*T^(4/15)/9.81^(1/3)*(500)^(1/5)*(500/(500-
0.9))*(500/0.9)^(-1/15) *(ViscosL/1.5e-3).^(-1/4);
PreGashold7 = 0.819*(10e-6/(pi*0.13^2/4)).^(2/3)
*(1./SurfTen').^(1/5)*rpm^(2/5)*T^(4/15)/9.81^(1/3)*(500)^(1/5)*(500/(500-
0.9))*(500/0.9)^(-1/15) *(ViscosL/1.5e-3).^(-1/4);
PreGashold8 = 0.819*(14e-6/(pi*0.13^2/4)).^(2/3)
*(1./SurfTen').^(1/5)*rpm^(2/5)*T^(4/15)/9.81^(1/3)*(500)^(1/5)*(500/(500-
0.9))*(500/0.9)^(-1/15) *(ViscosL/1.5e-3).^(-1/4);
Gashold5 = PreGashold5.*(1./(1+PreGashold5));
Gashold6 = PreGashold6.*(1./(1+PreGashold6));
Gashold7 = PreGashold7.*(1./(1+PreGashold7));
Gashold8 = PreGashold8.*(1./(1+PreGashold8));
Bubble5 = 0.7/0.8856/(5^2*rpm^7*T^13)^0.1836*0.1^4 .*SurfTen'.^0.6 * 2e-
6.^0.1028.*(1./500).^0.1672 *(ViscosL./1.5e-3).^0.1;
Bubble6 = 0.7/0.8856/(5^2*rpm^7*T^13)^0.1836*0.1^4 .*SurfTen'.^0.6 * 6e-
6.^0.1028.*(1./500).^0.1672 *(ViscosL./1.5e-3).^0.1;
Bubble7 = 0.7/0.8856/(5^2*rpm^7*T^13)^0.1836*0.1^4 .*SurfTen'.^0.6 * 10e-
6.^0.1028.*(1./500).^0.1672 *(ViscosL./1.5e-3).^0.1;

```



```

Bubble8 = 0.7/0.8856/(5^2*rpm^7*T^13)^0.1836*0.1^4 .*SurfTen'.^0.6 * 14e-
6.^0.1028.*(1./500).^0.1672 *(ViscosL./1.5e-3).^0.1;
Iarea5 = 6*Gashold5./Bubble5;
Iarea6 = 6*Gashold6./Bubble6;
Iarea7 = 6*Gashold7./Bubble7;
Iarea8 = 6*Gashold8./Bubble8;
figure
hold on
view(3)
grid on
mesh(ViscosL,SurfTen,Iarea5);
mesh(ViscosL,SurfTen,Iarea6);
mesh(ViscosL,SurfTen,Iarea7);
mesh(ViscosL,SurfTen,Iarea8);
hold off
title('Interfacial area Viscosity vs Surfacetension vary N2Flow')
PreGashold9 = 0.819*(6e-6/(pi*0.13^2/4)).^(2/3) *DenseL'.^(2/15)
*rpm^(2/5)*T^(4/15)/9.81^(1/3)*(1/0.05)^(1/5)*(1/(1-0))*(1/0.9)^(-
1/15)*(ViscosL/1.5e-3).^(-1/4);
Gashold9 = PreGashold9.*(1./(1+PreGashold9));
Bubble9 = 0.7/0.8856/(5^2*rpm^7*T^13)^0.1836*0.1^4 .*0.05.^0.6 * 6e-
6.^0.1028.*(1./DenseL').^0.1672 *(ViscosL./1.5e-3).^0.1;
Iarea9 = 6*Gashold9./Bubble9;
figure
hold on
view(3)
grid on
mesh(ViscosL,DenseL,Iarea5);
title('Viscosity vs Dense')
PreGashold10 = 0.819*(6e-6/(pi*0.13^2/4)).^(2/3) *DenseL'.^(2/15)
*rpm^(2/5)*T^(4/15)/9.81^(1/3)*(1./SurfTen).^(1/5)*(1/(1-0))*(1/0.9)^(-
1/15)*(0.01/1.5e-3).^(-1/4);
Gashold10 = PreGashold10.*(1./(1+PreGashold10));
%Bubble6 = 0.7/0.8856/(5^2*rpm^7*T^13)^0.1836*0.1^4 .*SurfTen'.^0.6 * 1e-
6.^0.1028 *(1./DenseL).^0.1672 *(0.01./1.5e-3).^0.1;
Bubble10 = 0.7/0.8856/(5^2*rpm^7*T^13)^0.1836*0.1^4 * 6e-6.^0.1028
*(1./DenseL').^0.1672 *SurfTen.^0.6*(0.01./1.5e-3).^0.1;
Iarea10 = 6*Gashold10./Bubble10;
figure
hold on
view(3)
grid on
mesh(SurfTen,DenseL,Iarea10);
title('Surfacetension vs DenseL')
PreGashold11 = 0.819*(6e-6/(pi*0.13^2/4)).^(2/3)
*(1./SurfTen').^(1/5)*rpm^(2/5)*T^(4/15)/9.81^(1/3)*(500)^(1/5)*(500/(500-
0.9))*(500/0.9)^(-1/15) *(ViscosL/1.5e-3).^(-1/4);

```

```

Gashold11 = PreGashold11.*(1./(1+PreGashold11));
Bubble11 = 0.7/0.8856/(5^2*rpm^7*T^13)^0.1836*0.1^4 .*SurfTen'.^0.6 * 6e-
6.^0.1028.*(1./500).^0.1672 *(ViscosL./1.5e-3).^0.1;
Iarea11 = 6*Gashold11./Bubble11;
figure
hold on
view(3)
grid on
mesh(ViscosL,SurfTen,Iarea11);
title('ViscosL vs Surftension')

```



ศูนย์วิทยทรัพยากร
จุฬาลงกรณ์มหาวิทยาลัย

C.3.2 Model for prediction of volumetric mass transfer coefficient characterization

```

function kLa_Dens_Viscos_VaryN2Flow_Temp3D
% Vary N2 Flow and Temperature
D = linspace(0.004e-9,4e-9,40); %Diffusivity
ViscosL = linspace(0.0005,0.02,40); %Pa.s
DenseL = linspace(100,1000,40); %kg/m3
E = linspace(0,5,40); %energy dissipation
Q = linspace(0e-6,1.4e-5,40); %N2 flow m3/s
Temp = linspace(50,250,40);
SurfTen = linspace(0.01,0.1,40);
%QN2=m3/sec
%Q=Q*(TV+273)/(25+273);
%Vs = Q/(pi*0.132/4); %m/s
T = 5/100; %meter
H = 10/100; %meter
rpm = 15; %round per sec.
Np=5;
mL = 1.6; %kg
mL1 = linspace(1.7,1.5,20);
Di = 0.13; %vessel diameter meter
Mw = linspace(50,1000,40);
%Bubble = 0.7/0.8856/(52*rpm7*T13)0.1836*0.14 .*SurfTen.0.6 *
Q'.0.1028.*(1./DenseL).0.1672.*(ViscosL./1.5e-3).0.1
% vary N2Flow
Bubble1 = 0.7/0.8856/(52*rpm7*T13)0.1836*0.14 .*0.05.0.6 * 2e-
6'.0.1028*(1./DenseL').0.1672 *(ViscosL./1.5e-3).0.1;
%calculate at volume liquid 0.1 m3, Viscosity N2 = 1.5e-3 Pa.s
%SurfTen = 0.05 N/m, Q=1e-5 m3/s
Bubble2 = 0.7/0.8856/(52*rpm7*T13)0.1836*0.14 .*0.05.0.6 * 6e-
6'.0.1028*(1./DenseL').0.1672 *(ViscosL./1.5e-3).0.1;
Bubble3 = 0.7/0.8856/(52*rpm7*T13)0.1836*0.14 .*0.05.0.6 * 1e-
5'.0.1028*(1./DenseL').0.1672 *(ViscosL./1.5e-3).0.1;
Bubble4 = 0.7/0.8856/(52*rpm7*T13)0.1836*0.14 .*0.05.0.6 * 1.4e-
5'.0.1028*(1./DenseL').0.1672 *(ViscosL./1.5e-3).0.1;
%PreGashold1 = 0.819*(Q'/(pi*0.132/4)).(2/3)
*(1./SurfTen).(1/5)*rpm(2/5)*T(4/15)/9.81(1/3)*(DenseL)(1/5)*(DenseL/(Dens
eL-DenseL))* (DenseL/DenseG)(-1/15)*(ViscosL/ViscosG)(-1/4);
PreGashold1 = 0.819*(2e-6'/(pi*0.132/4)).(2/3) *DenseL'.(2/15)
*rpm(2/5)*T(4/15)/9.81(1/3)*(1/0.05)(1/5)*(1/(1-0))(1/5)*(1/0.9)(-1/15)
*(ViscosL/1.5e-3).(-1/4);
%calculate at SurfTen = 0.05 N/m, Viscosity= 1 Pa.s,
% Viscosity N2 = 1.5e-3 Pa.s, Density N2=0.9 kg/m3, ViscosityL = 1 Pa.s
%Assume Density N2 very low compare to DenseL

```

```

PreGashold2 = 0.819*(6e-6/(pi*0.13^2/4)).^(2/3) *DenseL'.^(2/15)
*rpm^(2/5)*T^(4/15)/9.81^(1/3)*(1/0.05)^(1/5)*(1/(1-0))*(1/0.9)^(-1/15)
*(ViscosL/1.5e-3).^(-1/4);
PreGashold3 = 0.819*(1e-5/(pi*0.13^2/4)).^(2/3) *DenseL'.^(2/15)
*rpm^(2/5)*T^(4/15)/9.81^(1/3)*(1/0.05)^(1/5)*(1/(1-0))*(1/0.9)^(-1/15)
*(ViscosL/1.5e-3).^(-1/4);
PreGashold4 = 0.819*(1.4e-5/(pi*0.13^2/4)).^(2/3) *DenseL'.^(2/15)
*rpm^(2/5)*T^(4/15)/9.81^(1/3)*(1/0.05)^(1/5)*(1/(1-0))*(1/0.9)^(-1/15)
*(ViscosL/1.5e-3).^(-1/4);
Gashold1 = PreGashold1.*(1./(1+PreGashold1));
Gashold2 = PreGashold2.*(1./(1+PreGashold2));
Gashold3 = PreGashold3.*(1./(1+PreGashold3));
Gashold4 = PreGashold4.*(1./(1+PreGashold4));
%kL1 = 1/1000^(1/2)*3.7512e-7*rpm^0.8033*T^0.9918/H^(1/4)/18.79763^(0.3)
.*Mw'.^(1/4)*(Temp.^1/2 .*DenseL'.^(0.459/2) .* (1./ViscosL).^(3/4)
.*(1./Q).^0.0643)
kL1 = 1/1000^(1/2)*3.7512e-7*rpm^0.8033*T^0.9918/H^(1/4)/18.79763^(0.3)
*(1./2e-6).^0.0643.*500.^(1/4)*((180+273).^1/2 *DenseL'.^(0.459/2)
*(1./ViscosL).^(3/4) );
kL2 = 1/1000^(1/2)*3.7512e-7*rpm^0.8033*T^0.9918/H^(1/4)/18.79763^(0.3)
*(1./6e-6).^0.0643.*500.^(1/4)*((180+273).^1/2 *DenseL'.^(0.459/2)
*(1./ViscosL).^(3/4) );
kL3 = 1/1000^(1/2)*3.7512e-7*rpm^0.8033*T^0.9918/H^(1/4)/18.79763^(0.3)
*(1./1e-5).^0.0643.*500.^(1/4)*((180+273).^1/2 *DenseL'.^(0.459/2)
*(1./ViscosL).^(3/4) );
kL4 = 1/1000^(1/2)*3.7512e-7*rpm^0.8033*T^0.9918/H^(1/4)/18.79763^(0.3)
*(1./1.4e-5).^0.0643.*500.^(1/4)*((180+273).^1/2 *DenseL'.^(0.459/2)
*(1./ViscosL).^(3/4) );
%calculate at Molar volume H2O = 18.79763,
%Mw = 500, Temp 180
Iarea1 = 6*Gashold1./Bubble1;
Iarea2 = 6*Gashold2./Bubble2;
Iarea3 = 6*Gashold3./Bubble3;
Iarea4 = 6*Gashold4./Bubble4;
kLa1 = Iarea1.*kL1;
kLa2 = Iarea2.*kL2;
kLa3 = Iarea3.*kL3;
kLa4 = Iarea4.*kL4;
figure
hold on
view(3)
grid on
mesh(ViscosL,DenseL,kLa1)
mesh(ViscosL,DenseL,kLa2)
mesh(ViscosL,DenseL,kLa3)
mesh(ViscosL,DenseL,kLa4)
title('kLa Viscosity vs Density==>vary N2Flow')

```

```

hold off
% vary temp
% calculate at volume liquid 0.1 m3, Viscosity N2 = 1.5e-3 Pa.s
% SurfTen = 0.05 N/m, Q=1e-5 m3/s
Bubble6 = 0.7/0.8856/(5^2*rpm^7*T^13)^0.1836*0.1^4 .*0.05.^0.6 * 6e-
6'.^0.1028*(1./DenseL').^0.1672 *(ViscosL./1.5e-3).^0.1;
% PreGashold1 = 0.819*(Q/(pi*0.13^2/4)).^(2/3)
*(1./SurfTen).^(1/5)*rpm^(2/5)*T^(4/15)/9.81^(1/3)*(DenseL)^(1/5)*(DenseL/(DenseL-DenseL))*(DenseL/DenseG)^(-1/15)*(ViscosL/ViscosG)^(-1/4);
% calculate at SurfTen = 0.05 N/m, Viscosity= 1 Pa.s,
% Viscosity N2 = 1.5e-3 Pa.s, Density N2=0.9 kg/m3, ViscosityL = 1 Pa.s
% Assume Density N2 very low compare to DenseL
PreGashold6 = 0.819*(6e-6/(pi*0.13^2/4)).^(2/3) *DenseL'.^(2/15)
*rpm^(2/5)*T^(4/15)/9.81^(1/3)*(1/0.05)^(1/5)*(1/(1-0))*(1/0.9)^(-1/15)
*(ViscosL/1.5e-3).^(-1/4);
Gashold6 = PreGashold6.*(1./(1+PreGashold6));
% kL1 = 1/1000^(1/2)*3.7512e-7*rpm^0.8033*T^0.9918/H^(1/4)/18.79763^(0.3)
.*Mw'.^(1/4)*(Temp.^1/2 .*DenseL'.^(0.459/2) .* (1./ViscosL).^(3/4)
.*(1./Q).^0.0643)
kL5 = 1/1000^(1/2)*3.7512e-7*rpm^0.8033*T^0.9918/H^(1/4)/18.79763^(0.3)
*(1./6e-6').^0.0643.*500.^(1/4)*((120+273).^1/2 *DenseL'.^(0.459/2)
*(1./ViscosL).^(3/4) );
kL6 = 1/1000^(1/2)*3.7512e-7*rpm^0.8033*T^0.9918/H^(1/4)/18.79763^(0.3)
*(1./6e-6').^0.0643.*500.^(1/4)*((180+273).^1/2 *DenseL'.^(0.459/2)
*(1./ViscosL).^(3/4) );
kL7 = 1/1000^(1/2)*3.7512e-7*rpm^0.8033*T^0.9918/H^(1/4)/18.79763^(0.3)
*(1./6e-6').^0.0643.*500.^(1/4)*((200+273).^1/2 *DenseL'.^(0.459/2)
*(1./ViscosL).^(3/4) );
kL8 = 1/1000^(1/2)*3.7512e-7*rpm^0.8033*T^0.9918/H^(1/4)/18.79763^(0.3)
*(1./6e-6').^0.0643.*500.^(1/4)*((220+273).^1/2 *DenseL'.^(0.459/2)
*(1./ViscosL).^(3/4) );
% calculate at Molar volume H2O = 18.79763,
% Mw = 500, Temp 180
Iarea6 = 6*Gashold6./Bubble6;
kLa5 = Iarea6.*kL5;
kLa6 = Iarea6.*kL6;
kLa7 = Iarea6.*kL7;
kLa8 = Iarea6.*kL8;
figure
hold on
view(3)
grid on
mesh(ViscosL,DenseL,kLa5)
mesh(ViscosL,DenseL,kLa6)
mesh(ViscosL,DenseL,kLa7)
mesh(ViscosL,DenseL,kLa8)
title('kLa Viscosity vs Density==>vary temp')

```

```

hold off
%vary MW
kL9 = 1/1000^(1/2)*3.7512e-7*rpm^0.8033*T^0.9918/H^(1/4)/18.79763^(0.3)
*(1./6e-6).^0.0643.*250.^(1/4)*((180+273).^1/2 *DenseL'.^(0.459/2)
*(1./ViscosL).^(3/4) );
kL10 = 1/1000^(1/2)*3.7512e-7*rpm^0.8033*T^0.9918/H^(1/4)/18.79763^(0.3)
*(1./6e-6).^0.0643.*500.^(1/4)*((180+273).^1/2 *DenseL'.^(0.459/2)
*(1./ViscosL).^(3/4) );
kL11 = 1/1000^(1/2)*3.7512e-7*rpm^0.8033*T^0.9918/H^(1/4)/18.79763^(0.3)
*(1./6e-6).^0.0643.*700.^(1/4)*((180+273).^1/2 *DenseL'.^(0.459/2)
*(1./ViscosL).^(3/4) );
kL12 = 1/1000^(1/2)*3.7512e-7*rpm^0.8033*T^0.9918/H^(1/4)/18.79763^(0.3)
*(1./6e-6).^0.0643.*1000.^(1/4)*((180+273).^1/2 *DenseL'.^(0.459/2)
*(1./ViscosL).^(3/4) );
Iarea6 = 6*Gashold6./Bubble6;
kLa9 = Iarea6.*kL9;
kLa10 = Iarea6.*kL10;
kLa11 = Iarea6.*kL11;
kLa12 = Iarea6.*kL12;
figure
hold on
view(3)
grid on
mesh(ViscosL,DenseL,kLa9)
mesh(ViscosL,DenseL,kLa10)
mesh(ViscosL,DenseL,kLa11)
mesh(ViscosL,DenseL,kLa12)
title('kLa Viscosity vs Density==>vary Mw')
hold off

```

ศูนย์วิทยทรัพยากร
จุฬาลงกรณ์มหาวิทยาลัย

BIOGRAPHY

Mr. Surachat Chombanphaew was born on February 17th 1972 in Bangkok, Thailand and graduated from Kasetsart University, Faculty of Engineering in 1996 with a Bachelor's of Engineering in Chemical Engineering. He resumed studying in 1997 and got a Master's Degree of Chemical Engineering, Faculty of Engineering, Chulalongkorn University in 2001. In 2005, he started seeking a doctoral degree at the Department of Chemical Technology, Faculty of Science, Chulalongkorn University.



ศูนย์วิทยทรัพยากร
จุฬาลงกรณ์มหาวิทยาลัย